Dissertation

submitted to the

Combined Faculty of Natural Sciences and Mathematics

of the Ruperto Carola University Heidelberg, Germany

for the degree of

Doctor of Natural Sciences

Presented by

M.Sc. Marie Jacobovitz

born in: Orlando, Florida, USA

Oral examination: 14.12.2021

A comparative framework to investigate the intracellular residency of symbionts in Aiptasia

Referees:

Prof. Dr. Annika Guse

Prof. Dr. Thomas Holstein

Jun. Prof. Dr. Steffen Lemke

Dr. Doris Höglinger

Abstract

To survive in the nutrient-poor waters of the tropics, reef-building corals evolved the capacity to engage in a mutualistic symbiosis with unicellular dinoflagellates. This symbiosis creates both the structural and trophic foundation of the entire ecosystem – a highly productive ecosystem that is astonishingly rich in biodiversity. Most coral species reestablish this symbiosis with each new generation, meaning that coral progeny must select compatible symbionts from the environment. The symbionts are phagocytosed by the endodermal cells of the coral, where they reside in a specialized vacuole, i.e., the symbiosome, and a bidirectional nutrient exchange ensues. While immune suppression has been implicated in mediating symbiosis in corals, the cellular mechanisms connected to immune suppression that influence symbiont selection and maintenance are unknown. Furthermore, it is unclear how the modulation of immune pathways can simultaneously promote symbiont maintenance while thwarting invasion by non-beneficial microorganisms. To better understand how symbionts are stably integrated into host cells, we established a comparative framework using the endosymbiosis model Aiptasia, a small sea anemone closely related to corals. This comparative analysis was complemented with confocal microscopy and immunofluorescence, live imaging, transcriptomic analyses, and exogenous immune modulation to analyze various aspects of symbiosis establishment, from uptake to maintenance. We found that initial uptake of microalgae is largely indiscriminate as Aiptasia larvae phagocytose a vast array of particles, including symbionts, non-symbiotic microalgae, heat-killed microalgae, and beads. After phagocytosis, we found that non-symbiotic or heat-killed particles are expelled via vomocytosis, a process that is stochastic and dependent on extracellular-regulated kinase 5. Not only are these particles expelled, but they are frequently reacquired and expelled again, in what resembles a search for symbionts based on trial-and-error. The symbionts evade this expulsion and establish an intracellular lysosomal associated membrane protein 1 (LAMP1)-positive niche. Additionally, we found that LAMP1 accumulates around heat-killed microalgae, possibly in an attempt to digest the particles. However, even though the heat-killed non-symbiotic microalgae are intracellular longer than their healthy counterparts, they too are expelled, eventually. Thus, we revealed dual functionality for LAMP1 in intracellular niche establishment and its canonical association with degradative lysosomes. Analyzing transcriptomic data from symbiotic cells compared with non-symbiotic microalgae-containing cells revealed that symbiont-uptake induces broad immune suppression, sufficient to halt their

expulsion. Exogenously activating the innate immune system in Aiptasia larvae during infection with symbionts impairs symbiosis establishment. Using live imaging, we demonstrated that this compromised infection is a direct consequence of enhanced expulsion. Conversely, we showed that symbiosis establishment is bolstered when the toll-like receptor pathway is inhibited, specifically by interfering with MyD88 homodimer formation. In summary, we found that although some pre-phagocytic selection mechanisms exist, as heat-killing of microalgae influences uptake, the truly decisive symbiont selection mechanisms occur post-phagocytosis. Furthermore, our findings demonstrated that local immune suppression during symbiosis establishment is essential to bypass vomocytosis and initiate LAMP1-niche formation. This work revealed the role of an evolutionarily ancient innate immune response involved in symbiont selection and symbiosis establishment.

Zusammenfassung

Um in den nährstoffarmen Gewässern der Tropen überleben zu können, leben riffbildende Korallen in wechselseitiger Symbiose mit einzelligen Dinoflagellaten. Diese Symbiose bildet sowohl die strukturelle als auch die trophische Grundlage des gesamten Ökosystems - ein Ökosystem mit einer außerordentlichen Produktivität und einer erstaunlich großen biologischen Vielfalt. Die meisten Korallenarten bauen diese Symbiose mit jeder neuen Generation wieder auf. Das heißt, Korallennachkommen müssen kompatible Symbionten aus der Umwelt auswählen. Die Symbionten werden von den endodermalen Zellen der Koralle phagozytiert. Sobald sie intrazellulär sind, befinden sie sich in einer speziellen Vakuole, die als Symbiosom bezeichnet wird, und es findet ein bidirektionaler Nährstoffaustausch statt. Es ist bekannt, dass eine Suppression des Immunsystems die Symbiose ermöglicht, allerdings sind die mit der Immunsuppression verbundenen zellulären Mechanismen, die wiederum die Auswahl und den Erhalt der Symbionten beeinflussen, unbekannt. Darüber hinaus ist unklar, wie die Modulation der Immunwege gleichzeitig die Aufrechterhaltung der Symbionten fördern und die Invasion durch nicht nützliche Mikroorganismen verhindern kann. Um besser zu verstehen, wie Symbionten stabil in Wirtszellen integriert werden, haben wir einen vergleichenden Rahmen mit dem Endosymbiose-Modell Aiptasia geschaffen; einer kleinen Seeanemone, die eng mit Korallen verwandt ist. Wir ergänzten diese vergleichende Analyse mit konfokaler Mikroskopie und Immunfluoreszenz, Live-Imaging, transkriptomischer Analyse und exogener Immunmodulation, um verschiedene Aspekte der Symbiose-Etablierung, von der Aufnahme bis zur Aufrechterhaltung, zu analysieren. Unsere Experimente konnten zeigen, dass die anfängliche Aufnahme von Mikroalgen weitgehend wahllos erfolgt, da Aiptasia-Larven eine Vielzahl von Partikeln phagozytieren, darunter Symbionten, nicht-symbiotische Mikroalgen, hitzeabgetötete Mikroalgen und Plastikkugeln. Zudem haben wir festgestellt, dass nicht-symbiontische oder durch Hitze abgetötete Partikel nach der Phagozytose durch Vomozytose ausgestoßen werden - ein Prozess, der stochastisch ist und von der extrazellulär regulierten Kinase 5 abhängt. Diese Partikel werden nicht nur ausgestoßen, sondern auch häufig wieder aufgenommen und erneut ausgestoßen, was einer auf Versuch und Irrtum basierenden Suche nach Symbionten ähnelt. Die Symbionten entziehen sich dieser Ausstoßung und etablieren eine intrazelluläre, lysosomal assoziierte Membranprotein 1 (LAMP1)-positive Nische. Darüber hinaus haben wir festgestellt, dass sich LAMP1 in der Umgebung von hitzeabgetöteten Mikroalgen ansammelt, möglicherweise in dem Versuch, die Partikel zu verdauen. Obwohl die

hitzeabgetöteten nicht-symbiotischen Mikroalgen länger intrazellulär verbleiben als ihre gesunden Gegenstücke, werden auch sie schließlich ausgestoßen. So konnten wir eine doppelte Funktion von LAMP1 bei der Einrichtung intrazellulärer Nischen und der kanonischen Assoziation mit abbauenden Lysosomen nachweisen. Durch die Analyse transkriptomischer Daten von symbiotischen Zellen im Vergleich zu Zellen mit nicht-symbiotischen Mikroalgen fanden wir heraus, dass die Symbiontenaufnahme eine breite Immunsuppression induziert, die ausreicht, um ihre Ausstoßung zu stoppen. Die exogene Aktivierung des angeborenen Immunsystems in Aiptasia-Larven während der Infektion mit Symbionten beeinträchtigt die Etablierung der Symbiose drastisch. Mithilfe von Live-Imaging konnten wir zeigen, dass diese beeinträchtigte Infektion eine direkte Folge der verstärkten Ausstoßung ist. Umgekehrt konnten wir zeigen, dass die Etablierung der Symbiose gefördert wird, wenn der Toll-like-Rezeptor-Signalweg gehemmt wird, insbesondere durch die Störung der MyD88-Homodimerbildung. Zusammenfassend haben wir festgestellt, dass es zwar einige präphagozytäre Selektionsmechanismen gibt, da die Hitzeabtötung von Mikroalgen die Aufnahme beeinflusst, die wirklich entscheidenden Selektionsmechanismen für Symbionten jedoch erst nach der Phagozytose auftreten. Darüber hinaus haben unsere Ergebnisse gezeigt, dass eine lokale Immunsuppression während der Symbiosebildung wesentlich ist, um die Vomozytose zu umgehen und die Bildung von LAMP1-Nischen zu initiieren. Mit dieser Arbeit konnte die Rolle einer evolutionär alten angeborenen Immun-reaktion, die an der Symbiontenauswahl und Symbiosebildung beteiligt ist, enthüllt werden.

Acknowledgements

Over the last four years, and throughout the writing of this thesis, I have received a great deal of support, for which I am grateful. Firstly, I would like to thank my supervisor, Dr. Annika Guse, for granting me the opportunity to work in her lab. Your support was invaluable – your confidence in me eased my anxieties and kept me motivated. I have learned so much from you – not only did you navigate the lab through a global pandemic, but you managed to publish some excellent papers as well. Next, I must give a big thank you to my TAC members and examiners, Dr. Thomas Holstein, Dr. Steffen Lemke, and Dr. Doris Höglinger. I am truly grateful for your support and guidance throughout the years, which have shaped this thesis and me as a scientist.

I am thankful to all the members of the Guse lab, past and present. Sebastian – working on our paper together was quite the experience, and I am grateful to have shared it with you. And thank you for letting me borrow your noise-canceling headphones (this thesis would not exist otherwise). Ira – thank you for all your support and help over the years. You make everything run so seamlessly, and it is very much appreciated. Seb – Thank you for always making time to engage in lively conversations, offer up scientific advice, or brainstorm. Philipp – our scientific discussions were always engaging and a little bit goofy, which made my time in the lab a lot of fun. And beyond the lab, thank you for being my bouldering buddy. Also, a big thanks to all the students. I had such a great time working with all of you and learned so much myself.

Thank you to all the 6th-floor members. I enjoyed all of the social activities and discussions over the years. I can honestly say there was never a dull moment. I am so thankful to have found friends in you. Steffi – thank you for always bringing a smile to my face and radiating positivity. Niha – thank you for your endless support, willingness to listen to my problems, and always cooking the most delicious food for me. Our coffee breaks keep me going.

Lastly, I could not have completed this thesis without the love and support from my family and friends. Although there is an ocean between us, Mom – I am so thankful for your support and encouragement. You are always there for me. Nana – I miss you every day. You were always my #1 fan, and I wish we could celebrate this accomplishment together. Finally, Tomek – thank you for being my best friend and partner through it all. You are always there for me, and I am forever grateful.

Contributions

The work presented here is my own, apart from the contributions made by the following people: *C. velia* DIC images and infection data collected by Sebastian Rupp, heat-killed infection data and immunofluorescence images partially acquired by Viola Kühnel, live imaging of heat-killed microalgae acquired by Viola Kühnel, assessment of pH on symbiont growth performed by Sebastian Gornik, live imaging and quantification performed by Sebastian Rupp, transcriptomic data acquired by Philipp Voss and analyzed with assistance from Sebastian Gornik, heatmap created by Sebastian Rupp, ERK5/MAP2K5 phylogeny created by Sebastian Rupp, LPS treatment experiments and analysis performed by Sebastian Rupp, MyD88 inhibition experiments partially acquired by Sebastian Rupp, alignment of MyD88 sequences created by Sebastian Rupp – all which will be indicated in the respective figure legends. Due to the collaborative nature of the results presented in this thesis, I have utilized "we" throughout the text; however, it should be noted that I fully stand behind the results presented herein.

Publication of work presented in this thesis

The work presented in this thesis has partially been published in the following publication:

Jacobovitz, M.R., Rupp, S., Voss, P.A. *et al.* Dinoflagellate symbionts escape vomocytosis by host cell immune suppression. *Nat Microbiol* **6,** 769–782 (2021). https://doi.org/10.1038/s41564-021-00897-w

Table of contents

Table of Figures

List of Abbreviations

ANOVA – analysis of variance
AP1 – activator protein 1
Apo – aposymbiotic
ATP – adenosine triphosphate
BLAST – basic local alignment search tool
BSA – bovine serum albumin
C3 – complement protein
CALM – calmodulin-like
CCM – carbon concentrating mechanism
CMF-SW – calcium- and magnesium-free artificial seawater
CO_2 – carbon dioxide
DABCO – 1,4-diazabicyclo [2.2.2] octane
DIC – differential interference contrast
DMSO – dimethyl sulfoxide
DNA – deoxyribonucleic acid
dpf – days post fertilization
dpi – days post infection
EEA1 – early endosome antigen 1
EMT – epithelial to mesenchymal transition
ERK5 – extracellular signal-regulated kinase 5
F-actin – filamentous actin
FASW – filtered artificial seawater
GFP – green fluorescent protein
GTP – guanosine triphosphate
HCO_3^- – bicarbonate
HEK – human embryonic kidney
HK – heat-killed
hpi – hours post infection
IKK – inhibitor of nuclear factor kappa B kinase
IL-1R – interleukin-1 receptor
IRAK – interleukin-1 receptor-associated kinase
IκB – inhibitor of nuclear factor kappa B
IκBα – nuclear factor of kappa light polypeptide gene enhancer in B-cells inhibitor
JAK-STAT – janus kinase-signal transducer and activator of transcription protein
KEGG – Kyoto encyclopedia of genes and genomes
LAMP1 – lysosomal-associated membrane protein 1
LatB – latrunculin B
LGA – low gelling agarose
LPS – lipopolysaccharide
LRR – leucine rich repeat
MAMP – microbe associated molecular pattern

MAP2K5 – mitogen-activated protein kinase kinase 5
MAPK – mitogen-activated protein kinase
MALT1 – mucosa-associated lymphoid tissue lymphoma translocation protein 1-like
MPR – mannose-6-phosphate receptor
mRNA – messenger ribonucleic acid
mTORC – mechanistic target of rapamycin complex
MyD88 – myeloid differentiation primary response 88
NEMO – NF-κB essential modulator
NF-κB – nuclear factor kappa B
NLS – nuclear localization sequence
NOD – like receptor nucleotide-binding oligomerization domain
NPC2 – Niemann-Pick Type C2
PAR – photosynthetically active radiation
PBS – phosphate-buffered saline
PRR – pattern recognition receptor
PTM – post-translational modification
Rab5/6/7/8 – Ras-related protein 5/6/7/8
RIG-1-like receptor – retinoic acid inducible gene I
RT – room temperature
SCP – S. enterica-containing phagosome
SD – standard deviation
SEM – standard error of the mean
SNARE – soluble NSF attachment protein (SNAP) receptor
SR – scavenger receptor
SRA – sequence read archive
TAB1 – transforming growth factor β-activated kinase 1
TAK1 – TGF-β-activated kinase 1
TBS – tris-buffered saline
TGF-β – transforming growth factor beta
TIR – toll/interleukin-1 receptor
TLR – toll-like receptor
TNF – tumor necrosis factor
TRAF 3/6 – TNF receptor-associated factor 3/6
v-ATPase – vacuolar H+-ATPase
VAMP2 – vesical associated membrane protein 2
WASH – Wiskott-Aldrich syndrome protein and scar homolog
WASHC1 – WASH complex 1

1 Introduction

1.1 General Introduction

Coral reef ecosystems are rich in biodiversity. They are the marine equivalent of tropical rainforests in terms of species diversity and abundance, physical complexity, and high prevalence of coevolution amongst species. Globally, coral reefs cover a minuscule 0.2% of the seafloor yet provide habitat to one-quarter of all marine life (Reaka-Kudla, 1997; Souter et al., 2020; Spalding & Grenfell, 1997). These ecosystems are incredibly valuable for humankind as well, supporting hundreds of millions of people worldwide with coastal protection, fisheries, new biological compounds, and tourism (Costanza et al., 2014).

The physical structure of the reef itself provides shelter and creates feeding, spawning, and nursery grounds for many fish and other marine organisms. Reef-building organisms, among them stony corals, deposit calcium carbonate in the form of aragonite to generate these important three-dimensional structures, and form both the structural and trophic foundation of the entire ecosystem (Muscatine & Porter, 1977a; von Euw et al., 2017). Coral reefs are distributed across the sub-tropics and tropics, where the shallow waters are nutrient-poor, but due to a mutualistic symbiosis with photosynthetic dinoflagellates, corals can thrive in this oligotrophic environment.

Dinoflagellate symbionts live inside the coral tissue and transfer photosynthetic products to the host, which are essential for their survival. Although symbionts are taken up by phagocytosis, a process that classically culminates in the degradation of the phagocytosed particle (Huynh et al., 2007; Jaumouillé & Grinstein, 2016; Rosales & Uribe-Querol, 2017; Yellowlees et al., 2008), it is known that the symbionts remain intracellular to support host nutrition (Muscatine, 1990). This anomaly is compounded by the fact that the coral host possesses a complex innate immune system (Hemmrich et al., 2007; Mansfield & Gilmore, 2018; Miller et al., 2007). While recent investigations have explained aspects of this phenomenon, many questions remain unanswered. Questions such as: How do symbionts live within the constraints of the immune system? Moreover, how does immune suppression contribute to symbiont maintenance? How do symbionts circumvent phagolysosomal degradation? What is the nature of the symbiosome that enables intracellular persistence of symbionts? And how does the host preferentially select for symbionts while excluding non-symbiotic or potentially harmful microorganisms? The work presented in this thesis intends to address these questions.

1.2 Cnidarian-dinoflagellate symbiosis

The mutualistic endosymbiosis between cnidarians, including reef-building corals, and unicellular dinoflagellates from the family Symbiodiniaceae (previously genus *Symbiodinium*) (LaJeunesse et al., 2018; Muscatine & Porter, 1977b) is essential for the viability and success of coral reefs. The dinoflagellate symbionts are intracellularized by the host's endodermal cells via phagocytosis and are maintained in a specialized organelle, the symbiosome (Yellowlees et al., 2008). Once intracellular, a bidirectional nutrient exchange ensues, wherein the host provides shelter, protection from predation, a stable position within the water column, and inorganic nutrients to the endosymbiont, while the dinoflagellate symbiont transfers photosynthetically fixed carbon to the host, supporting host metabolism, growth, and reproduction (Muscatine, 1990). The appearance of coral reefs is thought to coincide with the establishment of this symbiosis 240 million years ago during the Triassic period (Muscatine et al., 2005).

Although some corals transmit symbionts to their offspring during sexual reproduction (vertical transmission), the vast majority of coral species produce aposymbiotic (i.e., symbiont-free) progeny, which means that each generation much establish symbiosis anew (horizontal transmission) (Baird et al., 2009). Because these larvae are provided with maternally derived yolk, they can survive for extended periods of time as they are dispersed over long distances in the open sea. Eventually, the larvae will settle and metamorphose into a sessile polyp. Therefore, the horizonal transmission strategy is hypothesized to support colonization with symbionts adapted to the local environment (Davies et al., 2017).

While symbiosis establishment can occur during the larval stage, it also occurs post-settlement in juvenile polyps or in mature polyps following a bleaching event. Bleaching refers to the loss of symbionts from corals, as dinoflagellate symbionts provide color to the otherwise transparent host organism. Bleaching events are increasing globally in both frequency and severity as a result of anthropogenic climate change. The rising temperature and acidity of the oceans disrupt the delicate balance between host and symbiont, which can ultimately be fatal for the bleached coral and, consequently, the entire ecosystem (Douglas, 2003; Hoegh-Guldberg et al., 1987; Hoegh-Guldberg & Smith, 1989). Fortunately, corals may recover after symbionts are expelled if symbiosis is reestablished in a timely manner. Adult corals have been shown to reacquire dinoflagellate symbionts and reestablish symbiosis following bleaching events; however,

acquiring symbionts by adult polyps is not as efficient as acquisition and symbiosis establishment by larvae (Baker, 2001; Lewis & Coffroth, 2004). As some hosts are populated by multiple symbiont strains, symbiont shuffling (i.e., the establishment of a new dominant symbiont strain within a host organism) has been shown to mediate host recuperation after a stress event; however, symbiont switching (i.e., the *de novo* acquisition of symbionts) is not a common occurrence (Ros et al., 2021). While the cnidarian-dinoflagellate symbiosis is ancient and has undoubtedly experienced a changing planet over the last 240 million years, these organisms are likely unable to withstand the unprecedented, rapid change in climate we are currently experiencing; and thus, protecting these precious and fragile organisms must be a priority (Knowlton et al., 2021).

1.2.1 Cnidaria

The phylum Cnidaria, one of the earliest diverging metazoan clades and sister group to Bilateria, comprises an assortment of relatively simple, primarily marine invertebrates. To date, more than 13,000 extant cnidarian species have been described (Collins, 2009; Daly et al., 2007; Kayal et al., 2018). Cnidaria is divided into three major clades. The first major clade, Medusozoa, comprises Cubozoa (box jellyfish), Hydrozoa (hydroids), Scyphozoa (true jellyfish), and Staurozoa (stalked jellyfish). The second clade, Anthozoa, contains more than half of all cnidarian species. Anthozoa is further subdivided into two subclasses, Hexacorallia (stony corals, black corals, and sea anemones) and Octocorallia (sea pens, sea fans, and soft corals). The third major clade, Endocnidozoa, includes Myxozoa and Polypodiozoa, all of which are endoparasitic invertebrates (Atkinson et al., 2018; Kayal et al., 2018) (Figure 1).

Cnidarians are diploblastic comprising two tissue layers, an outer ectoderm and an inner endoderm, separated by a jelly-like mesoglea. They possess a single orifice that functions as both mouth and anus that leads to the gastric cavity (Brusca, Richard C., 2002). All cnidarians possess stinging cells called cnidae, the taxa's namesake, which are primarily used for prey capture. Cnidae are capsular organelles containing a tightly coiled tubule, occasionally decorated with spines. Once triggered, the tubule is discharged explosively, accelerating up to 5 million g (Nüchter et al., 2006) (Figure 2). Despite their ability to capture prey and heterotrophically acquire nutrients, many cnidarians form symbioses with photosynthetic dinoflagellates to support nutrition in an otherwise nutrient-poor environment.

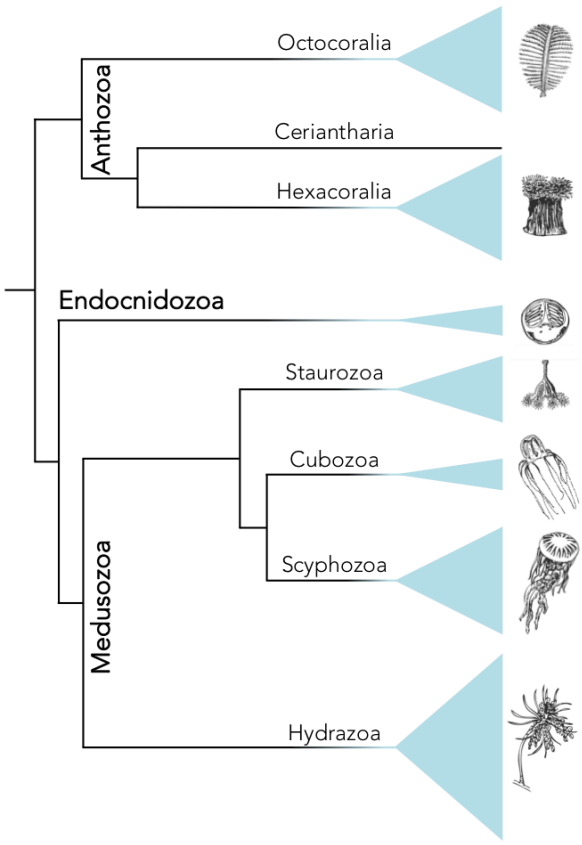

Figure 1 Cnidarian phylogeny
Three major clades of Cnidaria (Anthozoa, Endocnidozoa, and Medusozoa). Branch lengths are arbitrary. Adapted from (Kayal et al., 2018).

As cnidarians come in many different forms, cnidae are the only true unifying feature of the phylum. Most cnidarians are radially symmetric, but some species show biradial organization or are directionally asymmetric (C. W. Dunn, 2005). Additionally, while some cnidarians have three life stages – planula larvae, medusae, and polyps (i.e., Medusozoa), others only have two – planula larvae and polyps (i.e., Anthozoa) (Figure 3). The polyp form is also variable, as they can live solitarily or colonially, with or without an exoskeleton, with or without tentacles, or in benthic or pelagic zones (Daly et al., 2007). Regardless of the form, the biological innovations which arose in Cnidaria, such as cnidae, symbiosis with dinoflagellates, the plasticity of the life cycle, or coloniality, justify the remarkable ecological success of this phylum over the last 500 million years (Technau et al., 2012).

Just as the animals themselves are diverse, so are the mechanisms involved with reproduction. Cnidarians can reproduce both sexually and asexually and are either hermaphroditic (one animal producing both male and female gametes) or gonochoric (one animal produces one type

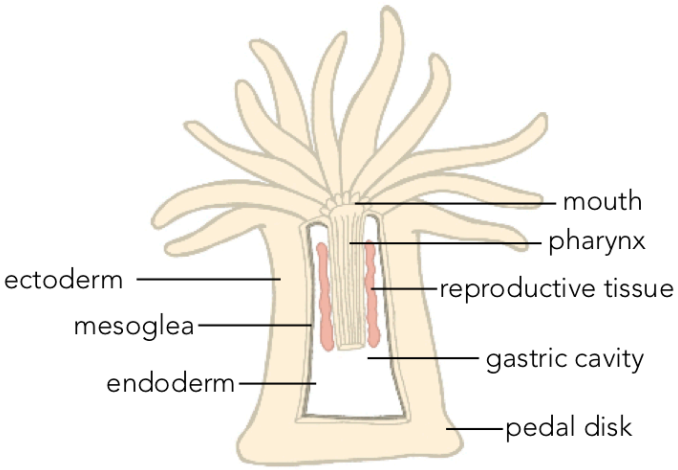

Figure 2 Cnidarian polyp anatomy
Simplified depiction of cnidarian polyp anatomy. Symbionts reside in the endodermal tissue and cnidae are found in the ectodermal tissue. Adapted from Hans Hillewaert.

of gamete, i.e., separate sexes) (Gleason & Hofmann, 2011). Transverse or longitudinal fission, budding, cyst formation, and tissue detachment have all been described to contribute to asexual reproduction in Cnidaria (Bocharova & Kozevich, 2011; Geller et al., 2005; Gleason & Hofmann, 2011). Asexual reproduction supports the growth and maintenance of colonies and can form new clonal populations (Fautin, 2002). Sexual reproduction methods vary depending on species, but one of the most impressive and best-known cnidarian sexual reproduction modes is that of mass spawning, e.g., by some reef-building corals. Mass spawning entails the highly synchronized release of gametes, deemed broadcast spawning, where external fertilization gives rise to aposymbiotic planula larvae. Typically, these events occur annually and involve the orchestration of all colonies from multiple species at a single location on the same day. Seasonality, temperature, and light cues all contribute to triggering this phenomenon (Keith et al., 2016; Mercier & Hamel, 2010). Fertilization may also occur internally, where embryos develop inside the parent polyp and are subsequently released as planula larvae, deemed brooding. Approximately 90 % of planulae from brooding parents are symbiotic, indicating that vertical transmission of symbionts is dominant for this reproductive mode (Baird et al., 2009; Gleason & Hofmann, 2011). The importance and extent of sexual versus asexual reproduction depend on species and specific populations, but the diversity in reproduction processes ultimately reflects the plasticity and adaptability of these organisms (Harrison, 2011).

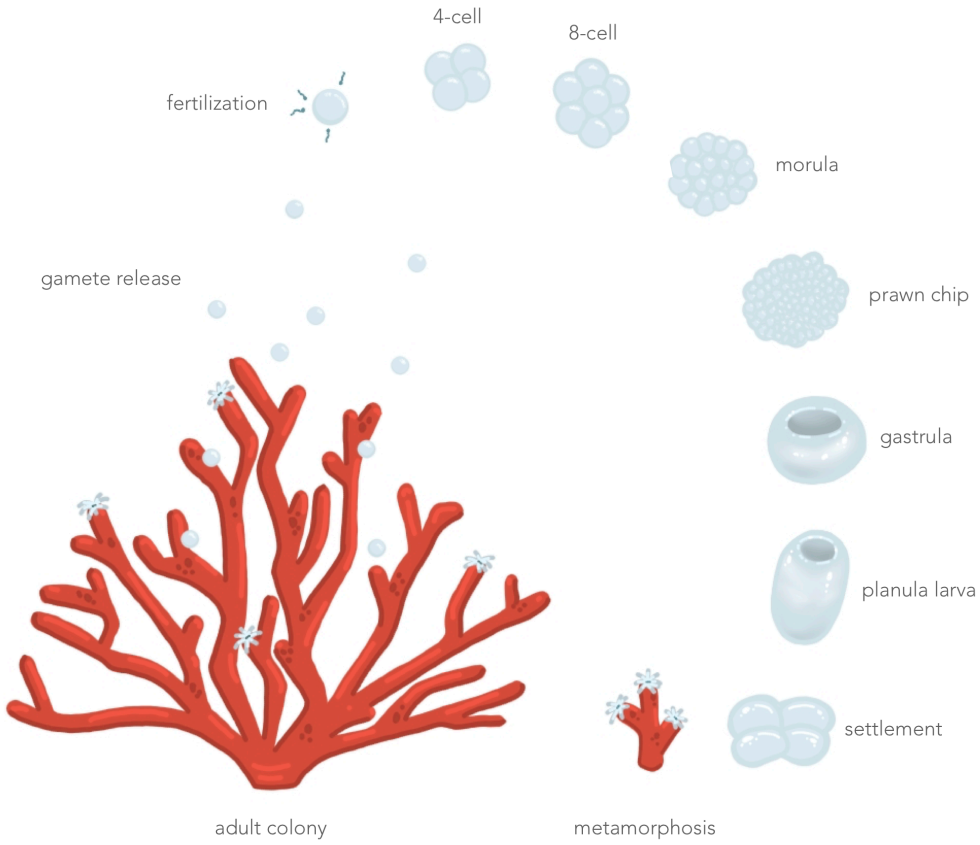

Figure 3 Sexual reproduction and life cycle of corals
Once a year, coral species synchronize the release of gametes. Depicted is an example of broadcast spawning, where a female coral release eggs into the sea water. External fertilization occurs and embryonic development follows. Approximately 48 hours post fertilization, a planula larva develops. At this stage, the organism is capable of establishing symbiosis. Once the larva finds a suitable location to settle, in combination with appropriate settlement cues, it will attach to the surface and eventually undergo metamorphosis.

1.2.2 Symbiodiniaceae

The intracellular symbionts that power coral reef ecosystems are unicellular eukaryotes from the family Symbiodiniaceae within the phylum Dinoflagellata. Dinoflagellata belongs to Alveolata, which includes ciliates, apicomplexans, and chromerids. Dinoflagellates are largely planktonic and found in all aquatic environments, but most commonly (87 %) inhabit marine waters. They represent one of the most abundant and diverse groups of single-celled aquatic eukaryotes, with an estimated 4,500 species described, 2,000 of which are extant (de Vargas et al., 2015; Guiry, 2012; Taylor et al., 2008). Dinoflagellata comprises photosynthetic autotrophs,

heterotrophs, and mixotrophs, which combine photosynthesis with phagocytosis or myzocytosis (Stoecker, 1999). Some heterotrophic and mixotrophic dinoflagellates (approximately 7 %) are parasites of both vertebrates and invertebrates, as well as other dinoflagellates (Coats, 1999). Only roughly 1 % of dinoflagellates are mutualistically symbiotic (Gomez, 2012).

Of the mutualistically symbiotic dinoflagellates, Symbiodiniaceae constitutes the largest group. These photosynthetic unicellular eukaryotes form symbioses with a multitude of hosts, including flatworms, mollusks, foraminifera, sponges, sea anemones, jellyfish, and corals (Burghardt et al., 2008; Coffroth et al., 2006; Douglas, 1995; Fay et al., 2009; Fitt & Trench, 1983; Rumpho et al., 2011). The systematics of Symbiodiniaceae was recently revised, with the former genus *Symbiodinium* now split into seven distinct genera: *Symbiodinium* (Clade A), *Breviolum* (Clade B), *Cladocopium* (clade C), *Durusdinium* (Clade D), *Effrenium* (Clade E), *Fugacium* (Clade F-Fr5), and *Gerakladium* (Clade G). Apart from *Effrenium* and *Gerakladium*, specific species belonging to all the other genera can engage in symbiosis with cnidarians (LaJeunesse et al., 2018).

Symbiodinaceae cells alternate between a coccoid stage (non-motile) and a smaller mastigote stage (motile and can undergo division), typically have golden brown pigmentation, and have mean cell sizes ranging from 6 μm (Clade B) to 12 μm (Clade E). Additionally, members of Symbiodinaceae share several features, including a pyrenoid (site of carbon fixation), ability to form endosymbioses, modified cell division *in hospite* (replication in coccoid stage), and seven amphiesmal vesicles (alveolar cell covering unique to Alveolata) in the mastigote stage (LaJeunesse et al., 2018)

1.3 Symbiosis establishment

The pairings between cnidarian host and dinoflagellate symbiont are intimate and specific. These relationships are not only stable during the lifetime of an individual host but also transcend generations over time – a fact that is even more astonishing when considering (1) the vast abundance and diversity of microorganisms present at the time of symbiosis establishment and (2) that the majority of symbiotic cnidarians give rise to aposymbiotic offspring. While the host organism is faced with the difficult task of seeking out the scarce symbiont from a plethora of other microbes, it is rare to find either partner without the other due to the obligatory nature of the relationship. Therefore, mechanisms must exist to guarantee symbiosis is established

(Nyholm & McFall-Ngai, 2004). A series of winnowing steps have been proposed to precede symbiont maintenance, with each step conferring a greater degree of specificity between partners. Symbiosis establishment can be broken down into three phases: (1) recognition and uptake, (2) symbiont selection, and (3) immune evasion/maintenance. Each phase relies on specific features exhibited by the interacting partners at the appropriate time (Davy et al., 2012).

1.3.1 Recognition and uptake

Recognition describes the initial molecular signaling between host and symbiont. To date, multiple mechanisms have been proposed to influence specificity and recognition. The beacon hypothesis explicates long-distance attraction, which was shown to be mediated, in part, by the endogenous GFP-related green fluorescence of some coral species, where green fluorescence attracted motile Symbiodiniaceae cells (Aihara et al., 2019; Hollingsworth et al., 2005). Larger proteins have been proposed to mediate initial recognition events in the local environment – specifically, the interaction between host pattern recognition receptors (PRRs) and microbe-associated molecular patterns (MAMPs). The lectin-glycan interaction is a well-known example of a PRR-MAMP interaction that has been heavily investigated in cnidarian-dinoflagellate symbioses. The surfaces of different Symbiodiniaceae cells have been shown to exhibit different glycan profiles, suggesting the unique surface makeup of symbionts could promote recognition via PRRs (Wood-Charlson et al., 2006). Additionally, some lectins were isolated from the seawater within which coral larvae were reared, further implicating lectin-glycan interactions in recognition (R. Takeuchi et al., 2021). However, infection is not always impaired when surface glycans of different symbiont strains are masked, indicating that lectin-glycan interactions are not the only gatekeeper for recognition (Parkinson et al., 2018).

Complement proteins have also been implicated in symbiosis establishment, specifically during the onset of symbiosis (Poole et al., 2016). In a process known as opsonization, complement proteins, known as opsonins, are secreted by the host and bind MAMPs. Once the opsonins are bound to the microbe, they are recognized by specific complement receptors on the host cell surface, initiating phagocytosis (Dunkelberger & Song, 2010). In one coral species, *Acropora millepora*, the complement protein, C3, was localized around symbionts and found in the epithelium, possibly in preparation for mounting an immune response or managing the microbiome (Kvennefors et al., 2010). Additional complement proteins have been characterized in cnidarians; however, their exact role in symbiosis is unclear as some studies

report their importance for symbiont uptake, while others report their reduced expression in the symbiotic state for immunosuppression (Poole et al., 2016; Shinzato et al., 2011).

Host scavenger receptors (SR) were also identified in Cnidaria and shown to play a role in successful colonization with symbionts (Lin et al., 2000; Neubauer et al., 2017; Poole et al., 2016; Wood-Charlson et al., 2006). Scavenger receptors are transmembrane glycoproteins that bind a wide array of microbial ligands, initiating phagocytosis (Rosenstiel et al., 2009). When comparing symbiotic with non-symbiotic host organisms, there appeared to be an upregulation of SRs in the symbiotic state (Lehnert et al., 2014; Rodriguez-Lanetty et al., 2006).

All of these recognition processes ultimately culminate in phagocytosis. And while it is known that symbionts are acquired by phagocytosis (Schwarz, 2008), there is no clear consensus on whether or not phagocytosis of symbionts occurs selectively. Ultimately, many factors have been described to contribute to symbiont recognition and phagocytosis; thus, it appears that no singular mechanism is responsible for this first step.

1.3.2 Symbiont selection

Symbiont selection relies on specificity between partners. Specificity is defined as the taxonomic range between symbiotic partners (Mandel, 2010; Moran, n.d.). Only compatible symbionts strains are suitable to be retained intracellularly, and those microalgae deemed incompatible will either be digested or expelled (S. R. Dunn & Weis, 2009). Specificity is likely determined by the long coevolution of partners, as cnidarian hosts have distinct preferences for specific Symbiodiniaceae species irrespective of the abundance of the preferential strain in the local environment. These specificities may have arisen as certain Symbiodiniaceae strains are thought to confer fitness benefits to their respective hosts compared to less compatible strains (Coffroth et al., 2006; Lajeunesse et al., 2004; LaJeunesse et al., 2018). In general, however, it appears that flexibility is more common than strict specificity, as hosts are known to harbor multiple strains simultaneously or can switch between dominant strains under stress conditions (Baker, 2003; Lesser et al., 2013). Furthermore, the developmental stage influences specificity as planula larvae are thought to be more promiscuous with partner selection than adult polyps (Cumbo, Baird, & van Oppen, 2013).

1.3.3 Immune evasion and maintenance

In general, parallels are often drawn between mutualistic and parasitic symbioses, and due to their implications for human health, a wealth of knowledge exists surrounding the immune evasion strategies employed by intracellular pathogenic microbes. Phagocytosis, involving the uptake of particles > 0.5 μm, is essential for immunity. In vertebrates, specialized cells, i.e., professional phagocytes, are dedicated to using phagocytosis for the ingestion and elimination of pathogens (Uribe-Querol & Rosales, 2020). Following recognition (see section 1.3.1), the pathogen will be engulfed and retained in a distinctive organelle, the phagosome. The phagosome will then go through a series of maturation steps resulting in fusion with lysosomes to create the phagolysosome, culminating in the degradation of the phagocytosed material (Figure 4) (Huynh et al., 2007; Jaumouillé & Grinstein, 2016; Rosales & Uribe-Querol, 2017). While some pathogens can escape from the phagosome (e.g., *Trypanosoma cruzi* and *Listeria monocytogenes)* or tolerate the phagolysosome (e.g., *Coxiella burnetii* and *Leishmania mexicana*), others actively alter phagosome maturation to avoid degradation and persist.

Different pathogens have evolved diverse approaches to evade this canonical process. For example, *Legionella pneumophila* interferes with lipid and protein sorting; *Salmonella enterica, Leishmania donovani*, and *Mycobacterium tuberculos*is impede vesicular trafficking; *M. tuberculosis* blocks lysosomal fusion machinery and maintains the early endosomal marker, Ras-related protein 5 (Rab5); and *L. donovani* inhibits fusion of vesicles with the phagosome (Flannagan et al., 2009; Méresse et al., 1999; Sacks & Sher, 2002). The prevailing belief in the field is that the symbiont resides in an arrested phagosome due to the presumed presence of the early endosomal marker, Rab5, and absence of the late endosomal marker, Rab7, along with transcriptomic data (Chen et al., 2003, 2004; Mohamed et al., 2016). However, vesicular trafficking is a dynamic process, and the use of one marker alone or analysis at one time point is not sufficient to classify the maturation state of an intracellular vesicle.

To ensure successful infection, some pathogens are known to interfere with cytokine signaling, and to this end, cytokine signaling has also been investigated in the cnidarian-dinoflagellate symbiosis. Transforming growth factor beta (TGF-β) is a cytokine, a small protein important for cell signaling, belonging to the transforming growth factor superfamily. Upon binding of

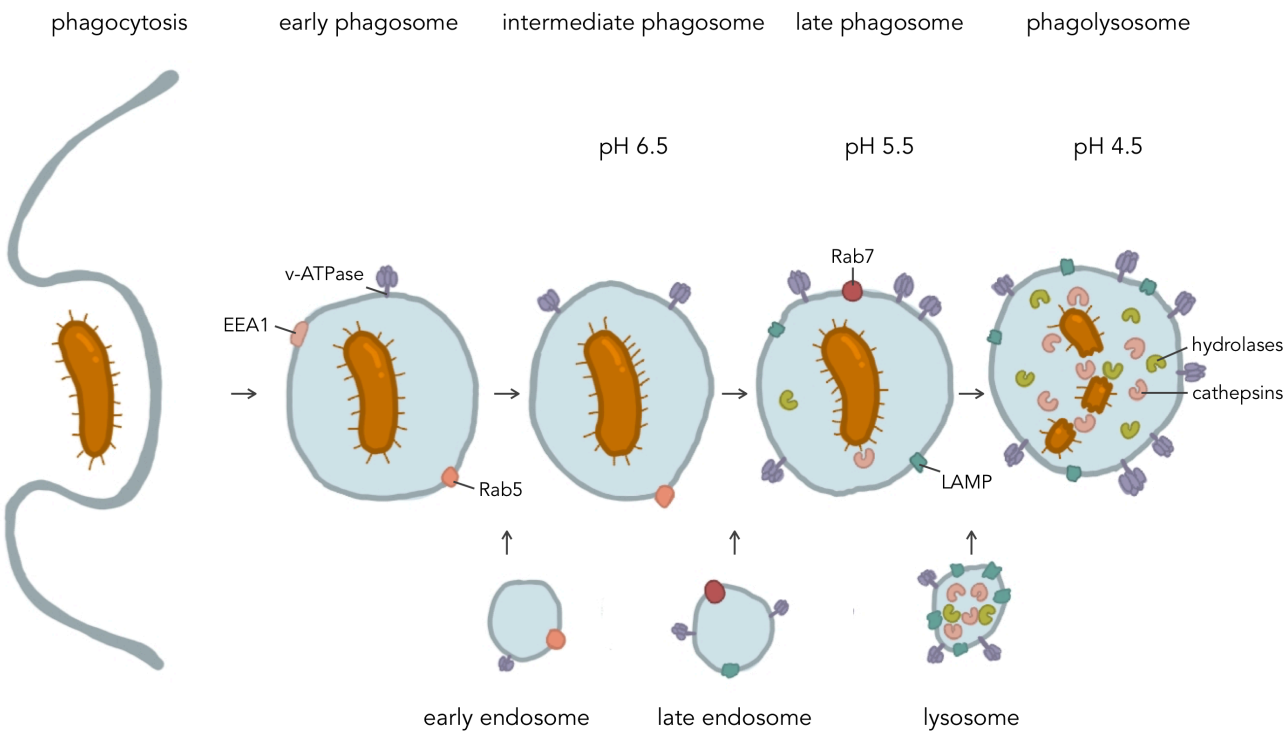

Figure 4 Phagosome maturation

Phagocytosis begins with the engulfment of particles (>0.5 µm). The newly formed phagosome, a plasma-membrane derived vacuole, will undergo a series of fusion and fission events with the endocytic pathway, and the pH of the phagosome progressively decreases due to the activity of the v-ATPase. This maturation process can be simplified into four stages: (1) Early: the phagosome membrane differs from the plasma membrane in that it is depleted of PtdIns(4,5)P2 and actin (Rab5, EEA1). (2) Intermediate: phagosomes still exhibit molecular markers of early endosomes but are in a transitional state (Rab5) (Lumen pH ~6.5). (3) Late: phagosomes lose early endosomal markers and acquire late endosomal markers (Rab7, hydrolases) (Lumen pH ~5.5). (4) Phagolysosome: phagosomes fuses with lysosomes (LAMP1/2, hydrolases, cathepsins), highly acidic and hydrolase-rich organelles that degrade the contents (Lumen pH ~4.5). Adapted from (Rosales & Uribe-Querol, 2017)

TGF-β to TGF-β receptors, a series of phosphorylation steps ensue, activating a signaling cascade that can induce transcription of genes important for cell proliferation, differentiation, tissue homeostasis, or immunity (Massagué, 2012). Depending on concentration and environment, TGF-β can be considered an anti-inflammatory cytokine, and *Plasmodium spp.* and *T. cruzi* are examples of pathogens that take advantage of TGF-β's immunosuppressive quality (Fadok et al., 1998; Ndungu et al., 2005; Waghabi et al., 2005; Wahl, 1994). *Plasmodium spp.* and *T. cruzi* possess TGF-β-activating molecules that can alter the outcome of infection (Ndungu et al., 2005; Waghabi et al., 2005). However, in *Fungia scutaria* coral larvae, interference with the TGF-β pathway impaired symbiosis establishment due to increased

nitric oxide secretion (Berthelier et al., 2017). These conflicting roles of TGF-β in managing pathogenic and mutualistic symbioses make it challenging to determine the precise role of this cytokine in symbiosis establishment as it is context-dependent.

Another pathway that some pathogens alter to promote survival is the toll-like receptor (TLR) pathway, specifically by modulating nuclear factor kappa B (NF-κB) activity. The intracellular parasite *Toxoplasma gondii,* for example, activates NF-κB to support the survival of their host cells. *T. gondii* uses a parasite-derived inhibitor of nuclear factor kappa B (IκB) kinase (IKK) to phosphorylate and subsequently ubiquitinylate the inhibitory IκB protein, which exposes the nuclear localization sequence (NLS) sequence of NF-κB. The released NF-κB dimers are then free to translocate to the nucleus, bind DNA, and activate transcription (Molestina & Sinai, 2005b, 2005a). The NF-κB pathway is 'target-rich' in terms of the possibilities for pathogenic and symbiotic microorganisms to efficaciously colonize host organisms. Activation of NF-κB is only one possibility to encourage survival. Depending on the status of the host cell, various pathogens can either activate or inhibit NF-κB signaling (Kawai & Akira, 2007; Rahman & McFadden, 2011). In symbiotic cnidarians, the role of NF-κB during symbiosis establishment and bleaching has been investigated. Organism-wide downregulation of NF-κB mRNA and protein was reported when aposymbiotic anemone larvae were infected with symbionts (Mansfield et al., 2017; Wolfowicz et al., 2016). When bleaching occurred, NF-κB mRNA and protein levels increased in anemones and NF-κB mRNA increased in the coral *Acropora palmata* (Desalvo et al., 2010; Mansfield et al., 2017). Modulation of the innate immune response can be an effective means of persistence for both symbionts and pathogens. However, signal transduction is highly complex, and the outcome of modulation is situational.

1.4 Aiptasia as a model to study symbiosis

The limited understanding surrounding symbiont recognition, selection, and maintenance in the coral-dinoflagellate symbiosis is largely a consequence of working with corals. Natural populations of corals are often threatened or endangered, and therefore the collection of specimens is challenging. Furthermore, the annual spawning of corals limits accessibility to planula larvae as well. Corals are less than ideal to maintain in the laboratory, as they tend to grow slowly, have calcareous exoskeletons that make physical manipulations difficult, and exhibit long generation times. The small sea anemone *Exaiptasia diaphana* (previously *E. pallida*; commonly, Aiptasia) is a tractable model system frequently used to investigate

symbiosis establishment at the cellular level (Baumgarten et al., 2015; Bucher et al., 2016; Davy et al., 2012; Hambleton et al., 2014; Weis et al., 2008; Wolfowicz et al., 2016).

Aiptasia (Actiniaria) is closely related to stony corals (Scleractinia) as both are members of Hexacorallia within Anthozoa (Figure 1). Corals and anemones share the same habitats and form symbioses with the same dinoflagellate symbionts from Symbiodiniaceae (Wolfowicz et al., 2016). It has been proposed that the symbiosis itself originated in their common ancestor; thus, much of the molecular and cellular machinery governing symbiosis is likely shared between Aiptasia and corals (Kayal et al., 2018). Dissimilar to corals, Aiptasia and other anemones live as solitary polyps and do not build calcareous exoskeletons. Furthermore, Aiptasia is easily maintained in the lab, amenable to experimentation, and adult anemones can be rendered aposymbiotic and maintained in the aposymbiotic state for indefinite periods of time when nutrition is supported heterotrophically (Matthews et al., 2016). Analogous to most coral species, Aiptasia gives rise to aposymbiotic offspring, and reliable protocols have been established to induce spawning with a blue light cue, yielding large quantities of larvae each week (Grawunder et al., 2015). Aiptasia larvae are small, transparent, and abundant, making cell biological and microscopic analyses straightforward. But beyond their ease of use, they represent the ideal system to assess the role of the innate immune response during symbiont selection because the planula larval stage is likely the natural period within the life cycle that the organism would encounter symbionts from the environment and establish symbiosis for the first time (Figure 5).

Aiptasia polyps are gonochoric and sexually reproduce by broadcast spawning. Embryonic development lasts approximately 48 hours, from fertilized egg to a planula larva capable of phagocytosing symbionts from the environment (Bucher et al., 2016). Larvae remain competent to establish symbiosis up to 14 days post fertilization (dpf); however, they can survive up to 10 weeks. To date, settlement and metamorphosis of Aiptasia larvae have not been observed under laboratory conditions. Aiptasia also undergoes asexual reproduction by pedal disc laceration, which lends itself to easily generating genetically identical lines and culture maintenance (Figure 5).

Many resources and biological tools have been developed for Aiptasia, including many traditional techniques (Bucher et al., 2016; Hambleton et al., 2014, 2019; Wolfowicz et al., 2016). Proteomic analyses are also on the rise (Medrano et al., 2019; Oakley et al., 2016), the

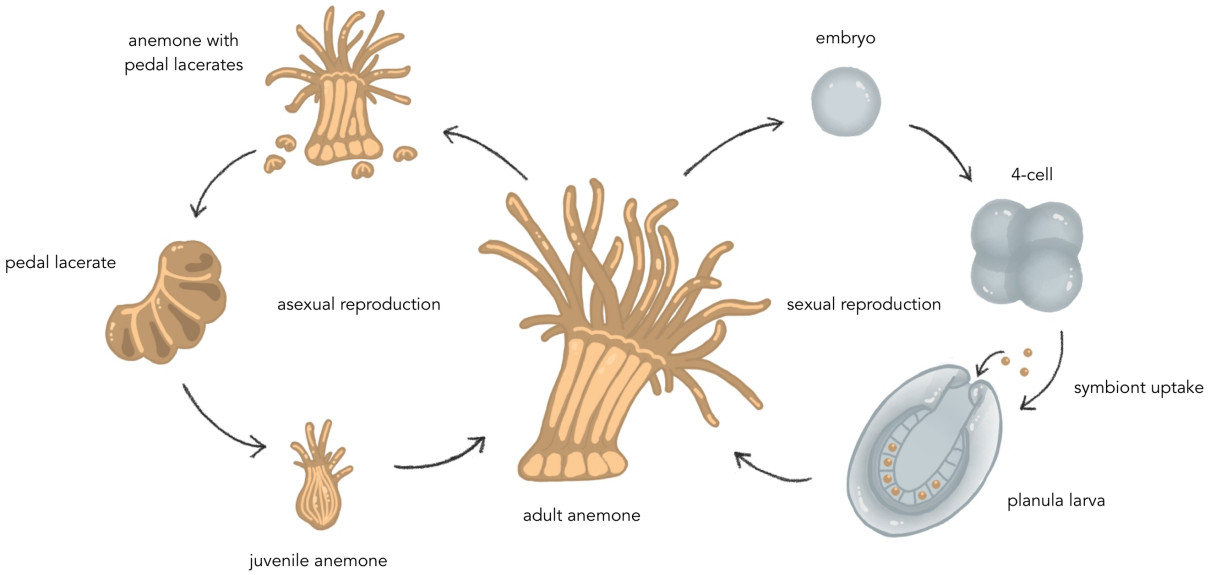

Figure 5 Aiptasia life cycle
Aiptasia undergo both sexual and asexual reproduction. Asexual reproduction occurs by pedal laceration (left) and sexual reproduction by broadcast spawning (right). Aiptasia larvae are naturally aposymbiotic, with symbiont acquisition by endodermal cells depicted. The transition from planula larva to adult anemone is currently not possible under laboratory conditions. Adapted from (Grawunder et al., 2015).

Aiptasia genome has been published, and a multitude of transcriptomic analyses have already been performed (Baumgarten et al., 2015; Lehnert et al., 2014; Matthews et al., 2017; Wolfowicz et al., 2016). Moreover, genetic manipulation of Aiptasia has been demonstrated (Bucher et al., 2017), and with the advent of simple gain and loss of function experiments on the horizon, we will have a better understanding of the molecular mechanisms facilitating symbiosis.

1.5 Aims

The overarching aim of this thesis is to better understand the cellular and molecular mechanisms dictating cnidarian-dinoflagellate symbioses, with the hope of providing valuable contributions to the comprehension of symbioses in general. Specifically, I have been fascinated and bewildered by the ability of two organisms to live and rely on each other so intimately, to the point where alterations to cellular and molecular processes evolved to facilitate the interaction. This symbiosis is central to sustaining biodiversity in reef ecosystems, yet we still have a fundamental lack of knowledge surrounding how symbionts are able to live within the

constraints of the immune system and how host organisms manage symbiotic interactions while excluding non-beneficial interactions.

This thesis builds upon previous work regarding cellular and molecular mechanisms pertaining to cnidarian immunity, symbiont selection and maintenance, and symbiotic interactions in general, although largely concerning host-pathogen interactions. We have taken a comparative approach using the model system Aiptasia. With this comparative system, we have combined microscopy, exogenous immune perturbations, transcriptomic analysis, and cell biology techniques to address the following specific aims:

The first aim set out to characterize host response to symbionts and non-symbiotic microalgae. I hypothesized that all microalgae would be taken up into endodermal cells, but only symbionts would be maintained, while the non-symbiotic microalgae would be lost, possibly by phagolysosomal degradation.

The second aim was to determine how symbionts are selectively maintained while non-symbiotic microalgae are not. I hypothesized that symbiont uptake would induce changes within the host at the cellular level, specifically by inhibiting the immune response.

The third aim was to determine how suppression of innate immunity contributes to symbiosis establishment and symbiont selection. I hypothesized that the immune suppression induced by symbiont-uptake would interfere with phagolysosomal degradation.

2 Results

2.1 Phagocytosis of microalgae is indiscriminate, but intracellular maintenance is specific

To understand the unique properties of the symbiosome and mechanisms allowing for intracellular maintenance of dinoflagellate symbionts, we established a comparative framework to analyze similarities and differences between host response to compatible symbionts (able to establish symbiosis) and incompatible particles (fail to establish symbiosis). The naturally aposymbiotic larvae of Aiptasia are capable of phagocytosing symbionts at 2 days post-fertilization (dpf) – once embryonic development is complete and the opening to the gastric cavity has formed (Bucher et al., 2016) – lending themselves to a simplistic yet powerful model to study the early stages of symbiosis establishment (Hambleton et al., 2014; Wolfowicz et al., 2016).

Breviolum minutum (previously *Symbiodinium minutum,* strain SSB01) (LaJeunesse et al., 2018; Xiang et al., 2013), the dinoflagellate symbiont, is readily phagocytosed into the endodermal cells of both Aiptasia larvae and adult polyps. Symbionts are maintained intracellularly in the endodermal cells and eventually proliferate to populate the tissue (Bucher et al., 2016). For comparison to the symbiont, we selected microalgae that were not previously reported to live in direct association with corals or anemones. The lipid-rich *Microchloropsis gaditana* and *Nannochloropsis oculata* are important production species for the biotechnology industry (Budisa et al., 2019; X. N. Ma et al., 2016), which led us to postulate that they could potentially be candidates for intracellular digestion, used to support host nutrition – an interesting fate compared to the maintenance of symbionts. Additionally, we included the apicomplexan-related *Chromera velia* in our analysis. *C. velia* has been shown to infect cnidarians with a broad geographic distribution, yet unlike symbionts, this infection does not develop into a stable partnership (Figure 6) (Cumbo, Baird, Moore, et al., 2013; Mohamed et al., 2018). Performing a standard infection assay, we added the respective microalgae species to distinct batches of Aiptasia larvae. We found that all of the microalgae introduced were taken up into the endodermal cells, which we confirmed using confocal microscopy (Figure 7).

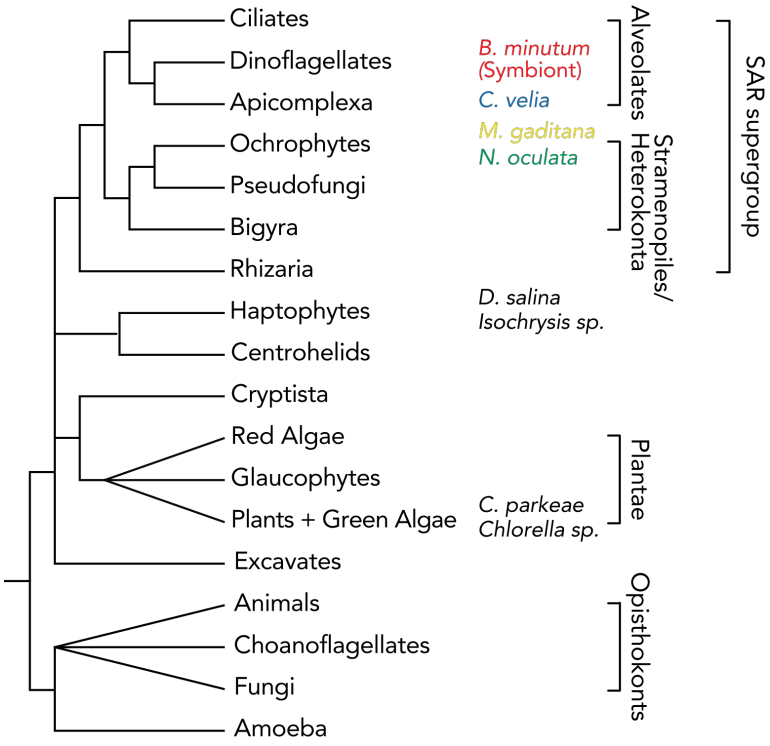

Figure 6 Diverse microalgae used to establish the comparative system

Phylogenetic relationship between microalgae used for the comparative analysis. Tree adapted from (Keeling & Burki, 2019). The stramenopiles, alveolates, and Rhizaria comprise the SAR supergroup, among which are the four microalgae used for the comparative analysis. Both members of Alveolata, *B. minutum* strain SSB01 (symbiont) belongs to the phylum Dinoflagellata, and *C. velia* belongs to the phylum Apicomplexa. *M. gaditana* and *N. oculata* both belong to the phylum Ochrophyta. We screened additional microalgae belonging to two phyla: *Dunaliella salina* and *Isochrysis species* (Haptophyta) and *Chlamydomonas parkeae* and *Chlorella species* (Chlorophyta) (data not included, published in (Jacobovitz et al., 2021), and additionally reported in my Master's thesis).

While symbionts are maintained, we next aimed to determine the residency time of the non-symbiotic microalgae. We infected aposymbiotic larvae for 24 hours with each of the microalgae species. Afterward, larvae were washed into fresh filtered artificial seawater (FASW), thereby removing any non-phagocytosed microalgae, and the infection was monitored over time (Figure 8a). We observed natural variation in the initial uptake of both symbiotic and non-symbiotic microalgae after 24 hours. The proportion of *M. gaditana*-infected larvae (85.2 %) was significantly higher than the proportion of *N. oculata*-infected larvae (35.7 %), while the proportion of symbiotic larvae (60.5 %) and *C. velia*-infected larvae (40.5 %) were between the two extremes.

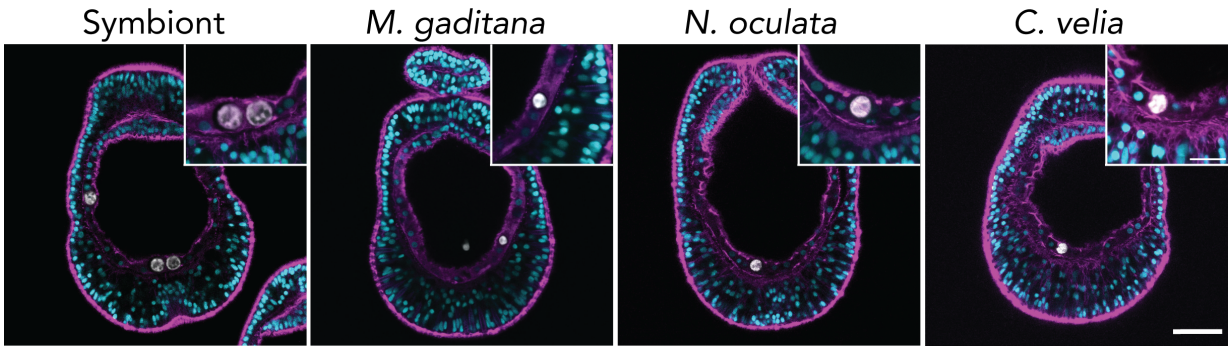

Figure 7 Indiscriminate uptake of microalgae by Aiptasia larvae
For the comparative analysis, we confirmed that all microalgae (symbionts, *M. gaditana*, *N. oculata,* and *C. velia*) were internalized into the endoderm of Aiptasia larvae. Microscopy images depict microalgae autofluorescence (white), Hoechst-stained nuclei (cyan), and phalloidin-stained F-actin (magenta). Scale bars represent 25 μm for whole larva and 10 μm for magnified inset (n=5, with a minimum of five larvae imaged per replicate).

Over time, the number of larvae containing symbionts remained relatively stable (67 % on average), whereas the number of larvae infected with non-symbiotic microalgae decreased (Figure 8b). The proportion of larvae infected with *N. oculata* decreased rapidly between 1 day and 2 days post-infection (dpi), from 35.7 % to 5.2 %, and remained below 5 % for the duration of the experiment. The proportion of *M. gaditana*-infected larvae also decreased rapidly after 1 dpi, from 85.2 % to 53 %. However, the subsequent reduction occurred steadily until 10 dpi: from 53 % to 34.1 % between 2 and 3 dpi, from 34.1 % to 15 % between 3 and 6 dpi, and from 15 % to 3.7 % between 6 and 10 dpi. The proportion of larvae infected with *C. velia* remained somewhat stable until 6 dpi (38 % on average), but between 6 and 10 dpi, there was a substantial reduction in the proportion of *C. velia*-infected larvae from 36.4 % to 10.4 % (Figure 8b).

Not only was the symbiont maintained during the 10-day observation period, but the number of symbionts per larva increased due to proliferation within the host (Figure 8c) (Hambleton et al., 2014). On average, between 1 and 10 dpi, there was an increase of 2.3 symbiont cells per larva. The mean number of non-symbiotic microalgae per larva decreased over time (Figure 8c). Based on these results, it appears that Aiptasia larvae readily phagocytose various microalgae from the environment – not only the symbiont. Thus, the post-phagocytic sorting of microalgae is an important step for symbiont selection. Furthermore, the loss of non-symbiotic microalgae is not uniform across the various species we examined; therefore, it appears that host response differs according to the internalized microorganism.

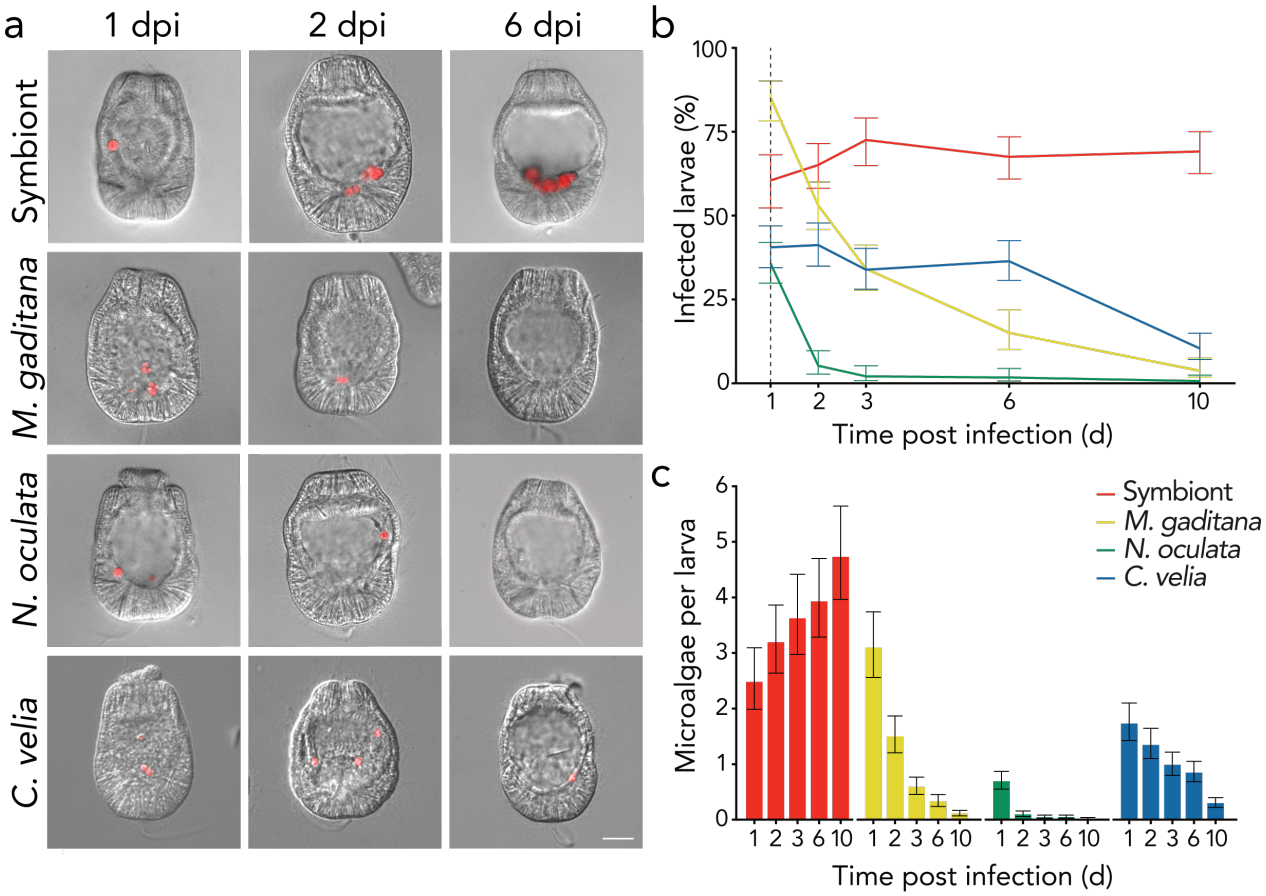

Figure 8 Establishment of a comparative system to investigate symbiont maintenance
a, At 4-6 dpf, Aiptasia larvae were infected with symbionts, *M. gaditana*, *N. oculata,* or *C. velia* for 24 hours, then washed into fresh FASW. Samples were fixed at 1, 2, and 6 dpi. Representative images of infection with merge DIC in grey and autofluorescence of microalgae photosynthetic pigments in red are shown. Scale bar represents 25 µm. **b,** After 24-hour infection with the respective microalgae, larvae were washed into fresh FASW (indicated by the dashed line at 1 dpi), and samples were taken at 1, 2, 3, 6, and 10 dpi. The percentage of infected larvae was then quantified. Error bars specify means ± 95% confidence intervals from five independent replicates. **c,** The average number of microalgae per larva was quantified after 24-hour infection from b. Error bars specify means ± 95% confidence intervals for five biological replicates with approximately 50 larvae per replicate. *C. velia* DIC images and *C. velia* infection data collected by Sebastian Rupp.

2.2 Healthy non-symbiotic microalgae are lost more rapidly than heat-killed microalgae

Due to the variation in the host clearance response to non-symbiotic microalgae, we next aimed to assess if the viability of the distinct microorganisms influenced their loss over time. To this end, we performed our standard infection assay as previously described with the addition of heat-killed microalgae. We then quantified the infections at 1, 2, and 3 dpi. As expected for the

symbiont control, the proportion of larvae infected with healthy symbionts remained stable over time. Over the 3 days, on average, 79 % of larvae were symbiotic (Figure 9a, Supplementary Figure 1), which further illustrated the natural variability in infection efficiency, even with the symbiont (compared to the average 67 % symbiotic larvae described above (Figure 8b)). In contrast, the proportion of larvae infected with heat-killed symbionts was only 31 % at 1 dpi, indicating that the viability status of the symbiont influences phagocytosis. We did not observe a reduction of heat-killed symbiont-infected larvae over the 3 days, on average, where only 30 % of larvae were infected.

Between 1 and 2 dpi, there was a considerable reduction in the proportion of larvae infected with healthy non-symbiotic microalgae compared with heat-killed non-symbiotic microalgae. For *M. gaditana*-infected larvae, the proportion of infected larvae decreased by 55.6 % for the control and 34.7 % for heat-killed. For *N. oculata*-infected larvae, the proportion of infected larvae decreased by 51.4 % for the control and by only 18.2 % for heat-killed. Although the

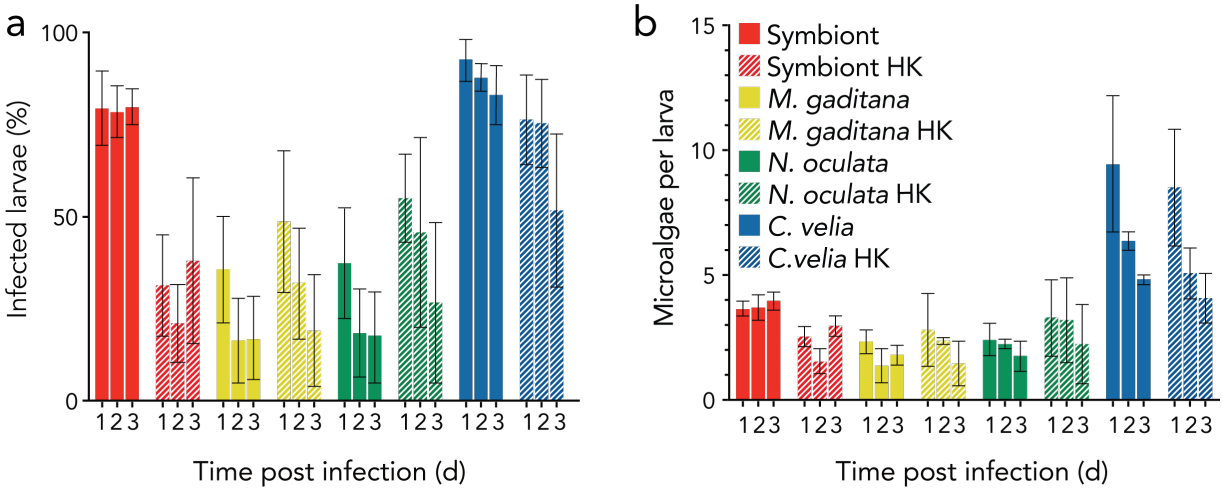

Figure 9 Investigations of microalgae viability on infection efficiency in Aiptasia larvae
a, At 4-6 dpf, Aiptasia larvae were infected with either healthy or heat-killed (HK) symbiont, M. gaditana, N. oculata, or C. velia for 24 hours, then washed into fresh FASW. Samples were fixed at 1, 2, and 3 dpi. The percentage of infected larvae was then quantified. Error bars represent SEM from three independent, biological replicates with 30 infected larvae per replicate. **b,** The average number of microalgae per larva was quantified after 24-hour infection from a. Error bars represent SEM from three independent, biological replicates with 30 infected larvae per replicate. Statistics are based on an ordinary two-way ANOVA, p-values adjusted using the Dunnets method. Data partially acquired by Viola Kühnel.

reduction was less drastic between 1 and 2 dpi for *C. velia*-infected larvae, there was still a larger reduction in the proportion of larvae infected with healthy *C. velia* compared with heat-killed, 5.4 % and 1.3 %, respectively.

Between 2 and 3 dpi, there was little to no change in the proportion of larvae infected with healthy non-symbiotic microalgae, whereas we observed a further reduction in the proportion of larvae infected with heat-killed non-symbiotic microalgae. Between 2 to 3 dpi, the proportion of heat-killed *M. gaditana*-infected larvae decreased by 40.6 %, heat-killed *N. oculata*-infected larvae decreased by 40 %, and heat-killed *C. velia*-infected larvae decreased by 32 % (Figure 9a). The mean number of heat-killed symbionts and healthy and heat-killed non-symbiotic microalgae per larva decreased over time (Figure 9b). Overall, it appears that the loss of healthy non-symbiotic microalgae occurs more rapidly than their heat-killed counterparts; therefore, the viability status of the microorganism influences both their uptake and intracellular residency time in Aiptasia larvae.

2.3 LAMP1 accumulates around healthy symbionts and heat-killed microalgae but not around healthy non-symbiotic microalgae

The uptake of symbionts occurs via phagocytosis (Schwarz et al., 1999). Typically, the phagosome formed post-phagocytosis will go through a series of maturation steps resulting in the phagosome fusing with lysosomes to create the phagolysosome, culminating in the degradation of the phagocytosed material (Huynh et al. 2007; Jaumouillé and Grinstein 2016; Rosales and Uribe-Querol 2017). Although symbionts are taken up by phagocytosis, it is known that the symbionts remain intracellular to allow bidirectional nutrient transfer between the partners (Muscatine 1990); however, the underlying mechanisms are unclear. We speculated that the loss of healthy and heat-killed non-symbiotic microalgae could result from lysosomal digestion, while healthy symbionts circumvent that fate. By utilizing lysosomal associate membrane protein 1 (LAMP1) as a marker for the lysosome, we sought to assess if the non-symbiotic-microalgae-containing-phagosomes are digestive. LAMP1 is highly glycosylated and plays an essential role in maintaining the integrity of the acidic and hydrolytic organelle (Wartosch, Bright, and Luzio 2015). We developed and optimized an Aiptasia-specific LAMP1 antibody to be used for our analyses (Figure 10).

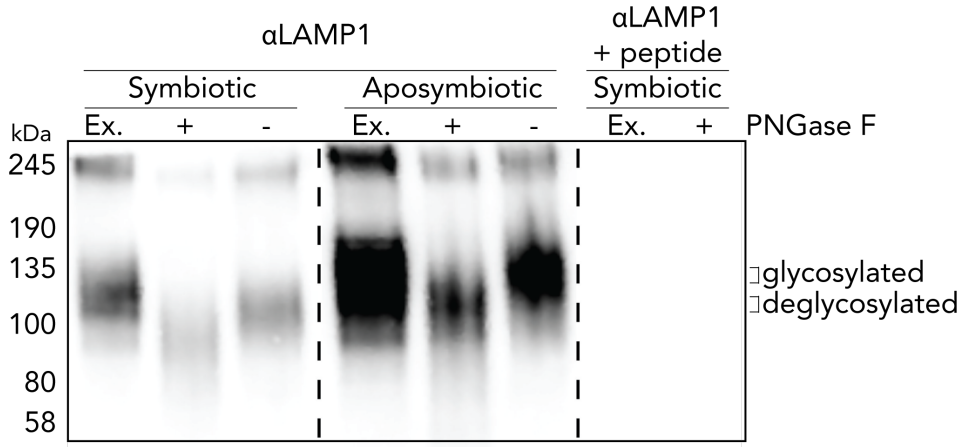

Figure 10 Establishment of Aiptasia-specific LAMP1 antibody

Verification by deglycosylation and western blot of the Aiptasia-specific LAMP1 antibody after purification. Although the predicted molecular weight of LAMP1 is 38 kDa, it contains many post-translational modifications (PTMs), namely glycosylation (Winchester, 2001). Homogenates of symbiotic and aposymbiotic adult Aiptasia CC7 were subjected to N-deglycosylation using PNGase F. A shift was observed, resulting in a band at a lower molecular weight than the control. Additionally, the LAMP1 antibody was blocked using the immunizing peptide to assess specificity.

Contrary to what we expected, healthy symbionts accumulated LAMP1 already at 6 hours post-infection (hpi), whereas the non-symbiotic microalgae did not (Figure 11a). This accumulation of LAMP1 around the symbiont persisted at 24 hpi. At both 6 and 24 hpi, *M. gaditana*- and *N. oculata*-containing phagosomes did not appear to accumulate LAMP1 in their direct vicinity; in fact, they seemed to be void of the protein altogether. However, upon closer inspection, it seemed as though there was space between the microalgae and the phagosome membrane. This space was never observed for symbiont-containing or *C. velia*-containing phagosomes. *C. velia*-containing phagosomes had only a slight accumulation of LAMP1 at 6 hpi but became weakly LAMP1 positive at 24 hpi (Figure 11a).

Conversely, all heat-killed microalgae, symbionts included, accumulated LAMP1 shortly after uptake and up to 24 hpi (Figure 11b). Although the autofluorescence of the microalgae was challenging to visualize after heat treatment, the phagosomes containing the heat-killed microalgae were delineated by LAMP1. We quantified these data by scoring the proportion of microalgae residing in LAMP1-positive, LAMP1-weak, or LAMP1-negative phagosomes at both 6 hpi (Figure 12a) and 24 hpi (Figure12b). There was little difference between healthy and

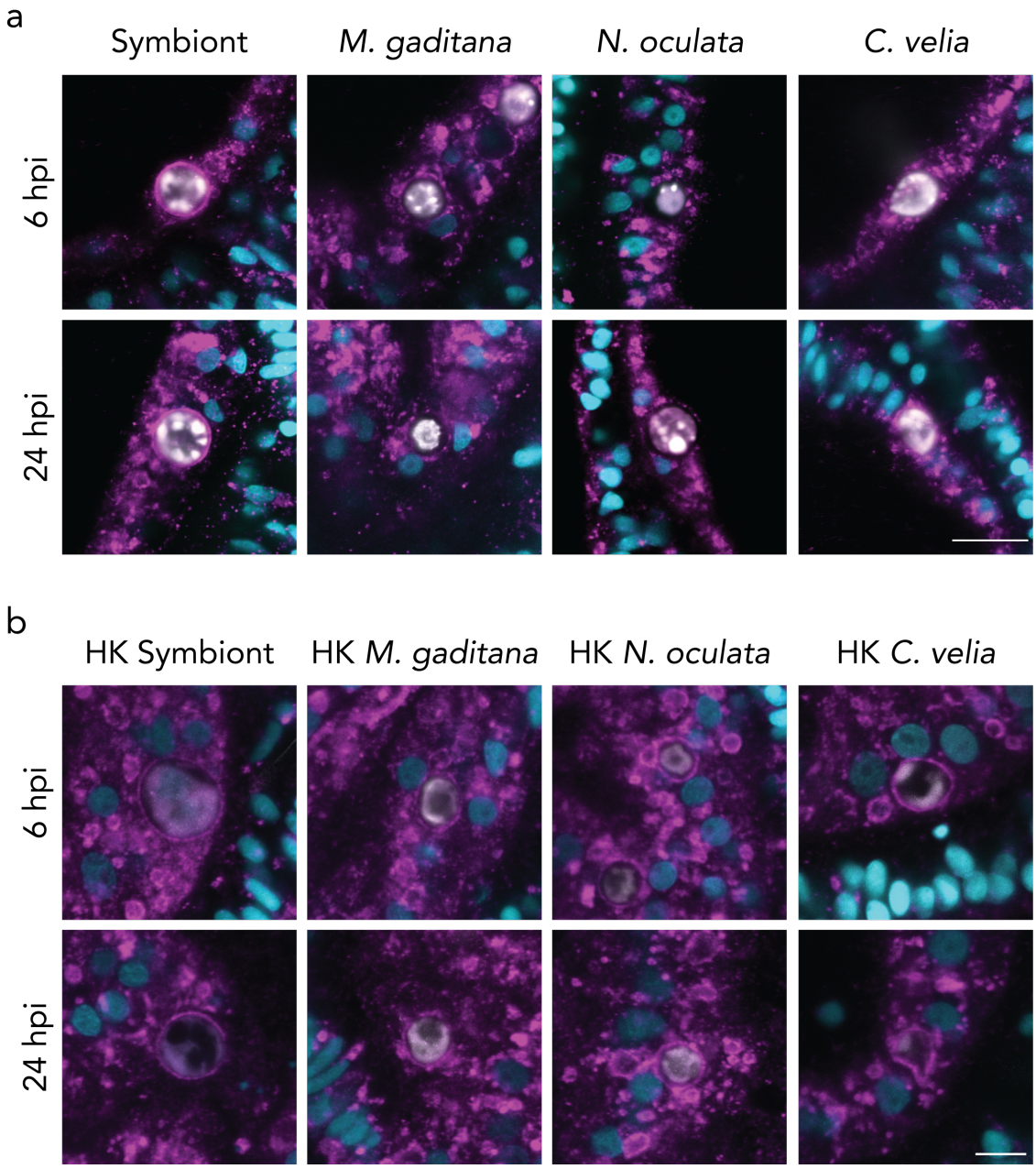

Figure 11 Distinct accumulation of LAMP1 around healthy symbionts and heat-killed non-symbiotic microalgae

a, LAMP1 was localized in Aiptasia larvae after 6- and 24-hour infection with healthy symbionts, *M. gaditana*, *N. oculata*, and *C. velia*. Only symbionts showed a strong accumulation of LAMP1 at both time points. *M. gaditana* and *N. oculata* appeared to have no or limited accumulation of LAMP1, and there appeared to be a gap between the microalgae and the phagosome. *C. velia* displayed intermediate LAMP1 accumulation. Images depict microalgae autofluorescence (white), Hoechst-stained nuclei (cyan), and LAMP1 (magenta). Scale bar represents 10 µm. (n=4, with 30 larvae per biological replicate). **b,** Additionally, LAMP1 was localized in Aiptasia larvae after 6- and 24-hour infection with heat-killed (HK) symbionts, *M. gaditana*, *N. oculata*, and *C. velia*. All HK microalgae accumulated LAMP1 to different degrees at both 6 and 24 hpi. Images depict microalgae autofluorescence (white), Hoechst-stained nuclei (cyan), and LAMP1 (magenta). Scale bar represents 10 µm. (n=4, with approximately 10 larvae per biological replicate).

heat-killed symbionts residing in LAMP1-positive symbiosomes (Figure 12a, b). At 6 hpi, 40.6 % of healthy *M. gaditana*-containing-phagosomes were void of LAMP1 altogether, whereas only 10 % of heat-killed *M. gaditana*-containing-phagosomes showed no accumulation of LAMP1. Interestingly, for heat-killed *M. gaditana*-containing-phagosomes, there was an increase in LAMP1-positive phagosomes from 32.8 % at 6 hpi to 53 % at 24 hpi. Similar to *M. gaditana* at 6 hpi, 37.5 % of healthy *N. oculata*-containing-phagosomes were LAMP1-negative, but only 5.3 % of heat-killed *N. oculata*-containing-phagosomes were LAMP1-negative. Furthermore, there was a 68 % increase in LAMP1-negative healthy *N. oculata*-containing-phagosomes between 6 and 24 hpi. For *C. velia*-containing phagosomes at 6 hpi, 67 % of healthy *C. velia*-containing phagosomes and 12 % of heat-killed *C. velia*-containing phagosomes were LAMP1-negative. At 24 hpi, for both healthy and heat-killed, there was an increase in LAMP1-positive and LAMP1-weak *C. velia*-containing phagosomes. There was

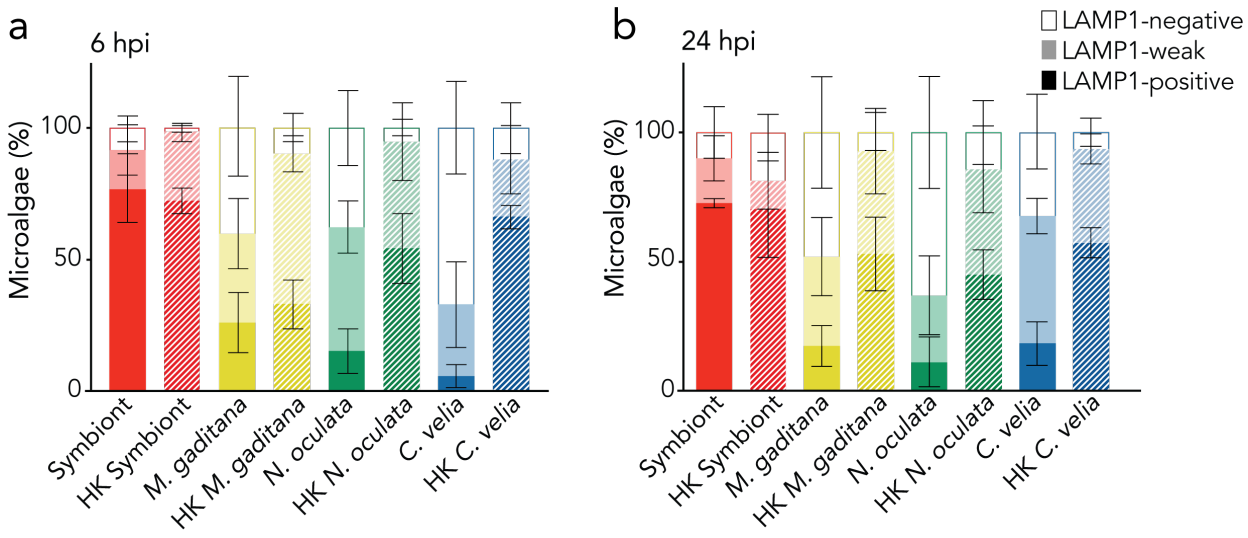

Figure 12 Increased LAMP1 accumulation around heat-killed non-symbiotic microalgae
LAMP1 accumulation was scored in Aiptasia larvae after 6- and 24-hour infection with healthy or heat-killed (HK) symbionts, *M. gaditana*, *N. oculata*, and *C. velia*. All HK microalgae accumulated LAMP1 to different degrees at both 6 and 24 hpi. LAMP1 accumulation was scored as either LAMP1-positive (solid), LAMP1-weak (50% opacity), LAMP1-negative (white). **a,** At 6 hpi, both healthy and HK symbionts accumulated LAMP1, where HK *M. gaditana, N. oculata,* and *C. velia* had more LAMP1-accumulation than the healthy controls. **b,** At 24 hpi, both healthy and HK symbionts accumulated LAMP1. As for 6 hpi, LAMP1 accumulated around HK *M. gaditana* and *N. oculata* more than the healthy controls. For HK *C. velia,* there was still more LAMP1-accumulation than the healthy control; however, the healthy *C. velia* accumulated more LAMP1 after 24 hpi compared to 6 hpi. Error bars represent SEM of four biological replicates, with approximately 10 larvae per replicate. Data partially acquired by Viola Kühnel.

103 % more LAMP1 accumulation at 24 hpi for healthy *C. velia*-containing phagosomes and 4.5 % more for heat-killed *C. velia*-containing phagosomes (Figure 12a, b).

Because healthy non-symbiotic microalgae do not accumulate LAMP1, their loss seems unlikely to result from intracellular digestion. However, the accumulation of LAMP1 around their heat-killed counterparts (together with the longer residency time between 1 and 2 dpi compared to the control (Figure 9a)) may indicate that the host cell is attempting to digest the dead particle. Our unexpected finding that LAMP1 heavily decorates the symbiosome shortly after uptake implicates a role for LAMP1 in niche formation and symbiosis establishment. Thus, it appears that the role of LAMP1 in dealing with both intracellular symbionts and non-symbiotic visitors is multi-faceted and complex.

2.4 Symbionts in culture can withstand low pH

If LAMP1-accumulation does indeed result from lysosomal fusion, then how are healthy symbionts able to withstand the harsh environment of this digestive organelle? One feature of the lysosome that makes this organelle particularly perilous is low pH, which is typically pH 4.5 (Mellman, 1986). Therefore, we investigated whether symbionts can tolerate such a low pH or not. For this, we grew symbiont cultures in growth media with varying degrees of acidity, ranging from pH 2.6 to pH 7.9, the latter of which represents a pH similar to seawater. We found little deviation between symbiont cultures grown at pH 7.9, pH 6.3, and pH 4.2 (Figure 13). Thus, it appears that symbionts can both survive and replicate as usual down to a lysosomal-like pH of 4.2. Interestingly, although the symbionts maintained at pH 2.6 did not grow as the cultures at higher pH, once they were transferred into new growth medium at pH 7.9 at 20 days, they resumed growth like normal (Figure 13), indicating that even at pH 2.6, the symbionts are able to survive for extended periods of time. It remains unclear if the LAMP1-positive symbiosome is derived from lysosomal fusion, and if so, if the organelle is hydrolytically active, however these data reveal that at least symbionts can tolerate lysosomal pH.

2.5 Non-symbiotic microalgae are cleared by expulsion

Due to the lack of evidence that non-symbiotic microalgae are digested, we still needed to determine how the non-symbiotic microalgae were lost (Figure 8b). Therefore, we chose to monitor their elimination directly by establishing live imaging. We performed our standard

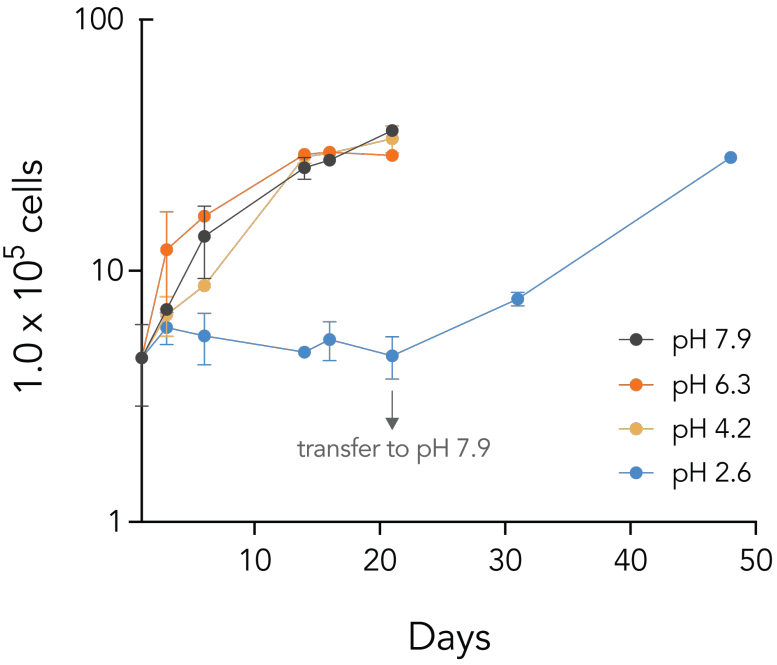

Figure 13 Symbionts in culture continue to grow at lysosomal-like pH
Symbionts were grown in IMK growth media with varying degrees of acidity (pH 7.9 (black), pH 6.3 (orange), pH 4.2 (yellow), and pH 2.6 (blue)). Cells were counted at 1, 3, 6, 14, 16, and 21 days. The cultures grown at pH 7.9, 6.3, and 4.2 grew relatively similar to each other. The culture at pH 2.6 showed no increase in cell number up to 21 days. At 21 days, symbionts grown at pH 2.6 were transferred into new growth medium at pH 7.9, and additional cell counts were made at 31 and 48 days. The culture recovered and continued to grow. Y-axis is log10-scaled. Error bars represent standard deviation. Data acquired by Sebastian Gornik.

infection assay by introducing the respective microalgae species for 24 hours. To further our comparative analysis, we also performed infections with fluorescent beads, comparable in size to symbionts, as a means of investigating host response to inert particles. The larvae were then embedded in low-gelling agarose (LGA) and z-stacks were acquired every 15 minutes for 48 hours. We differentiated between intracellular microalgae and microalgae that were non-phagocytosed in the gastric cavity by selecting larvae in which the movement of the microalga and the larva were synchronized. In the case of the symbiont, the vast majority of cells were retained during the imaging period. Additionally, we frequently observed the replication of symbionts within the larval host (11 replication events in 13 larvae) (Figure 14a). The retention and replication of symbionts under these live imaging conditions led us to believe that immobilization in LGA does not have a detrimental effect on either of the symbiotic partners.

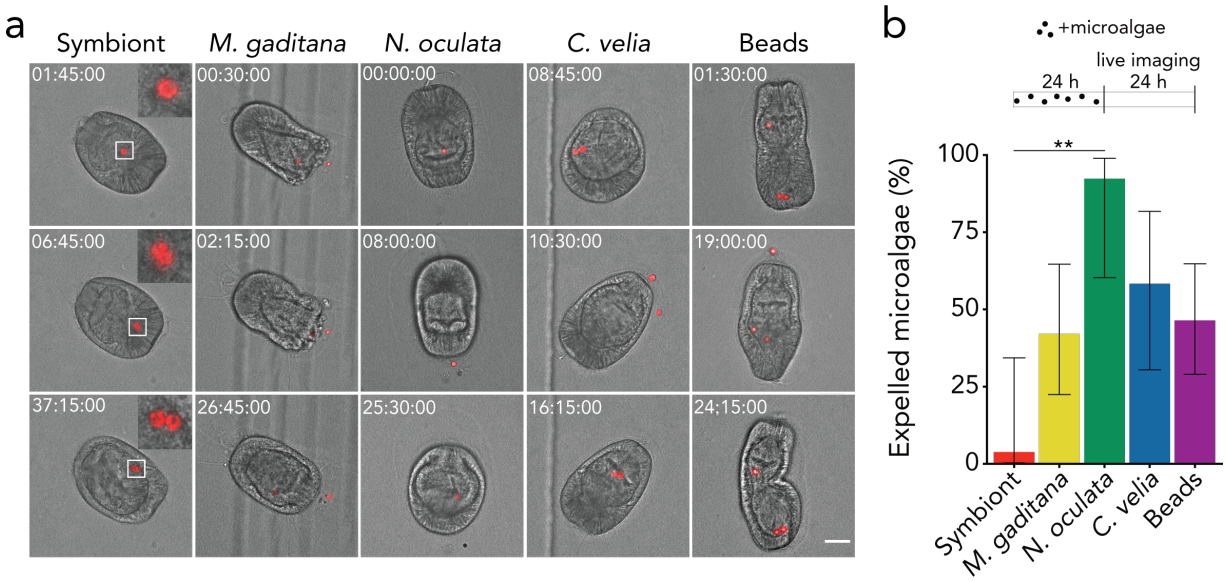

Figure 14 Non-symbiotic microalgae are expelled

Aiptasia larvae were live imaged after 24-hour infection with symbionts, *M. gaditana*, *N. oculata*, *C. velia,* or fluorescent beads. **a,** Symbionts were retained within the endoderm during the duration of imaging and even replicated. Non-symbiotic microalgae and beads were frequently expelled during the 48-hour live imaging session. Representative stills from imaging with corresponding time stamps coinciding with 24 hpi (hours, minutes, seconds), showing merge of DIC (grey) and autofluorescence of microalgae photosynthetic pigments or fluorescent beads (red). Scale bar represents 30 µm for whole larvae. Insets are threefold magnifications of the selected areas outlined by a white square. For related videos, see (Jacobovitz et al., 2021). **b,** After 24-hour infection, the expulsion of microalgae was quantified during a 24-hour live imaging session. The schematic above graph shows the addition of microalgae for 24 hours followed by 24-hour live imaging. 13 symbiotic larvae with a total of 27 symbionts, 7 *M. gaditana*-infected larvae with 19 *M. gaditana* cells, 7 *N. oculata*-infected larvae with 13 *N. oculata*-cells, 8 *C. velia*-infected larvae with 12 *C. velia* cells, and 11 bead-infected larvae with 28 beads were imaged. There was significantly more expulsion of cells from *N. oculata*-infected larvae ($p=0.0077$) compared to symbiotic larvae. Error bars represent means ± 95% confidence intervals. The schematic above graph signifies the duration of infection with microalgae (black dots) and live imaging. Data acquired by Sebastian Rupp.

Unlike the symbionts, most larvae infected with healthy non-symbiotic microalgae or beads expelled the particles during the duration of imaging (Figure 14a, b). During a 24-hour imaging session, we observed expulsion of particles in 57 % of *M. gaditana*-infected larvae, 87.5 % of *N. oculata*-infected larvae, 75 % of *C. velia*-infected larvae, and 100 % of bead-infected larvae. While some larvae contained more than one particle, we additionally quantified the total proportion of microalgae or beads expelled during the observation period. We observed the expulsion of 42.1 % *M. gaditana* cells, 92.3 % *N. oculata* cells, 58.3 % *C. velia* cells, and 46.4

% beads (Figure 14b). It should be noted that we did not observe the digestion of microalgae during live imaging; in fact, the microalgae retained their autofluorescence and appeared to remain intact post expulsion. Furthermore, we observed the frequent reacquisition of non-symbiotic microalgae and beads during the duration of imaging (Figure 14a). Based on these observations, we determined that expulsion of non-symbiotic microalgae is responsible for the reduction in infection over time (Figure 8b), whereas phagolysosomal digestion was not observed. Moreover, because the beads were also expelled, and the reacquisition of both beads and non-symbiotic microalgae occurred repeatedly, it is plausible that uptake and removal occur in a non-specific manner until suitable symbionts are encountered and taken up by the host endoderm.

2.6 Early infection variability is a result of expulsion and reacquisition of microalgae

Due to the variation in initial infection after 24 hours with the respective microalgae (Figure 8b) and the variability in their loss over time, we investigated the expulsion dynamics of early infection. During the first 12 hours after a 1-hour infection, we performed live imaging to observe the fate of symbionts and non-symbiotic microalgae. We found that symbionts and *C. velia* were expelled significantly less often when compared with *M. gaditana* and *N. oculata.* While only 12.5 % of symbionts and 27.6 % of *C. velia* cells were expelled during the first 12 hours of infection, 73.9 % of *M. gaditana* cells and 73.5 % of *N. oculata* cells were expelled (Figure 15a). Although *M. gaditana* and *N. oculata* were readily expelled early on, we also recorded their frequent reacquisition (Figure 15b), which is in line with the high infection efficiency of both microalgae species after 24 hpi, in particular, that of *M. gaditana* (Figure 8b). After the microalgae were washed out, we observed a reduction in larvae infected with non-symbiotic microalgae due to their expulsion.

Within the first 12 hours, we also noticed that the time to the first expulsion varied depending on the microalgae species. It should be noted that for some of the microalgae, we did not observe expulsion as depicted by the accumulation of data points at 12 hours (Figure 15c). We found that if symbionts were to be expelled, it occurred slightly earlier when compared with the non-symbiotic microalgae. Of the symbionts that were expelled, 80 % (4/5 expelled symbionts) were expelled within the first 1.5 hours of imaging, with the average time to the first expulsion of symbionts being 2.5 hours. Regarding the non-symbiotic microalgae that were expelled, *C. velia* cells were first expelled at 3.5 hours, and both *M. gaditana* and *N. oculata* at

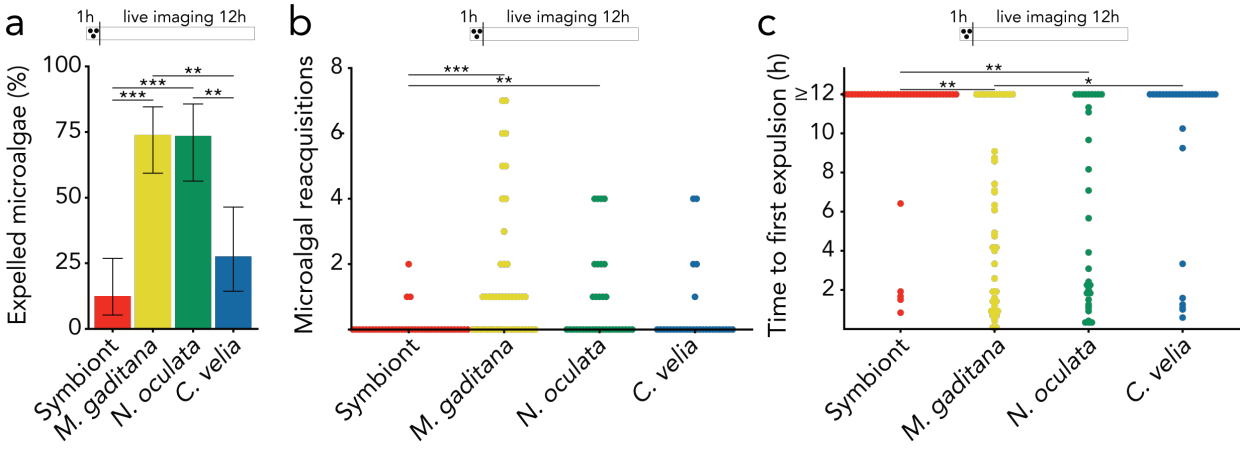

Figure 15 Expulsion and reacquisition of microalgae account for early infection variability
Aiptasia larvae were live imaged for 12 hours after 1-hour infection with symbionts, *M. gaditana*, *N. oculata*, or *C. velia,* which revealed significantly higher expulsion of non-symbiotic microalgae compared to symbionts. **a,** Compared to the symbiont, there was significantly more expulsion of *M. gaditana* ($p=0.0000058$) and *N. oculata* ($p=0.000021$) cells. Compared to *C. velia*, there was also significantly more expulsion of *M. gaditana* ($p=0.0014$) and *N. oculata* ($p=0.0035$). Error bars represent means ± 95% confidence intervals. **b,** *M. gaditana* ($p=0.00010$) and *N. oculata* ($p= 0.0049$) were reacquired significantly more often during the 12-hour live imaging session compared with symbionts. **c,** During the 12-hour live imaging session, the time to the first expulsion was highly stochastic. There were significant differences in time to expulsion between the symbiont and *M. gaditana* ($p=0.0025$), the symbiont and *N. oculata* ($p=0.0052$), and *M. gaditana* and *C. velia* ($p=0.036$). The non-expelled microalgae were set to 12 hours for analysis and quantification. Statistics are based on a two-sided generalized linear mixed model with pairwise p-values adjusted using the Tukey method. *$p < 0.05$, **$p < 0.01$, ***$p < 0.001$ (n=4 with approximately ten larvae each). Schematics above graphs signify the duration of infection with microalgae (black dots) and live imaging. Data acquired by Sebastian Rupp.

3.4 hours (Figure 15c). Beyond the average time to the first expulsion, we noticed that this process was stochastic, specifically for *M. gaditana* and *N. oculata*, where expulsion events were distributed somewhat randomly throughout the 12 hours of imaging.

2.7 Heat-killed non-symbiotic microalgae are retained longer than healthy microalgae

Based on our previous observations of reduced infection over time with heat-killed microalgae (Figure 9a), as well as the differential accumulation of LAMP1 around heat-killed-microalgae-containing phagosomes (Figure 12a, b), we next aimed to assess if heat-killed microalgae were expelled as their healthy counterparts and, if so, if the viability of the distinct microalgae influenced expulsion dynamics. After a 24-hour infection with heat-killed microalgae, infected larvae were live imaged for 16 hours. For the symbionts, we found that significantly more

healthy symbionts were maintained than heat-killed symbionts during the duration of imaging, 97.7 % and 36.6 %, respectively. We observed a similar tendency for *C. velia*-infected larvae, with slightly more maintenance of healthy *C. velia* when compared to heat-killed *C. velia* (75.0 % and 71.8 %, respectively). However, the opposite was true for both *M. gaditana* and *N. oculata*. Only 25.0 % of healthy *M. gaditana* cells were maintained during the 16-hour live imaging session, whereas 60.7 % of heat-killed *M. gaditana* cells were maintained. For *N. oculata*-infected larvae, only 17.8 % of healthy *N. oculata* cells were maintained compared with 79.3 % of heat-killed *N. oculata* (Figure 16a). Therefore, considerably more heat-killed *M. gaditana* and *N. oculata* were maintained compared with the control. Unlike the non-symbiotic microalgae, the heat-killing of symbionts negatively impacted their maintenance over time as they were expelled from the host.

Within the 16-hour observation period following the 24-hour infection with healthy and heat-killed microalgae, we found the time to the first expulsion varied depending on the viability of the microalgae. As previously mentioned, we did not observe expulsion for some of the microalgae as depicted by the accumulation of data points at 16 hours (Figure 16b). While the expulsion of healthy symbionts was atypical, we found that of the heat-killed symbionts expelled, it first occurred, on average, 6.5 hours after imaging began. Of the non-symbiotic microalgae to be expelled, healthy *M. gaditana* were first expelled at 3.7 hours and heat-killed *M. gaditana* at 5.6 hours. Healthy *N. oculata* cells were first expelled, on average, at 3.5 hours, and heat-killed *N. oculata* cells were first expelled at 5.3 hours. For *C. velia*-infected larvae, the first expulsion of healthy *C. velia* occurred at 3.5 hours, while the first expulsion of heat-killed *C. velia* occurred at 7.9 hours. Of the beads expelled, the first expulsion occurred at 1.1 hours (Figure 16b). Taken together, healthy non-symbiotic microalgae were expelled earlier than their heat-killed counterparts. Although the expulsion of the heat-killed microalgae was delayed, their expulsion was again stochastic, as we observed for the healthy non-symbiotic microalgae (Figure 15c).

2.8 Expulsion of incompatible microalgae does not depend on actin

We further set out to investigate the expulsion mechanism responsible for the sorting of symbionts from non-symbiotic microalgae. Since we did not observe digestion and the microalgae appeared healthy after expulsion and were readily reacquired, we specifically wanted to explore non-lytic expulsion mechanisms. The default mechanism for non-lytic

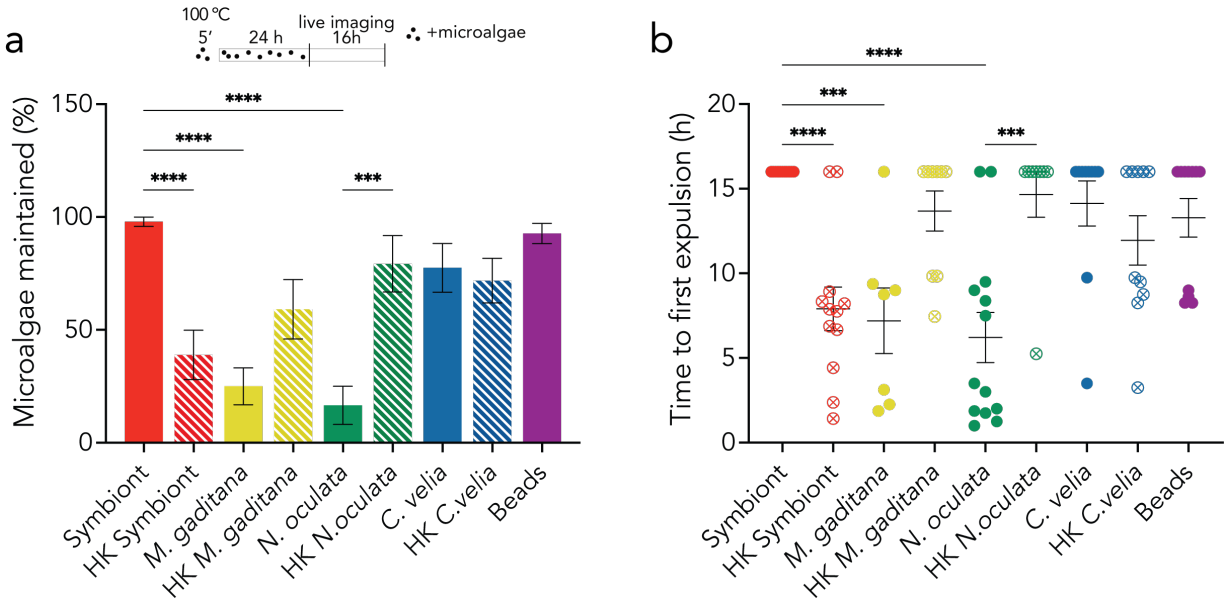

Figure 16 Heat-killed non-symbiotic microalgae are retained longer than healthy non-symbiotic microalgae

Aiptasia larvae were live imaged for 16 hours after a 24-hour infection with healthy or heat-killed (HK) symbionts, *M. gaditana*, *N. oculata*, *C. velia,* or beads, which revealed significantly longer retention of some HK non-symbiotic microalgae compared to healthy non-symbiotic microalgae. **a,** While healthy symbionts were maintained for the duration of imaging, significantly more HK symbionts were expelled. Conversely, more HK *M. gaditana* and HK *N. oculata* cells were maintained during imaging than their healthy counterparts. The schematic above graph signifies the duration of infection with microalgae (black dots) and live imaging. **b,** During the 16-hour live imaging session, the time to the first expulsion was stochastic, but with a longer time to first expulsion of HK *M. gaditana* and *N. oculata* compared with the healthy controls. The non-expelled microalgae were set to 16 hours for analysis and quantification. Quantified 21 symbiotic larvae with 49 symbionts, 18 HK-symbiont-containing larvae with 44 HK symbionts, 14 *M. gaditana*-infected larvae with 40 *M. gaditana* cells, 12 HK-*M. gaditana*-infected larvae with 17 HK-*M. gaditana* cells, 18 *N. oculata*-infected larvae with 44 *N. oculata* cells, 8 HK-*N. oculata*-infected larvae with 22 HK-*N. oculata* cells, 12 *C. velia*-infected larvae with 33 *C. velia* cells, 10 HK-*C. velia*-infected larvae with 29 HK *C. velia* cells, and 17 bead-infected larvae with 52 beads. Error bars indicate SEM and statistics are based on an ordinary one-way ANOVA. P-values were adjusted using the Tukey method. *$p < 0.05$, ** $p < 0.01$, *** $p < 0.001$. Data acquired by Viola Kühnel.

expulsion of indigestible material from amoebae is actin-dependent and occurs consistently ~80 minutes after phagocytosis. This process is regulated by the Wiskott-Aldrich syndrome protein and SCAR homolog (WASH) protein (Watkins et al., 2018).

To determine if the expulsion of non-symbiotic microalgae in Aiptasia larvae is actin-dependent, we treated larvae with an actin polymerization inhibitor, latrunculin B (LatB), during a 1-hour infection with *M. gaditana.* After determining the concentration of LatB that

affected the actin cytoskeleton but was not harmful to the larvae (Figure 17a), we performed live imaging for 12 hours to monitor expulsion dynamics when the functionality of actin is impaired. We found no significant difference in the expulsion of *M. gaditana* cells from larvae when we compared LatB-treated larvae with the control (Figure 17b). Furthermore, when

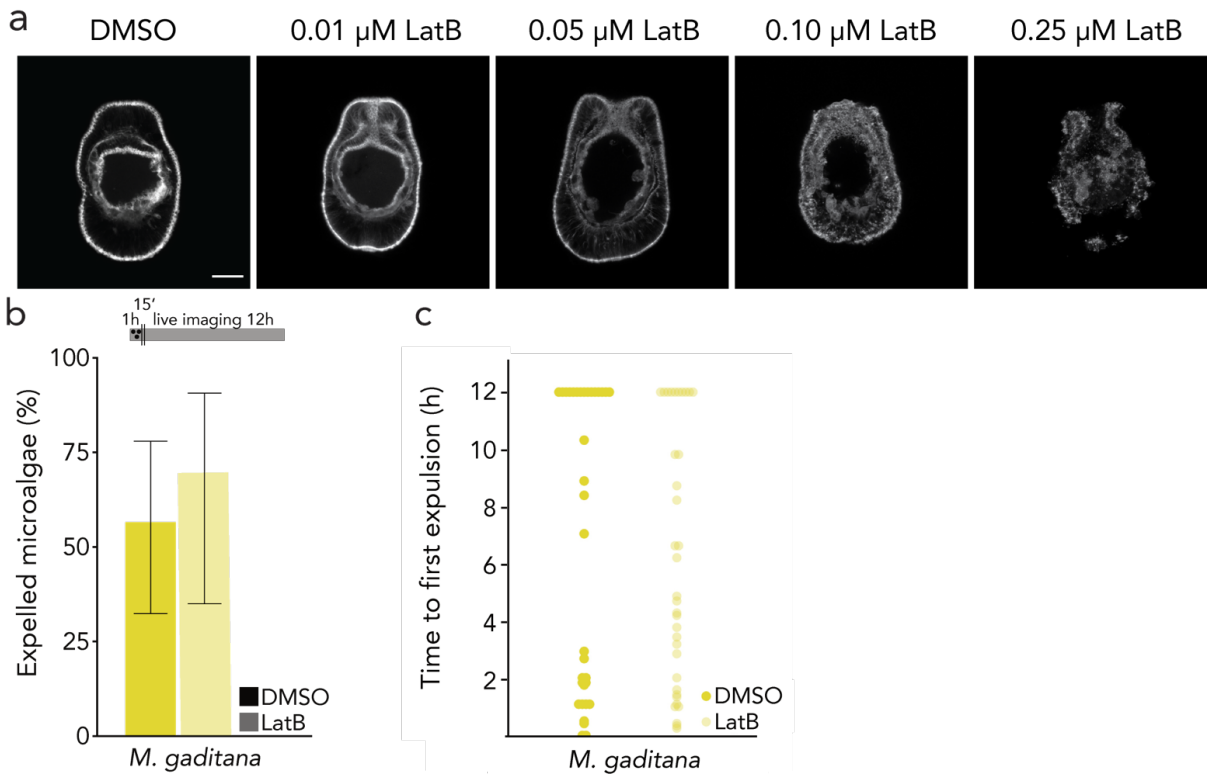

Figure 17 Actin polymerization inhibition does not interfere with the expulsion of *M. gaditana*
Latrunculin B (LatB) was used to inhibit actin polymerization in Aiptasia larvae to assess the role of actin in the expulsion of non-symbiotic microalgae. **a,** To determine a suitable concentration for live imaging, larvae were incubated in different concentrations of Lat B for 6 hours. Confocal microscopy was used to assess F-actin after phalloidin staining. 0.01 µM LatB did not appear to visually affect actin in larvae. 0.05 µM LatB substantially reduced F-actin levels but did not appear to harm larvae; therefore, it was the concentration selected to use for live imaging in b and c. 0.10 µM and 0.25 µM LatB were toxic to the larvae as they began to disintegrate**. b,** After a 1-hour infection and pretreatment with 0.05 µM LatB, larvae were live imaged for 12 hours. Actin polymerization inhibition by LatB had no effect on the expulsion of *M gaditana* cells from larvae. The schematic above graph signifies the duration of infection with *M. gaditana* (black dots), treatment with LatB (grey fill), and live imaging. **c,** Additionally, LatB treatment did not alter the time to the first expulsion of *M. gaditana,* indicating that this process does not rely on actin (n=3). Live imaging performed by Sebastian Rupp.

analyzing the time to the first expulsion after actin polymerization inhibition, we did not observe a significant difference between LatB-treated larvae and control (Figure 17c).

Additionally, we wanted to determine if WASH mediates expulsion of microalgae by using the same commercially available WASH complex 1 (WASHC1) antibody used for investigations in *Dictyostelium*. We did not observe WASHC1 accumulation around symbionts or non-symbiotic microalgae (Figure 18a), but it should be noted that WASHC1 was highly transient when localized in amoebae (Buckley et al., 2016). There is the possibility that we selected a time point where WASHC1 was not active as we imaged fixed samples. The antibody itself could have been insufficient at detecting Aiptasia WASHC1, but the peptide sequences between human WASHC1, from which the antibody was generated, and Aiptasia WASHC1 are more similar than when comparing the peptide sequences of human WASHC1 with *Dictyostelium* WASHC1. We were unable to detect WASHC1 in Aiptasia extracts by western blot, but we did detect it in human extracts (Figure 18b). Since the expulsion observed does not rely on actin, together with the fact that the timing of non-symbiotic microalgae expulsion is inconsistent and occurs after > 80 minutes post-phagocytosis, it appears that this process is likely not constitutive exocytosis.

2.9 Expulsion of microalgae is regulated by ERK5

Beyond constitutive exocytosis, an additional expulsion mechanism has been reported in amoeba and vertebrate macrophages, known as vomocytosis (Seoane & May, 2020). Vomocytosis deviates from constitutive exocytosis in that it is actin-independent and is a stochastic process, occurring between 2-12 hours post-phagocytosis (Johnston & May, 2010; H. Ma et al., 2006; Watkins et al., 2018). In fact, the expulsion of non-symbiotic microalgae does not rely on actin (Figure 17b) and appears to be highly stochastic (Figure 15c).

The extracellular signal-regulated kinase 5 (ERK5) is a known negative regulator of vomocytosis in vertebrate macrophages (Gilbert et al., 2017), together with the upstream mitogen-activated protein kinase kinase 5 (MAP2K5). To determine if ERK5 plays a role in mediating the expulsion of microalgae in Aiptasia larvae, we first needed to identify an ERK5 homolog in Aiptasia. We identified several MAP kinases and one ERK5 homolog, with a conserved ATP binding site (aa 61-69 in *H. sapiens* ERK5), as well as a MAP2K5 homolog

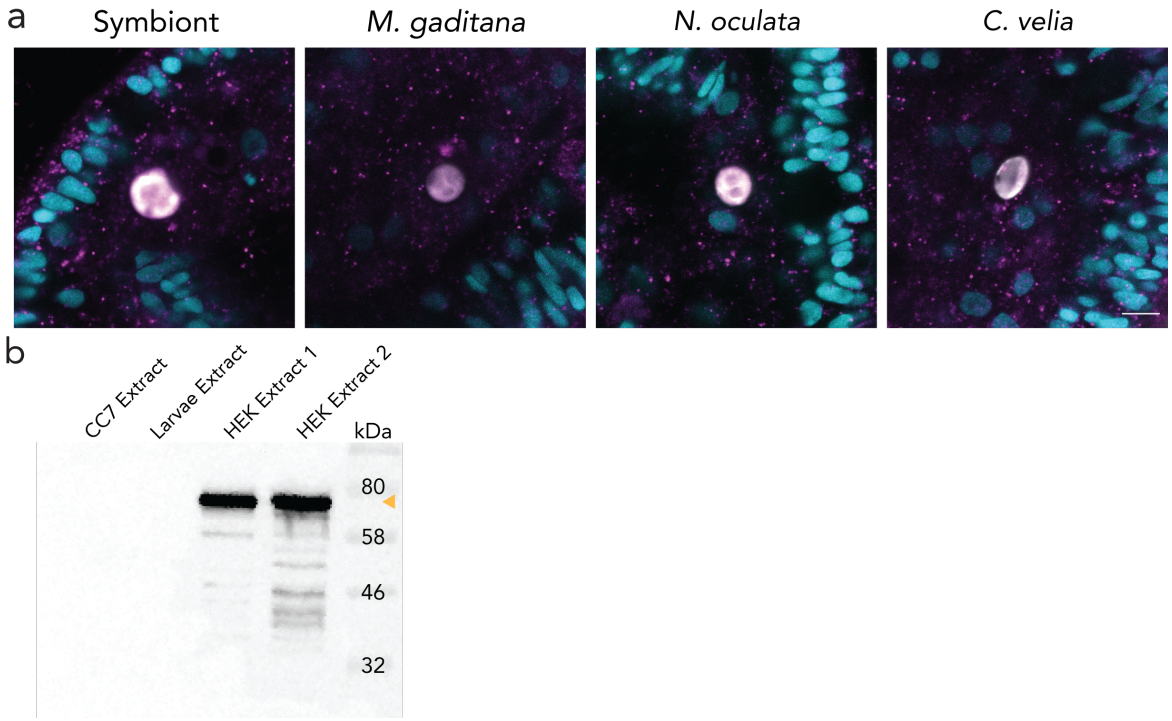

Figure 18 WASHC1 in Aiptasia

WASHC1 accumulation was assessed in Aiptasia larvae after a 6-hour infection with symbionts, *M. gaditana*, *N. oculata*, and *C. velia*. **a,** None of the microalgae appeared to accumulate WASHC1. Images depict microalgae autofluorescence (white), Hoechst-stained nuclei (cyan), and WASHC1 (magenta). Scale bar represents 10 µm. **b,** WASHC1 was not detected in Aiptasia polyp (CC7) or larvae extract by western blot. Although the predicted molecular weight of WASHC1 is 50.3 kDa, it typically appears around 70 kDa (indicated by yellow arrowhead). WASHC1 was detected at the expected molecular weight in two distinct HEK cell extracts indicating that the inability to detect Aiptasia WASHC1 is not due to a faulty antibody.

(Supplementary Figure 2). Using a specific ERK5 inhibitor XMD17-109, which targets the ATP binding site (Gilbert et al., 2017), we aimed to determine if ERK5 inhibition would stimulate expulsion of symbionts, which are typically retained. Upon treatment with XMD17-109, we saw a significant reduction in the proportion of symbiotic larvae when compared with the control (Figure 19a). Using live imaging, we confirmed that this reduced infection resulted from increased expulsion rather than reduced uptake. After a 1-hour infection and treatment with the ERK5 inhibitor, we monitored the larvae for 12 hours and observed a significant increase in symbionts expelled from larvae that had been treated with XMD17-109 compared with the control (Figure 19b).

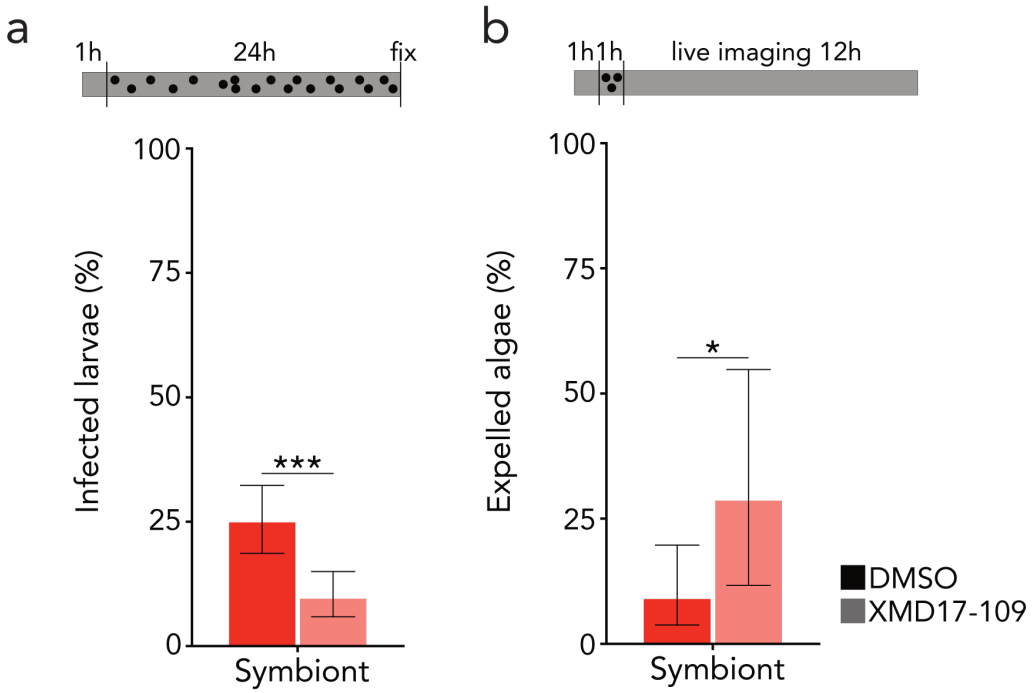

Figure 19 ERK5 inhibition enhances symbiont expulsion

The specific ERK5 inhibitor, XMD17-109, was used to assess infection with symbionts in Aiptasia larvae. **a,** There were significantly fewer symbiotic larvae when exposed to XMD17-109 compared to the control (p=0.000013) (n=6). **b,** The reduced infection was a direct result of increased expulsion. After a 1-hour infection, there was significantly more expulsion of symbionts from XMD17-109 treated larvae during the 12-hour observation period (p=0.013) than the control (n=5). Schematics above graphs signify the duration of infection with symbionts (black dots), treatment with XMD17-109 (grey fill), and live imaging (where applicable). Live imaging performed by Sebastian Rupp.

Additionally, we were curious if ERK5 inhibition interfered with LAMP1-niche formation that is typical for healthy symbiosomes (Figure 11a). After a 5-hour infection and treatment with the ERK5 inhibitor, we quantified LAMP1-positive symbiosomes and saw a massive reduction in LAMP1 accumulation around intracellular symbionts (Figure 20a, b). The stochastic nature of expulsion of non-symbiotic microalgae (Figure 15c), together with our findings that ERK5 acts as a negative regulator of symbiont expulsion, indicates that Aiptasia larvae use vomocytosis to release non-symbiotic microalgae or indigestible particles after they have been phagocytosed by the endodermal cells. Therefore, symbionts must circumvent vomocytosis in order to persist intracellularly and establish a LAMP1-positive niche.

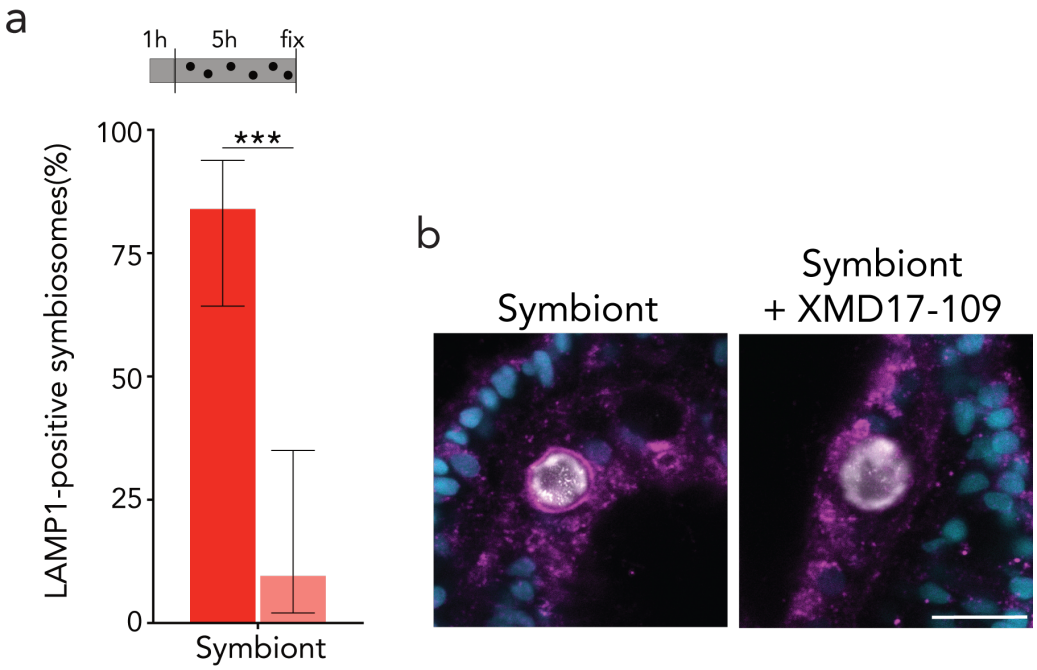

Figure 20 LAMP1-niche of symbionts fails to develop upon ERK5 inhibition
ERK5 inhibition by XMD17-109 interfered with LAMP1 accumulation around symbionts during early infection. **a,** Larvae treated with XMD17-109 had significantly fewer LAMP1-positive symbiosomes than the DMSO-treated control (p=0.0000027). The schematic above graph signifies the duration of infection with symbionts (black dots) and treatment with XMD17-109 (grey fill). Error bars represent means ± 95% confidence intervals. Statistics are based on a two-sided generalized linear mixed model accounting for repeated measurements. (n=3). **b,** Representative images of LAMP1 accumulation around symbionts compared with symbionts in larvae treated with XMD17-109. Images depict symbiont autofluorescence (white), Hoechst-stained nuclei (cyan), and LAMP1 (magenta). Scale bar represents 10 µm. (n=3).

2.10 Immune suppression induced by symbiont uptake is host cell-specific

To understand the mechanisms at play, directly succeeding symbiont uptake and preceding LAMP1-niche formation, ultimately suppressing symbiont vomocytosis, we turned to the innate immune system. Immune modulation is a well-studied prerequisite for establishing a vast array of symbioses, both parasitic and mutualistic, and has been shown to mediate cnidarian-dinoflagellate pairings (Ghosh & Stumhofer, 2014; Mansfield & Gilmore, 2018).

Moving forward, we explicitly wanted to understand if there was a link between vomocytosis and the innate immune response. To address this, we compared the expression levels of innate immune-related genes (based on KEGG (Kanehisa & Goto, 2000) annotations for Aiptasia) in

host cells that contain symbionts with cells that were either aposymbiotic or that contained non-symbiotic microalgae. We selected *M. gaditana* as the representative non-symbiotic microalgae for this analysis due to the dynamics of residency time – intracellular for enough time to perform the analysis, yet expelled relatively quickly after washout (Figure 8b). We performed our standard infection assay by incubating Aiptasia larvae with symbionts or *M. gaditana* for 24-

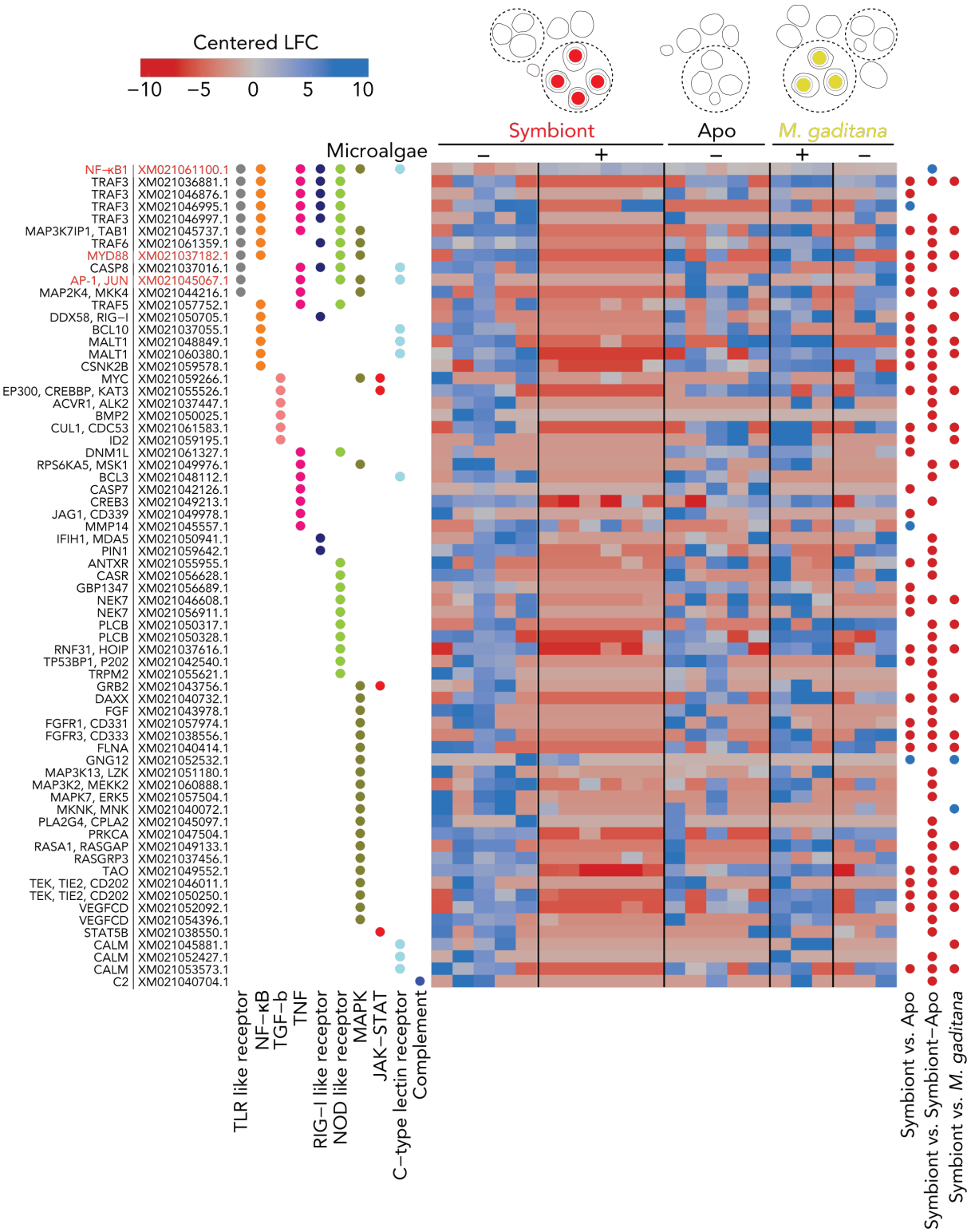

Figure 21 Cell-specific, comprehensive innate immune suppression in symbiont-containing cells
Transcriptomic analysis of Aiptasia cells revealed broad downregulation of genes across several immunity pathways in cells that contain symbionts. Numerous genes involved in innate immunity were differentially downregulated in cells that contained symbionts compared with all other cell types analyzed (aposymbiotic cells (Apo) from Apo larvae, Apo cells from symbiotic larvae, cells that contained *M. gaditana,* or Apo cells from *M. gaditana*-infected larvae). Gene names in red refer to specific genes of interest mentioned in this thesis. The NCBI RefSeq numbers are listed next to the gene names. The heatmap shows all differentially regulated genes within the KEGG pathways: TLR (ko04620), NF-κB (ko04064), TGF-β (ko04350), tumor necrosis factor (TNF) (ko04668), retinoic acid-inducible gene I (RIG-I)-like receptor (ko04622), nucleotide-binding oligomerization domain (NOD)-like receptor (ko04621), MAPK (ko04010), Janus-kinase (JAK)-signal transducer and activator of transcription protein (STAT) (ko04630), C-type lectin receptor signaling (ko04625), and complement and coagulation cascades (ko04610). Colors indicate the centered log[fold change] according to DESeq2 (red represents downregulation and blue represents upregulation). KEGG annotation was automated based on homology. Significantly differentially expressed genes are represented with blue (upregulated) or red (downregulated) dots in the respective cell-type comparison. Acquired by Philipp Voss, analyzed with assistance from Sebastian Gornik, and heatmap created by Sebastian Rupp.

48 hours. Once infected, larvae were dissociated into individual cells, and single cells were manually picked to represent each cell type that we were interested in comparing. 8-12 endodermal cells per classification were pooled and sequenced – (1) symbiont-containing cells, (2) *M. gaditana*-containing cells, (3) aposymbiotic cells from symbiotic larvae, (4) aposymbiotic cells from *M. gaditana*-infected larvae, and (5) aposymbiotic cells from uninfected larvae (Supplementary Figure 3).

This transcriptomic analysis revealed that the gene expression in symbiont-containing cells was distinct from all the other cell types. We found that cells that contained symbionts had significantly lower expression of genes distributed across ten innate immune pathways (Figure 21). These ten pathways were related to metazoan innate immunity based on KEGG, with some components present in multiple pathways and some genes classified with more than one transcript, for example, TRAF3, MALT1, and CALM. The pathways with the highest proportion of components that were down-regulated in symbiont-containing cells were the nuclear factor-κB (NF-κB) and activator protein 1 (AP-1)/Jun-related signaling pathways, involving approximately 20 % genes from each pathway (Figure 21, Supplementary Table 1). Interestingly, previous transcriptomic analysis in both Aiptasia larvae and adult polyps revealed organism-wide immune suppression upon symbiosis establishment (Lehnert et al., 2014; Mansfield et al., 2017; Wolfowicz et al., 2016); we further enhance these investigations by

providing evidence that this immune suppression is specific to only the symbiont-containing cells. Additionally, this uncovers the possibility that more information may have been overlooked due to the noise of aposymbiotic cells in previous analyses.

2.11 Immune stimulation enhances vomocytosis of symbionts in early stages of symbiosis establishment

The detection of symbionts and other microorganisms by cnidarian hosts typically begins with pattern recognition receptors (PRRs), which classically initiate an immune response (Rosenstiel et al., 2009). One signaling pathway activated by PRRs of particular interest, based on our findings, is the toll-like receptor (TLR) pathway. Our transcriptomic analysis revealed that most genes of the TLR pathway were significantly down-regulated in symbiont-containing cells compared with all other cell types analyzed (Figure 22). TLRs are PRRs that comprise an extracellular recognition domain with tandem copies of a leucine-rich repeat (LRR) motif, a transmembrane domain, and a cytoplasmic signaling (TIR) domain (Botos et al., 2011). While canonical TLRs have not been identified in Aiptasia, two TIR-domain-containing proteins and two LRR-domain-containing proteins have been identified (Baumgarten et al., 2015).

To assess the role of TLR-signaling in the early stages of symbiosis establishment, we instigated an immune response via the TLR pathway using lipopolysaccharides (LPS), a mammalian TLR ligand. We treated larvae for 1 hour before and during a 24-hour infection with symbionts and non-symbiotic microalgae and found that the proportion of symbiotic larvae was significantly reduced upon LPS treatment to 25 % of the control (Figure 23a). There was also a significant reduction in infection in *C. velia*-infected larvae in the presence of LPS; however, there were no substantial effects observed for *M. gaditana* or *N. oculata*-infected larvae (Figure 23a).

Although immune stimulation interferes with early symbiosis establish, once a stable symbiosome has formed and symbionts are intracellular for at least 24 hours, immune stimulation via LPS did not affect symbiont maintenance (Figure 23b). Thus, it appears that activation of the TLR pathway during early infection either inhibits uptake or enhances expulsion of symbionts and *C. velia;* yet, after symbionts are stably integrated into the host cell, exogenous immune stimulation fails to disrupt the symbiosis, likely due to transcriptional repression induced by symbiont uptake (Figure 21, 22).

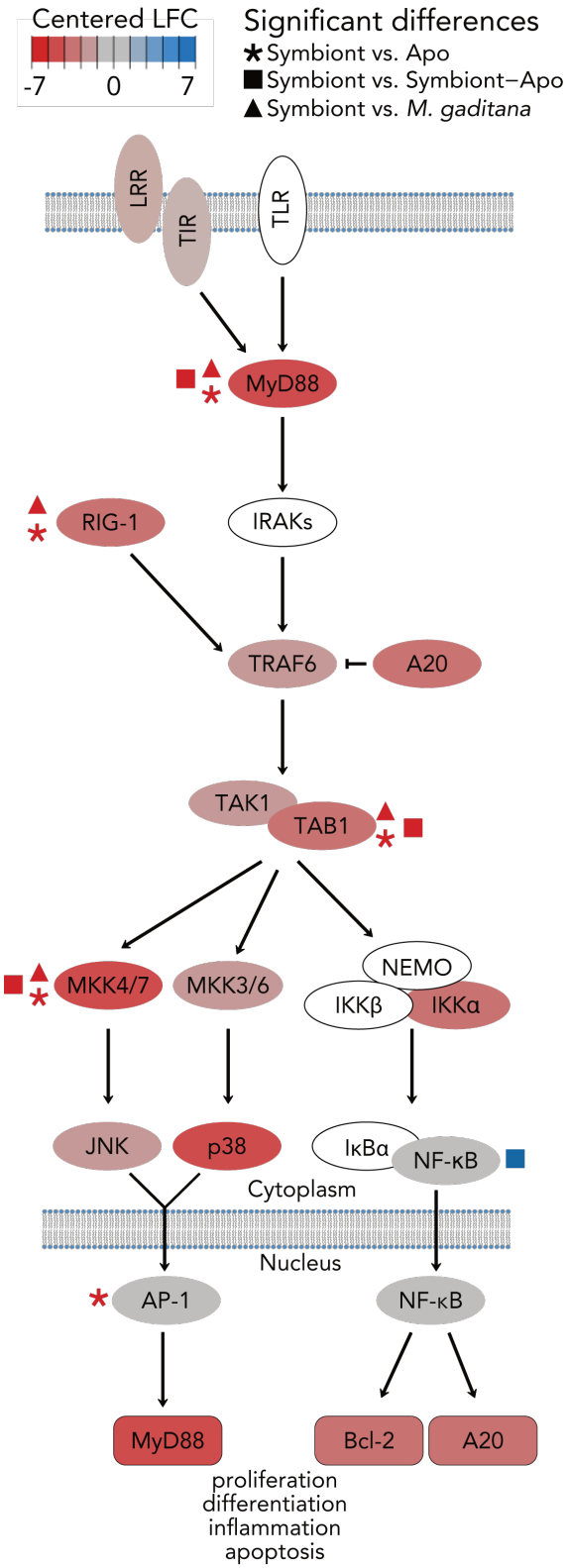

Figure 22 Multiple components of TLR pathway are suppressed upon symbiont uptake
A simplified TLR pathway according to KEGG annotations. The genes in white were not identified in Aiptasia. Colors indicate the centered log[fold change] according to DESeq2 (red represents downregulation and blue represents upregulation). Asterisks represent statistically significant differences between symbiotic and aposymbiotic cells from aposymbiotic larvae (Symbiont vs. Apo), squares represent significant differences between symbiotic and aposymbiotic cells from symbiotic larvae (Symbiont vs. Symbiont-Apo), and triangles represent significant differences between symbiont- and *M. gaditana*-containing cells (Symbiont vs. *M. gaditana*). Nuclear factor of kappa light polypeptide gene enhancer in B-cells inhibitor (IκBα) alpha, inhibitor of nuclear factor kappa-B kinase subunit (IKKα/β), interleukin-1 receptor-associated kinase (IRAK), NF-κB essential modulator (NEMO), transforming growth factor β-activated kinase 1 (TAB1), TGF-β-activated kinase 1 (TAK1), and TNF receptor-associated factor 6 (TRAF6). Acquired by Philipp Voss, analyzed with assistance from Sebastian Gornik, and pathway heatmap created by Sebastian Rupp.

To determine if TLR signaling during early infection inhibits uptake or enhances expulsion of symbionts, we performed live imaging on larvae treated with LPS. There was a significant increase in symbiont expulsion from larvae exposed to LPS compared with the control, where 45.2 % of symbionts were expelled when LPS was present, and only 10 % of symbionts were expelled without (Figure 23c). Therefore, active TLR signaling interferes with symbiosis

establishment by triggering the expulsion of symbionts. Because vomocytosis of non-symbiotic microalgae occurs frequently and stochastically during the 12-24 hours following phagocytosis, it is likely that immune stimulation by LPS does not further enhance the expulsion of *M. gaditana* or *N. oculata* (Figure 15c, 23a). Ultimately, we found vomocytosis to be the standard immune response utilized by Aiptasia larvae to remove non-symbiotic microalgae; symbiont uptake induces immune suppression that inhibits vomocytosis, which encourages intracellular persistence of symbionts and thus the beginnings of the symbiotic partnership.

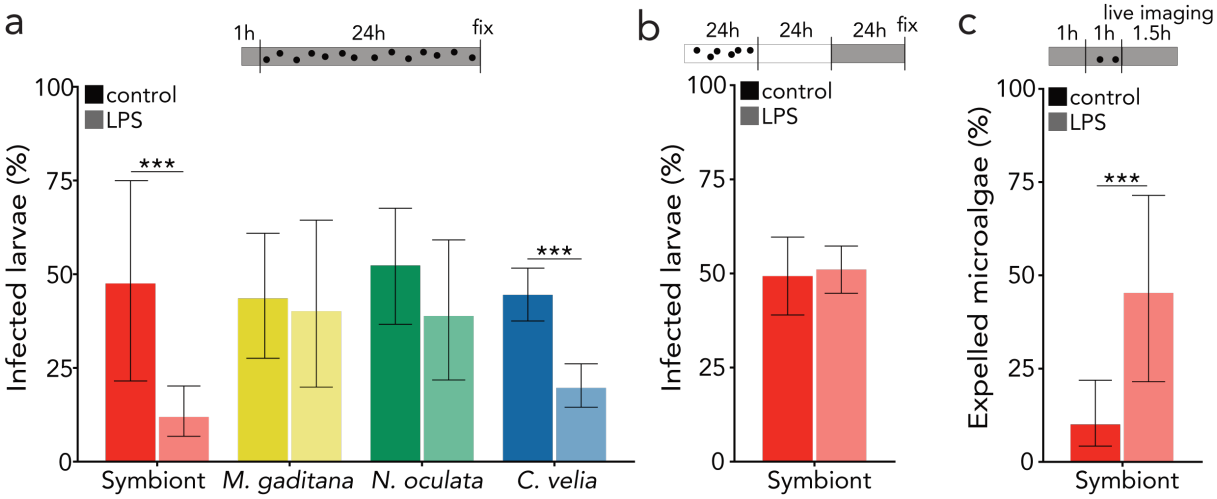

Figure 23 Stimulation of TLR pathway interferes with symbiosis establishment but not maintenance

a, After a 1-hour pretreatment with LPS, followed by a 24-hour treatment with LPS in addition to microalgae, the proportion of symbiotic larvae was significantly lower compared to the control (p=0.0000000024). There was also a statistically significant reduction in *C. velia*-infected larvae (p=0.00000000024). No significant effects were observed for *M. gaditana*- or *N. oculata*-infected larvae (n=5). **b,** After a 24-hour infection with symbionts, followed by a washout and additional 24 hours, LPS was added to assess immune stimulation post-symbiosis establishment. LPS treatment had no effect on symbiont maintenance (n=5). **c,** Live imaging after LPS treatment revealed that immune stimulation induced expulsion. Significantly more symbionts were expelled after LPS treatment compared with the control (p=0.00038) (LPS treatment: n=3 with a total of 42 symbionts, DMSO control: n=4 with a total of 50 symbionts). Error bars represent means ± 95% confidence intervals, with statistics based on a two-sided generalized linear mixed model accounting for repeated measurements. *p < 0.05, **p < 0.01, ***p < 0.001. Schematics above graphs signify duration of infection with microalgae (black dots), treatment with LPS (grey fill), and live imaging (where applicable). Data acquired by Sebastian Rupp.

2.12 MyD88 modulates TLR signaling during early symbiosis establishment

Myeloid differentiation primary response 88 (MyD88) is an adaptor molecule central to the intracellular signaling cascade that links TLRs and Interleukin-1 receptors (IL-1Rs) with their downstream kinases. This cascade ultimately activates the NF-κB and MAPK pathways (Barton & Kagan, 2009; O. Takeuchi & Akira, 2010). TLRs may recognize a vast array of microbial ligands, but the sensing converges a small handful of adaptors – the most crucial being MyD88. During infection with various microorganisms, MyD88 has been shown to be a key player in mediating an innate immune response (Ghosh & Stumhofer, 2014). Therefore, we sought to investigate the potential role of MyD88 in the early stages of symbiosis establishment in Aiptasia larvae.

Transcriptomic analysis revealed that in the early stages of symbiosis, expression of Aiptasia MyD88 was significantly lower than in cells across all other conditions (Figure 21, 22); thus, we were interested in understanding the role of MyD88 in both uptake and retention of microalgae. In regards to the role of MyD88 in the initial stages of microalgae uptake, we pretreated larvae for 1 hour with a MyD88 inhibitor peptide and then performed a 24-hour infection with all four microalgae species in the presence of the inhibitor. The MyD88 inhibitor blocks MyD88 homodimer formation by competitively binding to the MyD88 TIR domain (Dishon et al., 2018) (Supplementary Figure 4). MyD88 inhibition had no apparent effect on symbiont uptake or retention during the 24-hour infection, but interestingly, it appeared to somewhat negatively affect uptake or retention of the non-symbiotic microalgae (Figure 24a).

Thus, suppression of MyD88 activity in the first 24 hours of infection does not enhance uptake or retention of symbionts; however, it does seem to interfere with uptake or retention of non-symbiotic microalgae. To further investigate how MyD88 is implicated after microalgae are intracellular, we performed a 24-hour infection with all four microalgae species and then treated larvae with the MyD88 inhibitory peptide. We found a significant increase in the proportion of symbiotic larvae when MyD88 activity was inhibited (Figure 24b). However, for all other non-symbiotic microalgae, we observed no such effect (Figure 24b). Thus, while suppression of MyD88 activity may enhance symbiont retention between 24 and 48 hpi, it appears that reduced MyD88 activity is not solely responsible for maintaining intracellular microalgae.

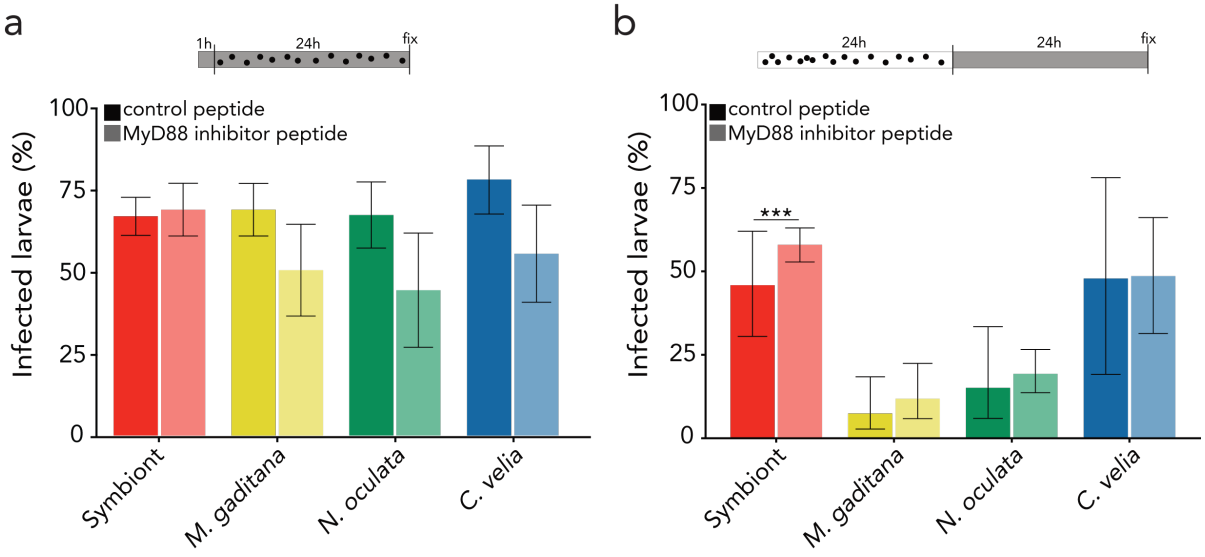

Figure 24 MyD88 inhibition enhanced maintenance of symbionts

a, MyD88 inhibition during infection with microalgae had no significant effect on infection. There was a slight reduction in non-symbiotic-microalgae-infected larvae when compared with control, although not significant. **b,** While MyD88 inhibition did not affect the maintenance of the non-symbiotic microalgae, MyD88 inhibition significantly enhanced the maintenance of symbionts after 24-hour infection and 24-hour treatment ($p=0.0000053$) ($n=10$ (symbionts); $n=3$ (*M. gaditana* and *C. velia*); $n=13$ (*N. oculata*)). Error bars represent means ± 95% confidence intervals, with statistics based on a two-sided generalized linear mixed model accounting for repeated measurements. ***$p < 0.001$. Schematics above graphs signify the duration of infection with microalgae (black dots) and treatment with MyD88 inhibitor peptide (grey fill). Data partially acquired by Sebastian Rupp.

3 Discussion

3.1 Post-phagocytic symbiont selection in Aiptasia

The selection of compatible symbionts is a critical first step in successful symbiosis establishment. Our data imply that symbiont selection mechanisms occur post-phagocytosis since all non-symbiotic microalgae we presented to aposymbiotic larvae were taken up into the endodermal cells (Figure 7). This finding is in line with previous investigations in other cnidarian species, which found that winnowing mechanisms exist to sort symbionts from non-symbionts after uptake (S. R. Dunn & Weis, 2009; Voolstra et al., 2009).

Although we observed the uptake of multiple microalgae species, it should be noted that the microalgae used in our comparative analysis were of comparable size. One important criterion that has been shown to influence symbiont uptake, and therefore selection, is size (Biquand et al., 2017; Wolfowicz et al., 2016). This size specificity also differs depending on the host. However, in general, it appears that smaller microalgae are phagocytosed more readily than their larger counterparts, not only when comparing different species but also when taking into consideration variability in cell size within one species (Biquand et al., 2017; Wolfowicz et al., 2016).

After uptake, the loss of non-symbiotic microalgae appeared unique to each species examined regarding timing. While most *N. oculata* cells were lost between 1 and 2 dpi, *M. gaditana* cells were maintained slightly longer over the 10-day observation period, and *C. velia* cells were maintained even longer; nevertheless, all were lost over time (Figure 8b). Accordingly, the timing of host response does not appear to be fixed for any phagocytosed particle but is specific to the individual microalgae. The viability status of the microalgae, both symbiotic and non-symbiotic, also affected both uptake and retention. Even though the healthy and heat-killed microalgae are of comparable sizes, there appeared to be either preferential uptake or retention of heat-killed *M. gaditana* and *N. oculata*. In contrast, heat-killing of symbionts and *C. velia* negatively impacted infection efficiency (Figure 9a). Additionally, healthy non-symbiotic microalgae were lost more rapidly than heat-killed (Figure 9a). All in all, we found that the uptake of microalgae is somewhat indiscriminate since we see the uptake of healthy and heat-killed symbiotic and non-symbiotic microalgae. However, viability status and non-symbiotic microalgae type influence both the efficiency of uptake and subsequent removal.

3.2 Pre-phagocytic versus post-phagocytic symbiont selection

Although phagocytosis seems unspecific, we observed differential uptake of microalgae depending on their viability status (Figure 9a). This observation is not entirely surprising since it has been shown that particular recognition mechanisms mediate the initial interaction between beneficial symbionts and host cells. For example, specific genes encoding complement proteins were upregulated during the onset of symbiosis in Aiptasia, molecules on the surface of symbionts (namely glycans) were identified to mediate host recognition and uptake in *Fungia scutaria* and *Aiptasia pulchella*, and host scavenger receptors were shown to play a role in successful colonization of Aiptasia with symbionts (Lin et al., 2000; Neubauer et al., 2017; Poole et al., 2016; Wood-Charlson et al., 2006).

The attraction of Symbiodiniaceae cells towards the green fluorescence of corals could bring the otherwise scarce symbionts closer to the host (Aihara et al., 2019; Hollingsworth et al., 2005). Once in the vicinity of the host, high molecular weight proteins or peptides, e.g., lectins, which do not diffuse efficiently over long distances, have been suggested to play a role in short-range attraction (R. Takeuchi et al., 2021). Based on our observations, it is conceivable that the heat-killing of symbionts interferes with pre-phagocytic recognition, which could explain the lower infection compared to the control.

On the one hand, the pre-phagocytic acquisition of symbionts is complex involving a multitude of factors. However, on the other hand, we see that some cnidarian larvae, Aiptasia included, are promiscuous with the uptake of microalgae, and the post-phagocytic sorting is essential for functional symbiosis establishment (Cumbo, Baird, & van Oppen, 2013; Jacobovitz et al., 2021). Thus, it appears that symbiont selection involves multiple winnowing steps, occurring prior to and following phagocytosis. While none of the steps alone is exclusively responsible for successful symbiosis establishment, some may be more influential than the others, as illustrated by the indiscriminate uptake of microalgae in Aiptasia larvae.

3.3 LAMP1-positive symbiosome and the arrested phagosome hypothesis

LAMP1 is a lysosomal membrane protein that is highly glycosylated, responsible for maintaining the integrity of this acidic and hydrolytic organelle (Wartosch, Bright, and Luzio 2015), and is commonly used as a lysosomal marker. However, because vesicular trafficking is a complex and diverse process, the presence of LAMP1 alone is not conclusive to classify this

organelle as a lysosome. The colocalization of other late endosomal/phagosomal markers such as the GTPase Rab7, v-ATPase, or cathepsins would better indicate the nature of the organelle. Regardless, we do not see the accumulation of LAMP1 around healthy non-symbiotic microalgae, which makes it clear that these microalgae are not being digested intracellularly (Figure 11a). Heat-killed non-symbiotic microalgae, on the other hand, do accumulate LAMP1 (Figure 11b; 12a, b). Although it cannot be said with certainty, this could be an attempt by the host cell to digest the dead microalgae. The healthy non-symbiotic microalgae may appear indigestible to the host based on some unknown factor. This attempt to digest could also account for the longer residency time for heat-killed non-symbiotic microalgae than healthy controls.

While LAMP1 accumulation could signify intracellular digestion of heat-killed non-symbiotic microalgae, its role in niche formation during symbiosis is far more interesting. While the non-symbiotic microalgae are lost, symbionts are maintained and reside in a LAMP1-positive niche (Figure 11a). Previous literature suggested that the symbiosome may be an arrested phagosome, which would allow symbionts to reside intracellularly and avoid degradation. Specifically, the early endosomal marker Rab5 was localized to the symbiosome in Aiptasia, and conversely, the late endosomal marker Rab7 was not. Furthermore, unhealthy or dead symbionts lost Rab5 and accumulated Rab7 (Chen et al. 2003, 2004). As previously mentioned, the complexity of vesicular trafficking makes using one marker to identify an organelle difficult; therefore, these investigations are not definitive proof that the symbiosome is an arrested phagosome.

Another example of the arrested phagosome hypothesis comes from a transcriptomic analysis in the coral *Acropora digitifera*. The authors suggest that the symbiosome is an arrested phagosome due to the upregulation of six vesicular trafficking genes in the symbiotic organism compared to the aposymbiotic control (Mohamed et al. 2016). The genes, however, were classified as such based on their mammalian homologs and not their function in *A. digitifera*. Furthermore, the genes are not specific to early endosome formation solely but are rather GTPases involved in vesicular trafficking in general. It is also important to note that the only significant differences observed were at the earliest time point (4 hpi), and they were lost at the later time points (12 and 48 hpi) (Mohamed et al. 2016). As phagosome maturation is a dynamic process and multiple markers will be present at any given time, transcriptomic data from only one time point that may not even represent a stable symbiosis is insufficient to characterize the symbiosome properly. Unfortunately, these investigations have led to assumptions in the field, and well-thought-out and stringent experiments will be necessary to understand this unique

organelle. Indeed, our results reveal that the symbiosome may not be an arrested phagosome after all.

3.4 Symbiosome as a modified lysosome

Beyond the early accumulation of LAMP1 around compatible symbionts, other clues suggest that the symbiosome may be a modified lysosome. Two lysosomal proteins, NPC2 and mTOR, have been localized to the symbiosome in Aiptasia (Hambleton et al. 2019; Voss et al. 2019). Niemann-Pick Type C2 (NPC2) is a protein located in late endosomes and lysosomes and is implicated in cholesterol transport (Hambleton et al. 2019; Subramanian and Balch 2008; Vanier and Millat 2004). Additionally, the active mechanistic target of rapamycin complex (mTORC) is positioned on lysosomes, which regulates a multitude of cellular processes, has been implicated in coral-dinoflagellate symbiosis (Voss et al. 2019).

Another characteristic feature of lysosomes is their low pH, which is ordinarily around 4.5 (Mellman 1986). v-ATPase is a membrane transport protein that acidifies the phagosome as it matures; it was not only found to be localized to the symbiosome membrane in the corals *Acropora yongei* and *Stylophora pistillata* but also actively acidified the symbiosome to pH ~4 (Barott et al. 2015). The low pH is thought to perpetuate a carbon concentrating mechanism (CCM), which drives photosynthesis by promoting the conversion of HCO_3^- (from the surrounding seawater) to CO_2 (Barott et al. 2015). Furthermore, our findings that reveal the symbiont's ability to survive and replicate at a lysosomal pH suggest that they could withstand the low pH of the symbiosome. The low pH and presence of three lysosomal markers are noteworthy suggestions that the symbiosome may be a modified lysosome; however, understanding the nature of this organelle will not be straightforward until we have additional evidence.

3.5 Pathogenic strategy to reside in modified lysosomes

The accumulation of LAMP1 suggests that lysosomes may, in fact, fuse with the symbiosome, but it is unknown if the symbiosome fuses with traditional lysosomes or if LAMP1 is acquired via a different route. It remains unclear which unique qualities of the symbiosome prevent symbiont digestion and, ultimately, allow symbionts to reside inside of animal cells. Oftentimes, parallels are drawn between mutualistic and pathogenic symbioses, and interestingly, LAMP1 recruitment has been hypothesized to play a critical role during infection

for a variety of pathogens (Madan et al. 2012). While some pathogens have strategies to arrest phagosome maturation and remain intracellular, others, such as *Listeria monocytogenes, Salmonella enterica, Cryptococcus neoformans,* and *Toxoplasma,* reside in LAMP1-positive vacuoles (Alvarez and Casadevall 2006; Birmingham et al. 2008; Levitz et al. 1999; Liss et al. 2017; Madan et al. 2012).

Salmonella enterica is a well-studied example of an intracellular pathogen that resides in a LAMP1-positive vacuole. *S. enterica*-containing phagosomes (SCPs) are devoid of hydrolytic enzymes but retain lysosomal membrane proteins; this was found to be mediated by the effector SifA, produced by *S. enterica*, which subverts the retrograde trafficking of mannose-6-phosphate receptors (MPRs) (Mcgourty et al. 2012). MPRs load hydrolytic enzymes into lysosomes (Coutinho, Prata, and Alves 2012); thereby, the activity of *S. enterica* attenuates the degradative capacity of lysosomes. Additionally, another *Salmonella* effector protein, SipC, was found to specifically bind host Syntaxin6, a SNARE protein involved in trafficking, to recruit the accessory molecules (i.e., vesicle-associated membrane protein 2 (VAMP2), Rab6, and Rab8) necessary to fuse with LAMP1-containing vesicles directly from the Golgi (Madan et al. 2012). Because the symbiosome is not only LAMP1-positive but also retains some other lysosomal features, we could speculate that symbionts reside in a lysosomal-like organelle that is void of hydrolytic enzymes as a result of the symbiont interfering with MPR trafficking; however, no effector molecules have been identified to support this hypothesis.

3.6 Healthy non-symbiotic microalgae are removed by vomocytosis

We found that diverse microalgae and beads were taken up into the endodermal cells of Aiptasia larvae, but they failed to establish a LAMP1-positive niche and were subsequently removed. Because (1) the microalgae appeared healthy after they were expelled from the larvae (Figure 14a) and (2) both the expelled microalgae and beads were frequently reacquired by the host (Figure 15b), we speculated that aposymbiotic larvae constitutively acquire and release microorganisms from the environment to probe for suitable symbionts. The phagocytosed microalgae that fail to initiate symbiosis are expelled back into the surrounding seawater via vomocytosis. We provide evidence that this expulsion is, in fact, vomocytosis and not constitutive exocytosis because the expulsion is (1) stochastic, (2) actin-independent, (3) ERK5-dependent, and (4) occurs for LAMP1-negative microalgae.

While the LAMP1-negative microalgae, i.e., healthy non-symbiotic microalgae, are readily expelled, it should be noted that we also see the expulsion of LAMP1-positive heat-killed microalgae. This expulsion, however, occurs much later than for the healthy controls. The longer residency time before expulsion (Figure 16b) and the accumulation of LAMP1 around heat-killed microalgae (Figure 11b; 12a, b) suggest that the host is attempting to digest the heat-killed microalgae. But ultimately, the host cell may have difficulty digesting the heat-killed microalgae since they too are eventually expelled. This could explain why we see the expulsion of both LAMP1-positive and LAMP1-negative microalgae, which is not the case for vomocytosis of *C. neoformans,* which are always LAMP1-negative (Smith et al., 2015).

The intracellular sorting via vomocytosis is likely independent of intracellular digestion as healthy non-symbiotic microalgae are sorted/expelled more quickly than the heat-killed equivalent (Figure 16b). The possibility that the expulsion of LAMP1-positive heat-killed microalgae occurs via a different route (i.e., constitutive exocytosis) is worth investigating. This could be assessed by live imaging heat-killed-microalgae-infected larvae treated with LatB. If heat-killed microalgae are retained when actin polymerization is inhibited, then it is probable that there is a second, actin-dependent expulsion mechanism at play to remove indigestible material from host cells, for instance. Furthermore, it will be important to disentangle the indigestibility of beads from heat-killed microalgae. While early sorting routinely relies on vomocytosis, heat-killed microalgae may leak nutrients or molecules that entice the host to begin intracellular digestion. Only after the initial vomocytosis is bypassed, a second expulsion mechanism may be required to remove the residual indigestible material.

3.7 Expulsion at the organismal level in both bleaching and regulating symbiont density

In the context of bleaching (loss of symbionts from the host during stress events), expulsion has been described as the primary mechanism by which symbiotic microalgae are lost from host tissue after heat stress (Hoegh-Guldberg et al., 1987; Hoegh-Guldberg & Smith, 1989; McCloskey et al., 1996). These observations were made by measuring symbiont population densities in the hosts before and after heat stress, as well as measuring symbiont concentrations in the surrounding water after extended periods of time (typically 24 hours post-heat stress). Furthermore, there is evidence to suggest that apoptosis and autophagy are induced in the host after exposure to high temperatures, which may account for symbiont expulsion from the host

organism (Downs et al., 2009; S. R. Dunn et al., 2002, 2004; S. R. Dunn & Weis, 2009), but no single pathway was found to be responsible for the expulsion of symbionts in bleaching.

Under normal conditions, observations of extruded symbiont pellets revealed that different anemone species expel pellets with varying compositions. The ratio of healthy symbionts, debris, and other microorganisms, as well as the life stage of symbionts, differed between the different species examined (Steele, 1977). Additionally, it was suggested that symbiont expulsion correlates with their division and ability to re-infect neighboring cells, but it is still unknown which pathway regulates symbiont density or spread throughout the organism.

Based on the literature, it may not be surprising that symbionts are expelled from the organism, but the exact mechanisms that occur at the cellular level are unknown. To date, there have been no observations with cellular resolution that show active symbiont expulsion post-phagocytosis. It should be noted that all previous work focused on adult polyps, whereas our investigations focused on symbiosis establishment during the larval stage.

3.8 Vomocytosis and why evolution favored tighter control

The first investigations of vomocytosis involved macrophages infected with *Cryptococcus neoformans* (Alvarez & Casadevall, 2006; H. Ma et al., 2006), but the field has since extended observations to various other hosts and intracellular partners (Seoane & May, 2020). Initially, it was thought that vomocytosis was a survival tactic utilized by fungal pathogens to escape from the phagocyte without instigating an immune response as the host cell remained undamaged during the getaway, a process that likely first arose in response to predation by amoebae (Chrisman et al., 2010). Vomocytosis was thought to be triggered by the pathogen since only healthy *C. neoformans* were expelled, while heat-killed *C. neoformans,* as well as beads, were not (Alvarez & Casadevall, 2006; H. Ma et al., 2006; Seoane & May, 2020); but our observations demonstrate this may not be pathogen-specific. We not only see the expulsion of heat-killed symbionts, but we also found healthy and heat-killed non-symbiotic microalgae and beads to undergo vomocytosis, suggesting this process is host-driven. Not only do Aiptasia larvae utilize vomocytosis to remove non-beneficial invaders, but it seems as though this mechanism is exploited to select suitable symbionts from the environment.

Discussion

The discrepancy between our observations and those made in vertebrate macrophages regarding who initiates vomocytosis, host or microorganism, can be partly explained when the environment is taken into consideration. For unicellular amoebae that are free-living, both constitutive exocytosis and vomocytosis are efficient ways to remove indigestible or potentially harmful material from the cell as it will simply be released back into the environment. The cells of multicellular organisms, on the other hand, do not have the luxury of releasing a pathogen as they run the risk of infecting neighboring cells or tissues; therefore, the retention and degradation of the material are vital for their survival.

As multicellularity arose during evolution, cooperation between cells became essential for the benefit of the organism as a whole (Cavalier-Smith, 2016). While phagocytosis and intracellular digestion are vital for both defense and nutrition in unicellular amoebae or ciliates, individual cells of multicellular organisms had to forfeit the ability to feed as they now needed to cooperate with their neighbors. This cooperation brought about mouths and guts, for example, where cells developed novel functions that supported the nutritional requirements of the organism as a whole and consequently encouraged complexity (Cavalier-Smith, 2016). Fascinatingly, it could be considered that Aiptasia represent the transition from unicellular life to multicellular complexity, as they comprise organized cells that form two tissue layers, yet these tissues are in constant contact with their environment. The strict regulation of vomocytosis by vertebrate macrophages is detrimental to symbiosis establishment as Aiptasia rely on this mechanism to select symbionts from the environment. Therefore, we can speculate that vomocytosis is not pathogen-specific but instead is an ancient clearance mechanism utilized by unicellular organisms and adopted by symbiotic cnidarians as a means of establishing symbiosis. During evolution, dinoflagellate symbionts developed the ability or had the appropriate features to circumvent expulsion by vomocytosis, and thus, escaping vomocytosis became a hallmark step in the evolution of intracellular life.

Accordingly, recent findings revealed that the mesodermal germ layer of bilaterians, which gives rise to the phagocytic cells of the innate immune system, is homologous to the endoderm of cnidarians, whereas the bilaterian endoderm is homologous to cnidarian pharyngeal ectoderm (Steinmetz, 2019). During gastrulation in *Nematostella vectensis*, the endoderm undergoes an epithelial to mesenchymal transition (EMT), where EMT is characteristic of the ingression of mesoderm (Kraus & Technau, 2006; Magie et al., 2007; Salinas-Saavedra et al., 2018). Additionally, mesodermal markers were expressed in the endoderm of *N. vectensis,* and

the ectodermal pharynx had an endodermal transcriptional profile (Martindale et al., 2004; Technau, 2020). These results contest Haeckel's theory that germ layer derivatives have similar functions and origins (Haeckel, 1873), but they are intriguing in the context of our observations, with more parallels being drawn between the phagocytic cells of vertebrates and the endoderm of Aiptasia.

3.9 Symbionts circumvent vomocytosis by cell-specific immune suppression

The endoderm of Aiptasia larvae plays a fundamental role in mediating beneficial and harmful interactions, both for nutrient acquisition and defense. As intracellular residents of the endoderm, dinoflagellate symbionts circumvent the immune response and establish a LAMP1-positive niche. Symbiont uptake induces cell-specific immune suppression, which, in turn, suppresses vomocytosis. Most non-symbiotic microorganisms or particles that make their way into an Aiptasia endodermal cell fail to induce immune suppression and will be effectively removed by vomocytosis. We identified a direct link between immune stimulation and vomocytosis in the early stages of symbiosis establishment (Figure 23a, c), but because symbiont-uptake induces extensive transcriptional immune suppression in the host cell, exogenous immune stimulation alone was not capable of prompting symbiont vomocytosis (Figure 23b).

Modulation of the host immune system is an inherent aspect of both pathogenic and mutualistic interactions, and mechanistically, symbionts are believed to utilize immune modulation strategies similar to pathogens to persist intracellularly. One example, involving TGF-β, revealed that in coral larvae inhibition of the TGF-β pathway impaired symbiosis establishment (Berthelier et al., 2017). Although our transcriptomic analysis reveals downregulation of several components of the TGF-β pathway (Figure 21), TGF-β can be either pro- or anti-inflammatory depending on concentration and context (Wahl, 1994); and because the levels and activity of TGF-β in vivo during symbiosis are unknown, it remains unclear if this cytokine or associated pathway is important for mediating cnidarian-dinoflagellate symbiosis.

In contrast to previous transcriptomic analyses that reported organism-wide downregulation of NF-κB mRNA and protein during symbiosis establishment in Aiptasia (Mansfield et al., 2017; Wolfowicz et al., 2016), our analysis, did not show suppression of NF-κB transcription in symbiont-containing cells (Figure 21). This suggests that at the level of the individual cell, NF-κB downregulation is not a prerequisite for symbiosis establishment. Unexpectedly, we

observed the upregulation of NF-κB transcription. Although our results do not reiterate previous findings, it could be that NF-κB suppression is important for organism-wide maintenance of a stable symbiosis but not for intracellular establishment in the host cell. Furthermore, because activation and inhibition are both possibilities to promote survival depending on context (e.g., activation to promote replication or prevent apoptosis; suppression to dampen immune response), it is likely that the NF-κB signaling pathway must be carefully managed to achieve long-term persistence.

It is clear that innate immunity signal transduction pathways are dynamic and complex, and the outcome of the immune response, either suppressive or stimulating, is context dependent. Targeting the various components of signal transduction involved in immunity is a highly effective and mutable strategy for intracellular pathogens or symbionts to survive within the constraints of their hosts' immune systems. However, both intracellular pathogens and symbionts must sustain a delicate balance between host-cell death and survival. And in the case of symbiotic organisms, the host immune system must simultaneously thwart invasion by harmful microorganisms and encourage the maintenance of symbionts.

3.10 Symbiont-uptake induces downregulation of MyD88

Although, NF-κB itself did not appear to mediate symbiosis establishment, our transcriptome, nevertheless, revealed a role for TLR signaling. The microbe associated membrane proteins (MAMPs) of various pathogens or symbionts will bind to TLRs at the host cell membrane or endolysosomal membrane. TLRs can recognize a vast number of MAMPs, albeit with a degree of specificity. Upon binding of a MAMP to a TLR, a signal cascade initiates in the cytoplasm of the host cell with the recruitment of adaptor proteins (Deguine & Barton, 2014; Peralta et al., 2007). To date, there are 13 members of the TLR family and 11 of these members rely on the adaptor MyD88 to advance the intracellular signal cascade (Akira et al., 2006; Kawai & Akira, 2007). Thus, MyD88 would be an ideal target to induce broad immune suppression in an effort to promote intracellular maintenance. For example, the pathogenic bacteria *Escherichia coli* strain CFT073, *Brucella melitensis,* and *Yersinia pestis* all express TIR-containing proteins that bind to MyD88 ultimately preventing downstream signaling (Cirl et al., 2008; Rana et al., 2011; Salcedo et al., 2013).

Our transcriptome revealed that MyD88 expression is significantly lower in cells that contain symbionts (Figure 21, 22), and therefore, its repression may be associated with symbiosis

establishment. The role of MyD88 in mediating host-microbe interactions was also explored in the cnidarian *Hydra vulgaris*. *H. vulgaris* polyps deficient in MyD88 were more susceptible to infection with the pathogenic bacteria, Pseudomonas aeruginosa, compared to control polyps (Franzenburg et al., 2012). Alternatively, MyD88-deficient polyps that were rendered germ-free had difficulty reestablishing the bacterial microbiota in the first two weeks following antibiotic treatment; however, after 19 weeks, the bacterial communities of the MyD88-deficient polyps resembled those of the control polyps in terms of diversity and proportions (Franzenburg et al., 2012). These findings indicate that in *H. vulgaris* polyps (1) MyD88 activity is important for preventing infection by pathogenic microorganisms, and (2) MyD88 activity mediates bacterial recolonization, but not homeostasis. While we found MyD88 to be transcriptionally repressed in symbiont-containing cells, we found that inhibition of MyD88 activity during infection did not yield an enhanced infection with symbionts compared to the control (Figure 24a). MyD88 inhibition did seem to interfere with uptake or retention of non-symbiotic microalgae during the 24-hour infection, however. Post-infection there were significantly more symbiotic larvae after MyD88 inhibition compared to the control (Figure 24b); whereas no such effect was observed for larvae infected with non-symbiotic microalgae. These findings further confirm the complexity of innate immune signaling in managing symbiotic interactions, just as with *H. vulgaris*. Although targeting this highly conserved and critical adaptor molecule seems straightforward and efficient, we cannot overlook the intricacies of the innate immune system, while appreciating the spatial, temporal, and contextual dynamics required for regulation.

3.11 Interplay of microorganisms in creating the holobiont

As previously discussed, the host must not only search for and encourage colonization by symbionts, but they must also defend themselves against invasion by potential pathogens. But just as the functionality of the immune system is not black and white, neither is the role of the countless microorganisms that these hosts encounter. There has been a concerted effort in recent years to expand focus and consider the impact that the microbiome has on the health of organisms. In addition to the dinoflagellate symbionts, bacteria, fungi, archaea, viruses, and other protists, such as *C. velia*, live in close proximity to or even on cnidarian hosts. The exact role of the cnidarian microbiome is still unknown; however, it is believed to support overall health of the host (van Oppen & Blackall, 2019). It has been suggested that bacterial members of the holobiont are important for providing nutrients or cycling nutrients, producing

antimicrobial compounds or outcompeting potentially harmful microorganisms to protect the host, or for larval settlement and metamorphosis (McDevitt-Irwin et al., 2017).

The composition of the microbiome is dynamic and is known to fluctuate according to life stage, location, or in response to stressors. Coral larvae, for example, tend to have a more diverse microbiome than adult polyps (Epstein et al., 2019; Lema et al., 2014; Littman et al., 2009) and it is believed that winnowing steps must occur to shape the adult holobiont. This winnowing could serve to meet the needs of the local environment where a free-swimming, planula larva will settle and undergo metamorphosis, for example. The mechanisms that regulate the composition of the microbiome are currently under investigation, however the immune suppression induced by symbiosis establishment has been proposed as a means of doing so (van Oppen & Blackall, 2019). Just as the host shapes the microbiome, so too does the microbiome influence the host and the innate immune system.

3.12 Updated model for symbiont selection and symbiosis establishment

(1) Phagocytosis of microalgae is indiscriminate for particles of the comparable size (6-8 μm)

(2) Sorting of symbionts and non-symbiotic microalgae occurs post-phagocytosis

(3) Non- symbiotic microalgae are expelled via vomocytosis

(4) Selection of symbionts requires local immune suppression to halt expulsion

(5) Symbionts establish a LAMP1-positive niche

4 Conclusions

Using this newly established comparative framework, we find that Aiptasia larvae phagocytose a wide array of microalgae and decisive symbiont selection mechanisms occur post-phagocytosis. Non-symbiotic microalgae are expelled via an ancient immune response that became more tightly regulated through evolution and progression of organismal complexity. Vomocytosis – and not phagolysosome degradation – is responsible for sorting symbionts from non-symbiotic microalgae. Symbiont-uptake induces broad immune suppression at the level of the individual cell, not at the organismal level as previously thought. Local immune suppression, to permit symbiont maintenance, could explain how host organisms are not easily susceptible to infection by pathogenic microorganisms once their immune response is suppressed. However, the temporal dynamics of immune suppression would need to be assessed, additionally, as well as the role of the other members of the holobiont, e.g., bacteria, archaea, and fungi. While the nature of the symbiosome still remains elusive, understanding how the LAMP1-niche is formed, as well as the degradative capacity of the organelle itself will provide insight into intracellular persistence and metabolic exchange. With this work, we contribute to the preexisting knowledge of the cellular and molecular mechanisms behind cnidarian-dinoflagellate symbioses, specifically aspects of cnidarian immunity and symbiont selection and maintenance.

5 Methods

5.1 Live organism culture and maintenance

5.1.1 Aiptasia culture conditions and spawning induction

Adult Aiptasia polyps from the clonal lines F003 (female) and CC7 (male) (Carolina Biological Supply Company 162865; Burlington, USA) were induced to spawn using the protocol described in (Grawunder et al., 2015). Aiptasia larvae were isolated from parent tanks via stepwise filtration and maintained in glass beakers in 0.22 µm filter-sterilized artificial seawater (FASW) (Coral Pro Salt; Red Sea Aquatics Ltd, Houston, USA) at 31–34 ppt salinity and exposed to 20–25 µmol m^{-2} s^{-1} of photosynthetically active radiation (PAR) as measured with an Apogee PAR quantum meter (MQ-200; Apogee, Logan, USA) during a diurnal 12-hour light/12-hour dark cycle at 26 ºC. Larvae were maintained at approximately 300 larvae per ml.

5.1.2 Microalgae culture conditions

Clonal axenic cultures of *Breviolum minutum* clade B (strain SSB01, symbiont) (Xiang et al., 2013), *Microchloropsis gaditana* CCMP526 (NCMA, Bigelow Laboratory for Ocean Sciences, Maine, USA), *Nannochloropsis oculata*, and *Chromera velia* (NORCCA K-1276, NIVA, Oslo, Denmark*)* were cultured in 0.22 µm filter-sterilized 1x Diago IMK medium (Wako Pure Chemicals, Osaka, Japan) in cell culture flasks, and exposed to a 12-hour light/12-hour dark cycle under 20–25 µ mol m^{-2} s^{-1} of PAR as measured with an Apogee PAR quantum meter (MQ-200; Apogee, Logan, USA). Sterile stocks of symbionts (SSB01), *N. oculata*, and *C. velia* were grown at 26 ºC and *M. gaditana* at 18 ºC. Infection cultures for all microalgae (including *M. gaditana*) were grown at 26 ºC for 1-2 weeks post splitting from sterile stock cultures before infection.

5.2 Infection assays

5.2.1 Infection assay using healthy microalgae

At least three batches of aposymbiotic Aiptasia larvae from distinct spawning events were collected as previously described and were maintained in FASW at 26 ºC in glass beakers. Larvae between 4- and 8-days post fertilization (dpf) were filtered and washed into new FASW before infection with 1.0 x 10^5 microalgae per ml of each of the microalgae species. All

infections were carried out at 26 ºC with a 12-hour light/12-hour dark cycle. After a 6- or 24-hour infection, the larvae were filtered to remove the microalgae and washed into new FASW.

5.2.2 Infection assay using heat-killed microalgae or polystyrene beads

For heat-killed microalgae and bead infection experiments, larvae were collected as previously described and concentrated to approximately 1000 larvae per ml in glass beakers. Microalgae were killed by heating to 100 ºC for 5 minutes, then cooled to room temperature (RT) before infection. 1.5 ml of larvae were distributed into 2 % Ficoll-coated 2 ml Eppendorf tubes and infected with 1.0×10^5 microalgae or beads (FSFR007, Bangs Laboratories, Inc., Indiana, USA) per ml of the respective particle type. Tubes containing larvae and microalgae or beads were rotated at 26 °C and exposed to a 12-hour light/12-hour dark cycle. After a 6- or 24-hour infection, the larvae were washed to remove the microalgae and fresh FASW was added.

5.3 Imaging and staining procedures

5.3.1 Infection quantification of fixed samples

Fixation of Aiptasia larvae occurred at 1-, 2-, 3-, 6-, and 10-day(s) post-infection (dpi). Infected larvae were incubated for 30 minutes with a 4 % formaldehyde solution (F1635, Sigma-Aldrich, Munich, Germany) at RT. After fixation, larvae were washed twice with 0.1 % Triton X-100 (PBS-Triton) (3051, Carl Roth GmbH, Karlsruhe, Germany) and once with 1x PBS. Samples were mounted in 87 % glycerol (G5516, Sigma-Aldrich) in PBS with the addition of 2.5 mg per ml 1,4-Diazabicyclo [2.2.2] octane (DABCO) (D27802, Sigma-Aldrich). For each biological replicate, at least 50 larvae per infection condition were counted. Additionally, representative differential interference contrast (DIC) and epi-fluorescent images capturing the autofluorescence of microalgae were taken. A Nikon Eclipse Ti inverted microscope with a Nikon Plan Fluor 40x air objective was used to acquire microscopy images, which were later analyzed and processed using Fiji software (Schindelin et al., 2012). Data were recorded in Microsoft Excel version 16.16.6.

5.3.2 Phalloidin staining to visualize F-actin

After a 24-hour infection, larvae were fixed for 30 minutes with a 4 % formaldehyde solution at RT. After fixation, larvae were transferred to 1.5 ml Eppendorf tubes and washed in 0.05 % PBS-Tween20 (P7949, Sigma-Aldrich) for 5 minutes. For permeabilization of larvae, samples

were incubated in a solution of 1 % PBS-Triton and 20 % DMSO (67-68-5, FisherScientific, Schwerte, Germany) and rotated at 0.25 rpm for 1 hour at RT. Next, the permeabilization solution was removed and larvae were resuspended in blocking solution: 5 % normal goat serum (005-000-121, Jackson ImmunoResearch Laboratories, Inc., Ely, UK) in 0.05 % PBS-Tween20. Larvae were rotated for 30 minutes in blocking solution at RT. After blocking, larvae were washed twice with 0.05 % PBS-Tween20. Next, Phalloidin Atto 565 (94072, Sigma-Aldrich) was diluted 1:200 in 0.05 % PBS-Tween20 and added to larvae, which were then rotated for 1 hour at RT and protected from light. Then, larvae were washed three times in 0.05 % PBS-Tween20. For visualization of nuclei, larvae were incubated for 30 minutes in 10 µg per ml Hoechst (B2883, Sigma-Aldrich) diluted in a buffer containing 0.1 % Triton X-100, 2 % bovine serum albumin (BSA) (A7906, Sigma-Aldrich), and 0.1 % sodium azide (S2002, Sigma-Aldrich) in Tris-buffered saline (TBS) (pH 7.4), while rotating at RT and protected from light; followed by three, 5 minutes washes with 0.05 % PBS-Tween20. Larvae were resuspended stepwise into glycerol from 30 % to 50 % to 100 % and mounted. Confocal images were acquired with a Leica TCS SP8 stand using 63x glycerol immersion objective (NA 1.30) using Leica LAS X software, and the analysis was performed using Fiji software (Schindelin et al., 2012). Hoechst was excited with the 405 nm laser line and detected at 410-501 nm, Atto 565 was excited with the 561 nm laser line and detected at 542-641 nm, and microalgae autofluorescence was excited with the 633 nm laser line and detected at 645-741 nm.

5.3.3 Live imaging of Aiptasia larvae

Live imaging chambers were prepared by adhering two 2.5 mm x 5 mm strips of non-toxic double-sided tape (TES5338, Tesa, Norderstedt, Germany) at the peripheral ends of a 35 mm µ-Dishes (81166, Ibidi, Gräfelfing, Germany). 1.5 % w/v low gelling agarose (LGA) (A4018, Sigma-Aldrich) was added to FASW and heated to 80 ºC to ensure it was fully dissolved and liquid. The temperature of the heat block was then set to 37 ºC and the liquid LGA remained at this temperature until use. 1 ml of larvae (approximately 300 larvae) were transferred to a 1.5 ml Eppendorf centrifuge tube. The larvae were pelleted after a quick vortex using a Sprout mini centrifuge (552021, Biozym Scientific GmbH, Hessisch Oldendorf, Germany). Working quickly to avoid polymerization of LGA at RT, a proportion of the larval pellet and the 37 ºC 1.5 % LGA were gently combined for a final LGA concentration of 1.14 %. The 1.14 % LGA-larvae mixture was added to the center of the imaging chamber between the two strips of double-sided tape. A 5 mm x 18 mm glass coverslip (cut to size beforehand) was carefully

pressed on top of the LGA-larvae mixture so that it rested on the double-sided tape at both ends. 2 ml of FASW were added to the Ibidi plate so that the sample was completely submerged. Z-stacks were acquired every 5 or 15 minutes (as indicated) in DIC and TexasRed channels. Microscopy images were acquired with a Nikon Eclipse Ti inverted microscope using a Nikon Plan Fluor 20x air objective. Images were analyzed and processed using Fiji software (Schindelin et al., 2012). Data were recorded in Microsoft Excel version 16.16.6.

5.3.4 Aiptasia-specific anti-LAMP1 antibody purification

An Aiptasia-specific antibody against the LAMP1 homolog (LOC110235349) was generated in rabbit against the peptide IIGRRKSQRGYEKV (KXJ16564.1) coupled to the adjuvant keyhole limpet hemocyanin (DJ-Diagnostik BioScience, Göttingen, Germany). Using the third and final (4^{th}) bleeds, the antibody was affinity purified using the synthetic peptide coupled to N-hydroxysuccinimide esters-activated sepharose (17090601, GE Health Care Life Sciences) according to the manufacturer's protocols.

5.3.5 Western blot LAMP1 antibody validation and deglycosylation assay

Aiptasia polyps (two aposymbiotic and two symbiotic adults) were separately homogenized in 50 mM Tris-HCl pH 7.5, 200 mM NaCl, and 1 % NP-40 with 2x Halt Protease Inhibitor Cocktail (78430, Thermo Fisher Scientific), followed by two rounds of 25 pulses at duty cycle 40 %, output control 1.8 of sonication on ice (Sonifier 250, Branson Ultrasonics). Next, the homogenate was centrifuged at maximum speed for 10 minutes at 4 °C, and then the supernatant was transferred to a new 1.5 ml Eppendorf tube. For N-deglycosylation, PNGase F (P0704S, New England BioLabs Inc.) was used following the manufacturer's protocol with a modification wherein the reaction was kept for 3 hours at 37 °C followed by overnight at RT. As a control for the western blot analysis, 0.5 mg per ml of LAMP1 antibody was neutralized with 1 mg per ml of LAMP1 peptide (IIGRRKSQRGYEKV) in 4 % milk in 0.1 % PB-Triton overnight at 4 ºC. Untreated extracts were diluted 1:1 in 5X loading dye and heated to 100 °C; PNGase F treated extracts were diluted 1:1 in 5X loading dye and heated to 60 °C for 5 minutes. Samples were loaded into and run on a 4-20 % precast gel (4561095, Bio-Rad Laboratories Inc.) at 90 V for 15 minutes, followed by 200 V for 1 hour at RT in 1x SDS running buffer. The proteins were transferred onto a nitrocellulose membrane at 0.37 A for 1 hour and 15 minutes at RT in 1x transfer buffer (100 ml methanol, 100 ml 10X transfer buffer, 800 ml water). After transfer, the membrane was blocked in 4 % milk in 0.1 % Triton X-100 in PBS for 1 hour at

RT. The blot was cut in two: half was incubated in LAMP1 antibody diluted 1:2000 in blocking buffer, and the other half was incubated with neutralized LAMP1 antibody, both rocking overnight at 4 °C. The blots were then washed in 0.1 % Triton X-100 in PBS three times for 15 minutes at RT. Goat-α-rabbit-HRP (Jackson ImmunoResearch) was added at 1:5000 for 1 hour at RT, protected from light. After incubation with secondary antibody, the blots were washed in 0.1 % Triton X-100 in PBS three times for 15 minutes, followed by one wash in 1x PBS. The blot was developed using a 1:1 enhanced chemiluminescent solution (GERPN2232, Sigma-Aldrich) and the signal was detected and acquired with an enhanced chemiluminescent imager (ChemoCam, Intas).

5.3.6 Western blot WASHC1

Aiptasia polyps (two aposymbiotic and two symbiotic adults) were separately homogenized in 180 µl 1x TBS (chilled) with 2 µl of 100x Halt Protease Inhibitor Cocktail (78430, Thermo Fisher Scientific). Then, 20 µl of 1x TBS 10 % Triton X-100 (chilled) was added for a final concentration of 1 % Triton X-100 and kept on ice. Additionally, larval extract and human embryonic kidney (HEK) cell extract was made by pelleting the cells or 10,000 larvae using the Sprout mini centrifuge (552021, Biozym Scientific GmbH, Hessisch Oldendorf, Germany) and resuspending the pellets in 180 µl 1x TBS (chilled) with 2 µl of 100x Halt Protease Inhibitor Cocktail. The larvae were then subjected to sonication with 20 pulses, duty cycle 40 %, output control 1.8, and immediately placed on ice when finished. All samples were then rotated at 4 ºC for 30 minutes. They were then centrifuged at 15000g at 4 ºC for 10 minutes. The supernatants were then transferred into new tubes, 20 µl of 5x loading dye was added, and samples were incubated for 5 minutes at 100 ºC. Pellets were resuspended in 200 µl lysis buffer (180 µl 1x TBS + 20 µl 1xTBS with 10 % Triton X-100). Then, 20 µl of 5X loading dye was added to 80 µl of the resuspended pellet sample and boiled for 5 minutes at 100 ºC. All samples were then loaded into and run on a 12 % polyacrylamide gel at 90 V for 15 minutes, followed by 200 V for 1 hour at RT in 1x SDS running buffer. The proteins were transferred onto a nitrocellulose membrane at 0.37 A for 1 hour and 15 minutes at RT in 1x transfer buffer (100 ml methanol, 100 ml 10X transfer buffer, 800 ml water). After transfer, the membrane was blocked in blocking buffer (0.1 % Tween 20 in 1x TBS) for 1 hour at RT. The blot was incubated in WASHC1 antibody (HPA002689, Sigma-Aldrich) diluted 1:250 in blocking rocking overnight at 4 °C. The blots were then washed in 0.1 % Tween 20 in TBS three times for 15 minutes at RT. Goat-α-rabbit-HRP (Jackson ImmunoResearch) was added at 1:5000 for

1 hour at RT, protected from light. After incubation with secondary antibody, the blots were washed in 0.1 % Tween 20 in TBS three times for 15 minutes, followed by one wash in 1x TBS. The blot was developed using a 1:1 enhanced chemiluminescent solution (GERPN2232, Sigma-Aldrich) and the signal was detected and acquired with an enhanced chemiluminescent imager (ChemoCam, Intas).

5.3.7 Immunofluorescence staining (LAMP1)

After a 6- or 24-hour infection, larvae were fixed for 45 minutes with a 4 % formaldehyde solution at RT, followed by three washes in 0.2 % PBS-Triton and one wash in PBS. Larvae were then permeabilized in 0.2 % PBS-Triton for 1.5 hours while rotating at RT. Then, the permeabilization solution was removed and larvae were resuspended in blocking solution (5 % normal goat serum and 1 % BSA in 0.2 % PBS-Triton) and rotated for 1 hour at RT. Aiptasia-specific rabbit-α-LAMP1 (see above) was diluted 1:100 in blocking solution and added to larvae to incubate overnight at 4 °C while rotating. The following day, the excess, unbound primary antibody was removed by three consecutive 15-minute washes in 0.2 % PBS-Triton. Goat-α-rabbit AlexaFluor488 (ab150089, Abcam, Berlin, Germany) was diluted 1:500 in blocking solution and added to larvae to incubate for 1.5 hours at RT, protected from light and rotating. Larvae were washed two times in 0.2 % PBS-Triton to remove secondary antibody solution. In order to visualize nuclei, larvae were incubated for 15-minute with 10 µg per ml Hoechst staining solution protected from light at RT while rotating. Finally, larvae were washed twice with 0.2 % PBS-Triton and once with PBS. Samples were mounted in 87 % glycerol in PBS with the addition of 2.5 mg per ml DABCO. Confocal images were acquired with a Leica TCS SP8 stand using 63x glycerol immersion objective (NA 1.30) using Leica LAS X software, and the analysis was performed using Fiji software (Schindelin et al., 2012). Hoechst was excited with the 405 nm laser line and detected at 410-501 nm, Alexa488 was excited with the 496 nm laser line and detected at 501-541 nm, and microalgae autofluorescence was excited with the 633 nm laser line and detected at 645-741 nm.

5.3.8 Immunofluorescence staining (WASHC1)

After a 6-hour infection, larvae were fixed for 45 minutes with a 4 % formaldehyde solution at RT, followed by three washes in 0.2 % PBS-Triton and one wash in PBS. Larvae were then permeabilized in 0.2 % PBS-Triton for 1.5 hours while rotating at RT. Then, the permeabilization solution was removed and larvae were resuspended in blocking solution (5 %

normal goat serum and 1 % BSA in 0.2 % PBS-Triton) and rotated for 1 hour at RT. α-WASHC1 (HPA002689, Sigma-Aldrich) was diluted at 1:100 for 1 µg/ml in blocking solution and added to larvae to incubate overnight at 4°C while rotating. The following day, the excess, unbound primary antibody was removed by three consecutive 15-minute washes in 0.2 % PBS-Triton. Goat-α-rabbit AlexaFluor488 (ab150089, Abcam, Berlin, Germany) was diluted 1:500 in blocking solution and added to larvae to incubate for 1.5 hours at RT, protected from light and rotating. Larvae were washed two times in 0.2 % PBS-Triton to remove secondary antibody. In order to visualize nuclei, larvae were incubated for 15-minute with 10 µg per ml Hoechst staining solution protected from light at RT while rotating. Finally, larvae were washed twice with 0.2 % PBS-Triton and once with PBS. Samples were mounted in 87 % glycerol in PBS with the addition of 2.5 mg per ml DABCO. Confocal images were acquired with a Leica TCS SP8 stand using 63x glycerol immersion objective (NA 1.30) using Leica LAS X software, and the analysis was performed using Fiji software (Schindelin et al., 2012). Hoechst was excited with the 405 nm laser line and detected at 410-501 nm, Alexa488 was excited with the 496 nm laser line and detected at 501-541 nm, and microalgae autofluorescence was excited with the 633 nm laser line and detected at 645-741 nm.

5.4 Cell-type-specific transcriptomic analysis

5.4.1 Sample collection via cell picking and sequencing

At 6-7 dpf, approximately 300 larvae per ml were infected with either 1.0 x 10^5 symbiont cells per ml, 1.0 x 10^5 *M. gaditana* cells per ml, or left uninfected for 24 to 48 hours. For each biological replicate from distinct spawning events, 3-5 larvae were incubated for 5 minutes in 5 ml of Calcium- and Magnesium-free artificial seawater (CMF-SW, doi:10.1101/pdb.rec12053). In order to remove ectodermal cells, larvae were then placed in a solution of 70 µl of 0.5 % Pronase (10165921001, Sigma-Aldrich) and 1 % sodium thioglycolate (T0632, Sigma-Aldrich) in CMF-SW for approximately 2 minutes. Additionally, ectodermal cells were further removed from larvae by physical disruption as they were pipetted up and down 3-5 times. The naked endoderm was transferred to fresh FASW, while the remaining ectodermal cells were carefully removed with a pipette. Endodermal cells were further separated using tweezers. A custom microcapillary needle (Science Products GB100T-8P) pulled to a diameter of 8-12 µm (Micropipette Puller P-97, Sutter Instrument) was used to pick cells. Groups of approximately 7-20 cells representative of each condition – either

symbiotic, aposymbiotic from symbiotic animals, aposymbiotic from aposymbiotic animals, *M. gaditana*-containing cells, or microalgae-free cells from *M. gaditana*-containing larvae – were picked. At the time of picking, cells were taken up into capillaries containing 4.3 µl of lysis buffer (0.2 % Triton X-100, 1 U per µl Protector RNase inhibitor (3335399001, Sigma-Aldrich), 1.25 µM oligo- dT30VN, and 2.5 mM dNTP mix). After selection, the cells were flushed out of the capillary in the lysis buffer and flash frozen. RNA reverse transcription and 21 PCR cycles to pre-amplify cDNA were used to generate sequencing libraries as described in (Picelli et al., 2014). After cDNA library preparation, samples were sequenced on a NextSeq500 (Illumina) with 75-base pair paired-end reads. The reads can be accessed via the NCBI sequence read archive (SRA) under two SRA projects, SRP229372 and SRP233508. The SRA project SRP229372 references groups of cells from aposymbiotic or symbiotic larvae, and the accession numbers for each group of cells are as follows: endodermal cells from aposymbiotic larvae (SRX7119772-7119776), symbiont-containing cells (SRX7119782-7119787), aposymbiotic cells from symbiotic larvae (SRX7119777-7119781). The SRA project SRP233508 references groups of cells from larvae infected with *M. gaditana*, and the accession numbers for each group of cells are as follows, *M. gaditana*-containing cells (SRX7229078-7229080) and microalgae-free cells from *M. gaditana*-containing larvae (SRX7229075-7229077).

5.4.2 Computational methods

Using the Aiptasia genome version GCF_001417965.1, paired reads were mapped with HISAT2 version 2.1.0 using default settings (except for –X 2000 --no-discordant --no-unal --no-mixed). Default settings in Trinity version 2.5.1 with salmon version 0.10.2 were used to quantify transcripts. For all samples, a Perl script supplied with Trinity was used to generate the principal component analysis. DEseq2 was used to analyze differential expression (Love et al., 2014) (log2-fold change ≥ 1, adjusted p-value ≤ 0.05) in R! version 3.5.2 (R Core Team, 2018). Innate immunity pathways were graphed as found in KEGG (Kanehisa & Goto, 2000), using the R! package “ComplexHeatmap” (Gu et al., 2016) in KNIME (Berthold et al., 2008). The TLR pathway transcriptome analysis was generated in R! using the mean corrected log fold expressions from Deseq2 in “pathview” (Luo & Brouwer, 2013). The KNIME workflow used for this analysis can be found at https://doi.org/10.24433/CO.0872345.v1.

5.5 Exogenous perturbations to Aiptasia or symbionts

5.5.1 LPS treatment of Aiptasia larvae

Five batches of aposymbiotic Aiptasia larvae from distinct spawning events between 4- and 8-dpf were filtered and washed into new FASW at approximately 300-500 larvae per ml. For each replicate, larvae were then divided into two groups (treatment vs. control) and incubated with either 20 µg per µl LPS (from *Escherichia coli* O127:B8, Sigma-Aldrich) or without for 1 hour. Infections with 1.0 x 10^5 microalgae per ml of each of the microalgae species were carried out at 26 ºC with a 12-hour light/12-hour dark cycle. The larvae were fixed after a 24-hour infection in 4 % formaldehyde for 30 minutes. Samples were then washed in PBS and subsequently mounted in 100 % glycerol. For each biological replicate, at least 100 larvae per infection condition were counted. The autofluorescence of the microalgae was used for counting and quantification, which was carried out using a Nikon Eclipse Ti inverted microscope with a Nikon Plan Fluor 20x air objective. Data were recorded in Microsoft Excel version 16.16.6.

5.5.2 ERK5 inhibitor treatment of Aiptasia larvae

Six batches of aposymbiotic Aiptasia larvae from distinct spawning events between 4- and 8-dpf were filtered and washed into new FASW at approximately 300-500 larvae per ml. For each replicate, larvae were then divided into two groups (treatment vs. control) and incubated with either 1 µM XMD17-109 (0.1 % DMSO, Carl-Roth) or 0.1 % DMSO for 1 hour. Infection with 1.0 x 10^5 symbiont cells per ml was carried out at 26 ºC with a 12-hour light/12-hour dark cycle. The larvae were fixed after a 24-hour infection in 4 % formaldehyde for 30 minutes. Samples were then washed twice in 0.2 % PBS-Triton, followed by one wash in PBS, and subsequently mounted in 87 % glycerol in PBS with the addition of 2.5 mg per ml DABCO. For each biological replicate, at least 100 larvae per infection condition were counted. Utilizing autofluorescence of symbiont cells, counting and quantification were carried out using a Nikon Eclipse Ti inverted microscope with a Nikon Plan Fluor 20x air objective. Data were recorded in Microsoft Excel version 16.16.6.

5.5.3 LPS post-infection treatment

Five batches of aposymbiotic Aiptasia larvae from distinct spawning events between 4- and 8-dpf were filtered and washed into new FASW at approximately 300-500 larvae per ml. Infection with 1.0 x 10^5 symbiont cells per ml was carried out at 26 ºC with a 12-hour light/12-hour dark

cycle for 24 hours. Then, the larvae were filtered to remove non-phagocytosed symbiont cells from the water and were kept for an additional 24 hours at 26 ºC. For each replicate, half of the infected larvae were exposed to 20 µg per ml of LPS for 24 hours while the other half remained untreated at 26 ºC; after 24 hours, all samples were fixed with 4 % formaldehyde for 30 minutes at RT. Samples were then washed in PBS and subsequently mounted in 100 % glycerol. For each biological replicate, at least 100 larvae per treatment condition were counted. A Nikon Eclipse Ti inverted microscope was used to visualize the autofluorescence of symbiont cells. Counting and quantification were carried out using a Nikon Plan Fluor 20x air objective. Data were recorded in Microsoft Excel version 16.16.6.

5.5.4 Live imaging of early infection with LPS treatment

Three to four batches of aposymbiotic Aiptasia larvae from distinct spawning events between 4- and 8-dpf were filtered and washed into new FASW at approximately 300-500 larvae per ml. For each replicate, larvae were then divided into two groups (treatment vs. control) and incubated with either 20 µg per µl LPS or without for 1 hour. Then, 1.0 x 10^5 symbiont cells per ml were added, and samples were incubated at 26 ºC for 1 hour. They were then mounted in live imaging chambers as previously described. In LPS treated larvae, LPS was added to both the LGA and the surrounding FASW. Z-stacks were acquired every 15 minutes for 1.5 hours in DIC and TexasRed channels. Microscopy images were acquired with a Nikon Eclipse Ti inverted microscope using a Nikon Plan Fluor 20x air objective. Images were analyzed and processed using Fiji software (Schindelin et al., 2012). Data were recorded in Microsoft Excel version 16.16.6. For each independent experiment (n=3, LPS treatment; n=4, control), between 6 and 14 larvae with a total of 42 (LPS) symbiont cells or 50 (control) symbiont cells were observed.

5.5.5 Live imaging of early infection with ERK5 inhibitor treatment

Five batches of aposymbiotic Aiptasia larvae from distinct spawning events between 4- and 8-dpf were filtered and washed into new FASW at approximately 300-500 larvae per ml. For each replicate, larvae were then divided into two groups (treatment vs. control) and incubated with either 1 µM XMD17-109 (0.1 % DMSO) or 0.1 % DMSO for 1 hour. Then, 1.0 x 105 symbiont cells per ml were added and samples were incubated at 26 ºC for 1 hour. They were then mounted in live imaging chambers as previously described. In XMD17-109 treated larvae, XMD17-109 was added to both the LGA and the surrounding FASW. Z-stacks were acquired

every 15 minutes for 12 hours in DIC and TexasRed channels. Microscopy images were acquired with a Nikon Eclipse Ti inverted microscope using a Nikon Plan Fluor 20x air objective. Images were analyzed and processed using Fiji software (Schindelin et al., 2012). Data were recorded in Microsoft Excel version 16.16.6. For each independent experiment, between 6 and 14 larvae with a total of 7-24 symbiont cells were observed.

5.5.6 MyD88 inhibitor peptide treatment of infected larvae

Between 3 and 13 batches of aposymbiotic larvae from distinct spawning events at 6 dpf were filtered and washed into new FASW at approximately 300-500 larvae per ml. Infections with 1.0 x 10^5 microalgae cells per ml with symbiont, *M. gaditana*, *N. oculata*, and *C. velia* were carried out at 26 ºC with a 12-hour light/12-hour dark cycle for 24 hours. Then, the larvae were filtered to remove non-phagocytosed microalgae cells from the water and 10 units per ml penicillin and 10 µg per ml streptomycin (P4333 Sigma-Aldrich) were added. For each replicate, half of the infected larvae were exposed to 50 µM of MyD88 inhibitor peptide, while the other half was treated with 50 µM control peptide (NBP2-29328, Novus Biologicals, Centennial, CO, USA) for 24 hours at 26 ºC. After 24 hours, all samples were fixed with 4 % formaldehyde for 30 minutes at RT, and infection efficiency was quantified as previously described.

5.5.7 MyD88 inhibitor peptide treatment during infection with microalgae

Four batches of aposymbiotic larvae from distinct spawning events at 6 dpf were filtered and washed into new FASW at approximately 300-500 larvae per ml. For each replicate, 10 units per ml penicillin and 10 µg per ml streptomycin (P4333 Sigma-Aldrich) were added, and half of the infected larvae were exposed to 50 µM of MyD88 inhibitor peptide, while the other half was treated with 50 µM control peptide (NBP2-29328, Novus Biologicals, Centennial, CO, USA) for 24 hours at 26 ºC. After 24 hours, 1.0 x 10^5 microalgae cells per ml of symbiont, *M. gaditana*, *N. oculata*, or *C. velia* were added and infections were carried out at 26 ºC with a 12-hour light/12-hour dark cycle for 24 hours. All samples were fixed with 4 % formaldehyde for 30 minutes at RT, and infection efficiency was quantified as previously described.

5.5.8 LAMP1-accumulation after ERK5 inhibition with XMD17-109

Three batches of aposymbiotic Aiptasia larvae from distinct spawning events between 4- and 8-dpf were filtered and washed into new FASW at approximately 300-500 larvae per ml. For

each replicate, larvae were then divided into two groups (treatment vs. control) and incubated with either 1 µM XMD17-109 (0.1 % DMSO, Carl-Roth) or 0.1 % DMSO for 1 hour. Infection with 1.0 x 10^5 symbiont cells per ml was carried out for 5 hours at 26 ºC with a 12-hour light/12-hour dark cycle. The larvae were fixed after a 5-hour infection in 4 % formaldehyde for 30 minutes. Samples were then washed twice in 0.2 % PBS-Triton, followed by one wash in PBS. LAMP1 was localized in larvae using the immunofluorescence protocol described above. After staining, samples were mounted in 87 % glycerol in PBS with the addition of 2.5 mg per ml DABCO. LAMP1-positive symbiosomes were assessed using confocal microscopy by acquiring images with a Leica TCS SP8 stand with a 63x glycerol immersion objective (NA 1.30) and using Leica LAS X software. The analysis was performed using Fiji software (Schindelin et al., 2012). Hoechst was excited with the 405 nm laser line and detected at 410-501 nm, Alexa488 was excited with the 496 nm laser line and detected at 501-541 nm, and microalgae autofluorescence was excited with the 633 nm laser line and detected at 645-741 nm. For the DMSO control, LAMP1-positive symbiosome were quantified in 20 infected larvae per replicate; however, due to reduced infection efficiency caused by XMD17-109 treatment, only 8, 4, and 7 larvae were able to be assessed per replicate.

5.5.9 Assessment of cytoskeleton to determine the concentration of LatB

Aposymbiotic Aiptasia larvae were treated with 0.01, 0.05, 0.1, or 0.25 µM Latrunculin B (LatB) for 6 hours. After treatment, larvae were fixed in 4 % formaldehyde for 30 minutes. Samples were then washed twice in 0.2 % PBS-Triton, followed by one wash in PBS. The cytoskeleton was evaluated in larvae using the Phalloidin staining protocol described above. After staining, samples were mounted in 87 % glycerol in PBS with the addition of 2.5 mg per ml DABCO. At 0.05 µM LatB, larvae were healthy and visually appeared intact, but the amount of F-actin present was drastically reduced compared to the DMSO control.

5.5.10 Live imaging after 1-hour infection with *M. gaditana* and Lat B treatment

Three batches of aposymbiotic Aiptasia larvae from distinct spawning events between 4- and 8-dpf were filtered and washed into new FASW at approximately 300-500 larvae per ml. Then, 1.0 x 10^5 *M. gaditana* cells per ml were added and samples were incubated at 26 ºC for 1 hour. After a 1-hour infection, larvae were divided into two groups (treatment vs. control) and incubated with either 0.05 µM Lat B or DMSO as a control. They were then mounted in live imaging chambers as previously described. In Lat B treated larvae, 0.05µM Lat B was added

to both the LGA and the surrounding FASW. In control larvae, DMSO was added to both the LGA and the surrounding FASW. Z-stacks were acquired every 5 minutes for 12 hours in DIC and TexasRed channels. A Nikon Eclipse Ti inverted microscope with a Nikon Plan Fluor 20x air objective was used to acquire microscopy images, which were then analyzed and processed using Fiji software (Schindelin et al., 2012). Data were recorded in Microsoft Excel version 16.16.6. For each biological replicate, between 8 and 10 larvae with a total of 8-16 *M. gaditana* cells were observed.

5.5.11 Acidic growth medium for symbiont cultures

Hydrogen chloride was slowly added in small quantities to 1x Diago IMK medium (Wako Pure Chemicals, Osaka, Japan) and pH was measured using a digital pH meter. Four media with varying pH were generated (pH 7.9, 6.3, 4.2, and 2.6). One clonal axenic culture of *Breviolum minutum* clade B (strain SSB01, symbiont) (Xiang et al., 2013) was spun down to pellet symbiont cells, and cells were then distributed into cell culture flasks containing the pH adjusted IMK media. All cultures were exposed to a 12-hour light/12-hour dark cycle under 20–25 μ mol m^{-2} s^{-1} of PAR as measured with an Apogee PAR quantum meter (MQ-200; Apogee, Logan, USA). For pH 7.9, 6.3, 4.2, and 2.6, samples were taken at 1, 3, 6, 14, 16, and 21 days and symbiont cells were counted using a TC20 automated cell counter (1450102, Bio-Rad). For pH 2.6, samples were taken additionally at 31 and 48 days after they were transferred to pH 7.9 IMK media. At the end of the experiment, the pH was again measured for each of the samples and they remained the same from the start of the experiment. Data were recorded and the figure created using Prism version 9.2.0.

5.6 Phylogenies and computational analyses

5.6.1 ERK5 / MAP2K5 phylogeny

Human ERK5 (MAPK7) and MEK5 (MAP2K5) were searched via reciprocal BLAST. The sequences were then used to classify and assemble the Aiptasia MAPK and MAP2K repertoires. The Aiptasia MAPK and MAP2K sequences were blasted using BLASTP against other organisms from public databases. Sequences from *H. echinata* were retrieved from https://research.nhgri.nih.gov/hydractinia/download/ and manually translated. Utilizing ClustalW (GONNET, goc: 3, gec: 1.8), the protein sequences were then deduplicated and aligned. TrimAI was used for automated trimming with standard parameters

(http://trimal.cgenomics.org/, (Capella-Gutiérrez et al., 2009)). To determine best-fitting amino acid substitution models, ModelFinder (-m MF -msub nuclear -nt AUTO) within FigTree was used, followed by generation of Maximum likelihood trees. FigTree 1.4.4 (http://tree.bio.ed.ac.uk/software/figtree/) and Adobe Illustrator CC 2018 and Affinity Designer v1.9.1 were used to finalize trees.

5.6.2 Statistical notes

Statistical analysis, R-script, raw data, biological/technical repeat information, and results are located at https://doi.org/10.24433/CO.0872345.v1. A two-sided generalized linear mixed model was analyzed in R v4.0.3 using the gam function from the mgcv-package (R Core Team, 2018). Larvae treatment (e.g., addition of LPS or LatB) in a biological replicate was recorded with the random Intercept "s(Well_ID, bs="re")". The random intercept "s(Repeat.Date.,bs='re')" was used to record experiments that were performed simultaneously. For the graphs in Figure 8, multiple comparisons were performed using the emmeans package with the default Tukey correction methods of p-values. Figure 9, Figure 12, and Figure 16 were created using Prism version 9.2.0 and a multiple comparison 2way ANOVA with Tukey test (alpha=0.05) were used for statistical analysis.

6 Supplementary Material

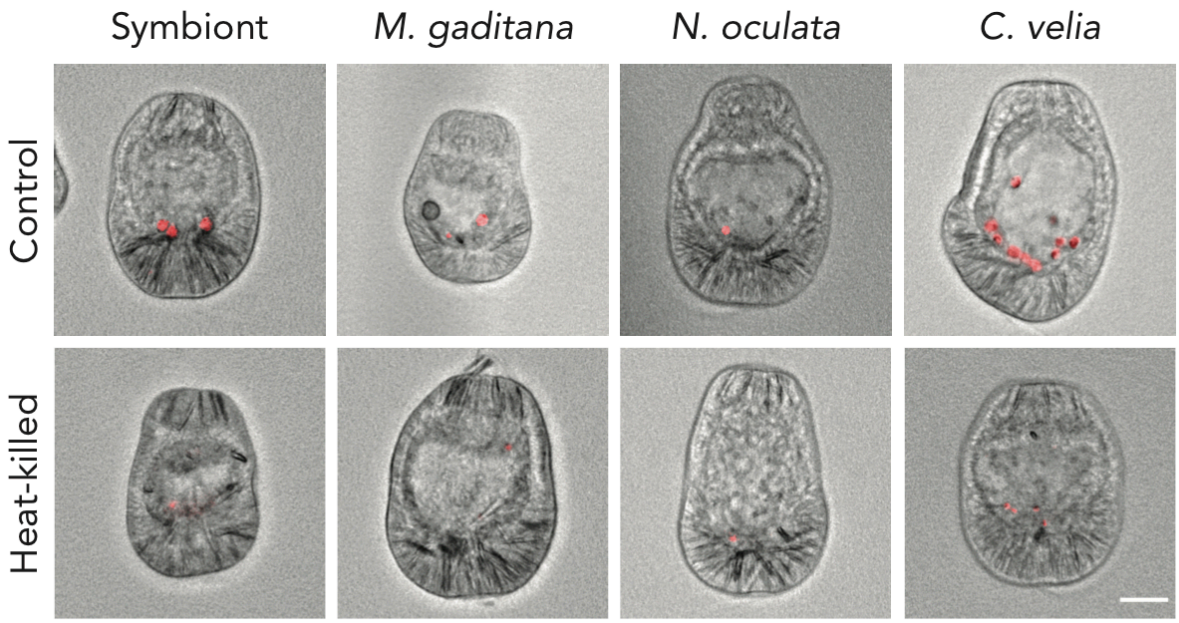

Supplementary Figure 1 Infection with heat-killed microalgae in Aiptasia larvae
Aiptasia larvae infected for 24 hours with healthy or heat-killed symbionts, *M. gaditana*, *N. oculata,* or *C. velia*. Representative images (merge of DIC and microalgae autofluorescence (red)) of Aiptasia larvae infected with healthy (control) and heat-killed microalgae. Due to reduced autofluorescence of heat-killed microalgae, quantifying infection was not as straightforward as with the control. Scale bar represents 25 µm.

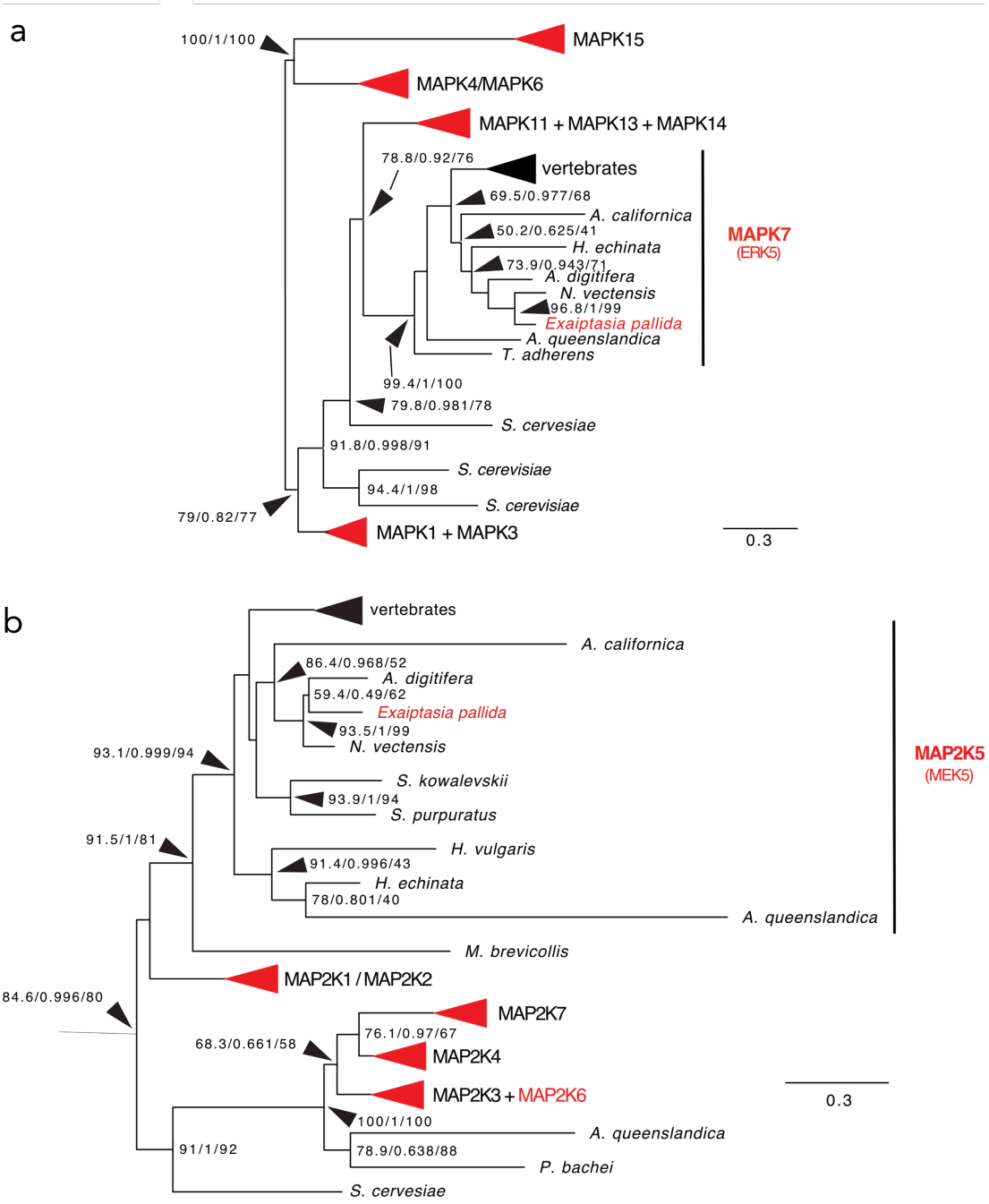

Supplementary Figure 2 Aiptasia homologs of ERK5 and MAP2K5

Phylogenetic analysis of Aiptasia ERK5 and MAP2K5. **a,** Collapsed tree of Aiptasia MAPK compared to several other species. Aiptasia MAPK7 (ERK5) clusters within MAPK7 (ERK5). **b,** Collapsed tree of Aiptasia MAP2K compared to several other species. Aiptasia MAP2K5 (MEK5) clusters within MAP2K5 (MEK5). Red arrowheads or red writing demonstrate the presence of an Aiptasia homolog. Created by Sebastian Rupp.

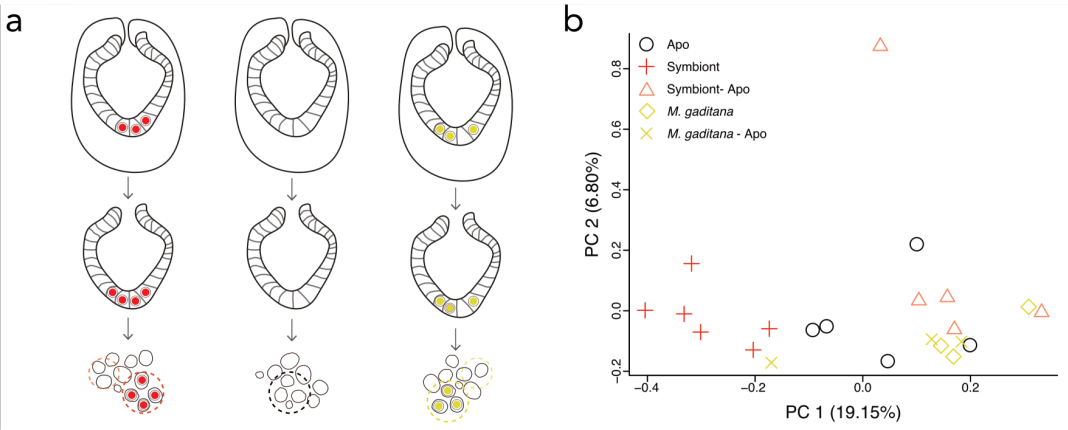

Supplementary Figure 3 Transcriptomic analysis of specific cell types

a, Schematic of cells selected for cell-type-specific transcriptome. Infected Aiptasia larvae were infected with symbionts or *M. gaditana*, and then the ectodermal cells were removed. The remaining endodermal cells were dissociated and picked following the criteria: aposymbiotic cells from symbiotic larvae (Symbiont-Apo), symbiotic cells from symbiotic larvae (Symbiont (red)), aposymbiotic cells from aposymbiotic larvae (Apo), cells containing *M. gaditana* from *M. gaditana*-infected larvae (*M. gaditana* (yellow)), and aposymbiotic cells from *M. gaditana*-infected larvae (*M. gaditana*-Apo). **b,** Principal Component Analysis (PCA) plot of host gene expression across different conditions. Acquired by Philipp Voss and analyzed with assistance from Sebastian Gornik.

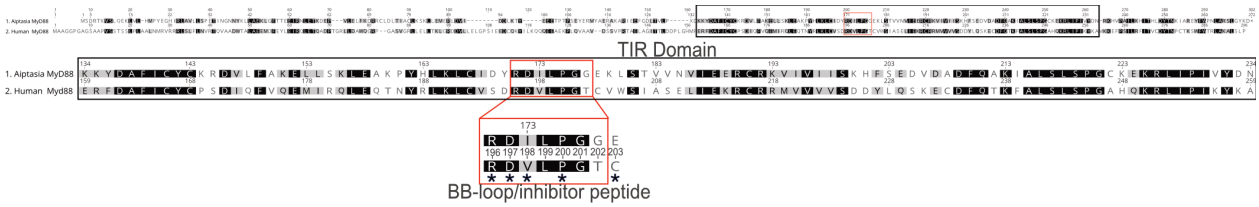

Supplementary Figure 4 Human and Aiptasia MyD88 amino acid sequence similarity

The amino acid sequence similarity between human MyD88 and Aiptasia MyD88. MyD88 comprises a death domain (DD), an interdomain (ID), and a C-terminal TIR domain. (Hardiman et al., 1996). The TIR domains between human and Aiptasia, delineated by a black box in the top alignment, are well conserved with approximately 50% sequence similarity. The downstream signaling cascade for immune activation via MyD88 begins with MyD88 homodimerization. The TIR domain is important for homodimerization. Specifically, within the TIR domain, the BB-loop is critical for homodimerization. The BB-loop is a solvent-exposed stretch of seven amino acid residues with the sequence RDLVPGT. Peptides (such as the one used in this thesis) that mimic the amino acid sequence of the BB-loop can block homodimerization and, therefore, the intracellular signaling cascade that it initiates (Loiarro et al., 2005; Ruggiero et al., 2010). The BB-loops, delineated by a red box in the second alignment, are nearly identical, with all critical residues conserved between human and Aiptasia. Identical amino acids have black backgrounds, similar amino acids have gray backgrounds, and the amino acids with white backgrounds are not similar according to blosume62 scoring. Created by Sebastian Rupp.

Signaling Pathway	Genes in Kegg-pathway	Transcripts in Aiptasia	Sym vs. Apo	Sym vs. Sym-Apo	Sym-Apo vs. Apo	*M.g* vs. Apo	*M.g* vs. *M.g*-Apo	*M.g*-Apo vs. Apo	Symbiont vs. *M.g*
C-type lectin receptor	82	61	6 (9.84%)	8 (13.11%)	2 (3.28%)	2 (3.28%)	2 (3.28%)	2 (3.28%)	4 (6.56%)
Complement and coagulation cascades	81	14	0 (0%)	1 (7.14%)	0 (0%)	0 (0%)	0 (0%)	0 (0%)	0 (0%)
JAK-STAT	139	25	1 (4%)	4 (16%)	1 (4%)	1 (4%)	1 (4%)	0 (0%)	1 (4%)
MAPK	235	156	13 (8.33%)	25 (16.03%)	3 (1.92%)	1 (0.64%)	3 (1.92%)	2 (1.28%)	13 (8.33%)
NF-kappa B	97	48	10 (20.83%)	11 (22.92%)	3 (6.25%)	0 (0%)	3 (6.25%)	4 (8.33%)	6 (12.5%)
NOD-like receptor	142	119	14 (11.76%)	16 (13.45%)	1 (0.84%)	1 (0.84%)	5 (4.2%)	6 (5.04%)	6 (5.04%)
RIG-I-like receptor	53	41	5 (12.2%)	7 (17.07%)	1 (2.44%)	0 (0%)	3 (7.32%)	4 (9.76%)	2 (4.88%)
TGF-beta	83	44	3 (6.82%)	5 (11.36%)	3 (6.82%)	0 (0%)	1 (2.27%)	2 (4.55%)	3 (6.82%)
TNF	92	60	12 (20%)	12 (20%)	2 (3.33%)	4 (6.67%)	6 (10%)	7 (11.67%)	5 (8.33%)
Toll-like receptor	76	40	8 (20%)	8 (20%)	3 (7.5%)	1 (2.5%)	2 (5%)	4 (10%)	4 (10%)
Unique genes within pathways	761	389	36 (9.25%)	53 (13.62%)	11 (2.83%)	6 (1.54%)	15 (3.86%)	15 (3.86%)	25 (6.43%)

Supplementary Table 1 Statistics of innate immune suppression from transcriptome

Account of innate immunity genes over 10 immune pathways modulated in response to symbiosis establishment. KEGG pathways represented: C-type lectin receptor signaling (ko04625), complement and coagulation cascades (ko04610), JAK-STAT (ko04630), MAPK (ko04010), NF-κB (ko04064), NOD-like receptor (ko04621), RIG-I-like receptor (ko04622), TGF-β (ko04350), TNF (ko04668), and TLR (ko04620), as well as unique genes within pathways. Some genes were present across multiple pathways, and some transcripts were annotated as the same gene (e.g., TRAF3). Acquired by Philipp Voss and analyzed by Sebastian Rupp.

7 References

Aihara, Y., Maruyama, S., Baird, A. H., Iguchi, A., Takahashi, S., & Minagawa, J. (2019). Green fluorescence from cnidarian hosts attracts symbiotic algae. *Proceedings of the National Academy of Sciences*, *116*(6), 2118–2123. https://doi.org/10.1073/pnas.1812257116

Akira, S., Uematsu, S., & Takeuchi, O. (2006). Pathogen recognition and innate immunity. *Cell*, *124*(4), 783–801. https://doi.org/10.1016/j.cell.2006.02.015

Alvarez, M., & Casadevall, A. (2006). Phagosome Extrusion and Host-Cell Survival after Cryptococcus neoformans Phagocytosis by Macrophages. *Current Biology*, *16*(21), 2161–2165. https://doi.org/10.1016/j.cub.2006.09.061

Atkinson, S. D., Bartholomew, J. L., & Lotan, T. (2018). Myxozoans: Ancient metazoan parasites find a home in phylum Cnidaria. *Zoology*, *129*(May), 66–68. https://doi.org/10.1016/j.zool.2018.06.005

Baird, A. H., Guest, J. R., & Willis, B. L. (2009). Systematic and biogeographical patterns in the reproductive biology of scleractinian corals. *Annual Review of Ecology, Evolution, and Systematics*, *40*, 551–571. https://doi.org/10.1146/annurev.ecolsys.110308.120220

Baker, A. C. (2001). Reef corals bleach to survive change. *Nature*, *411*(6839), 765–766. https://doi.org/10.1038/35081151

Baker, A. C. (2003). Flexibility and Specificity in Coral-Algal Symbiosis: Diversity, Ecology, and Biogeography of Symbiodinium. *Annual Review of Ecology, Evolution, and Systematics*, *34*, 661–689. https://doi.org/10.1146/annurev.ecolsys.34.011802.132417

Barott, K. L., Venn, A. A., Perez, S. O., Tambutté, S., & Tresguerres, M. (2015). Coral host cells acidify symbiotic algal microenvironment to promote photosynthesis. *Proceedings of the National Academy of Sciences*, *112*(2), 607–612. https://doi.org/10.1073/pnas.1413483112

Barton, G. M., & Kagan, J. C. (2009). A cell biological view of toll-like receptor function: Regulation through compartmentalization. *Nature Reviews Immunology*, *9*(8), 535–541. https://doi.org/10.1038/nri2587

Baumgarten, S., Simakov, O., Esherick, L. Y., Liew, Y. J., Lehnert, E. M., Michell, C. T., Li, Y., Hambleton, E. A., Guse, A., Oates, M. E., Gough, J., Weis, V. M., Aranda, M., Pringle, J. R., & Voolstra, C. R. (2015). The genome of *Aiptasia* , a sea anemone model for coral symbiosis. *Proceedings of the National Academy of Sciences*, *112*(38), 11893–11898. https://doi.org/10.1073/pnas.1513318112

Berthelier, J., Schnitzler, C. E., Wood-Charlson, E. M., Poole, A. Z., Weis, V. M., & Detournay, O. (2017). Implication of the host TGFβ pathway in the onset of symbiosis between larvae

of the coral Fungia scutaria and the dinoflagellate Symbiodinium sp. (clade C1f). *Coral Reefs*, *36*(4), 1263–1268. https://doi.org/10.1007/s00338-017-1621-6

Berthold, M. R., Cebron, N., Dill, F., Gabriel, T. R., Kötter, T., Meinl, T., Ohl, P., Sieb, C., Thiel, K., & Wiswedel, B. (2008). KNIME: The Konstanz information miner. *Studies in Classification, Data Analysis, and Knowledge Organization*, 319–326. https://doi.org/10.1007/978-3-540-78246-9_38

Biquand, E., Okubo, N., Aihara, Y., Rolland, V., Hayward, D. C., Hatta, M., Minagawa, J., Maruyama, T., & Takahashi, S. (2017). Acceptable symbiont cell size differs among cnidarian species and may limit symbiont diversity. *Nature Publishing Group*, *11*(7), 1702–1712. https://doi.org/10.1038/ismej.2017.17

Birmingham, C. L., Canadien, V., Kaniuk, N. A., Steinberg, B. E., Higgins, D. E., & Brumell, J. H. (2008). Listeriolysin O allows Listeria monocytogenes replication in macrophage vacuoles. *Nature*, *451*(7176), 350–354. https://doi.org/10.1038/nature06479

Bocharova, E. S., & Kozevich, I. A. (2011). Modes of reproduction in sea anemones (Cnidaria, Anthozoa). *Biology Bulletin*, *38*(9), 849–860. https://doi.org/10.1134/S1062359011090020

Botos, I., Segal, D. M., & Davies, D. R. (2011). The structural biology of Toll-like receptors. *Structure*, *19*(4), 447–459. https://doi.org/10.1016/j.str.2011.02.004

Brusca, Richard C., and G. J. B. (2002). Invertebrates, Second Edition. *Molecular Phylogenetics and Evolution, Vol. 111*, *1*, xx + 936.

Bucher, M., Jones, V. A. S., Hambleton, E. A., & Guse, A. (2017). *Microinjection to deliver protein and mRNA into zygotes of the cnidarian endosymbiosis model*. 1–24.

Bucher, M., Wolfowicz, I., Voss, P. A., Hambleton, E. A., & Guse, A. (2016). Development and Symbiosis Establishment in the Cnidarian Endosymbiosis Model Aiptasia sp. *Scientific Reports*, *6*, 1–11. https://doi.org/10.1038/srep19867

Buckley, C. M., Gopaldass, N., Bosmani, C., Johnston, S. A., Soldati, T., Insall, R. H., & King, J. S. (2016). WASH drives early recycling from macropinosomes and phagosomes to maintain surface phagocytic receptors. *Proceedings of the National Academy of Sciences of the United States of America*, *113*(40), E5906–E5915. https://doi.org/10.1073/pnas.1524532113

Budisa, A., Haberle, I., Konjevic, L., Blazina, M., Djakovac, T., Spalj, B. L., & Hrustic, E. (2019). Marine microalgae microchloropsis gaditana and pseudochloris wilhelmii cultivated in oil refinery wastewater - a perspective on remediation and biodiesel production. *Fresenius Environmental Bulletin*, *28*(11), 7888–7897.

Burghardt, I., Stemmer, K., & Wägele, H. (2008). Symbiosis between Symbiodinium (Dinophyceae) and various taxa of Nudibranchia (Mollusca: Gastropoda), with analyses of long-term retention. *Organisms Diversity and Evolution*, *8*(1), 66–76. https://doi.org/10.1016/j.ode.2007.01.001

Capella-Gutiérrez, S., Silla-Martínez, J. M., & Gabaldón, T. (2009). trimAl: A tool for automated alignment trimming in large-scale phylogenetic analyses. *Bioinformatics*, *25*(15), 1972–1973. https://doi.org/10.1093/bioinformatics/btp348

Cavalier-Smith, T. (2016). Origin of animal multicellularity: precursors, causes, consequences — the choanoflagellate /sponge transition, neurogenesis and the Cambrian explosion. *Philosophical Transactions of the Royal Society B: Biological Sciences*, *372*, 20150476. https://doi.org/http://dx.doi.org/10.1098/rstb.2015.0476

Chen, M. C., Cheng, Y. M., Hong, M. C., & Fang, L. S. (2004). Molecular cloning of Rab5 (ApRab5) in Aiptasia pulchella and its retention in phagosomes harboring live zooxanthellae. *Biochemical and Biophysical Research Communications*, *324*(3), 1024–1033. https://doi.org/10.1016/j.bbrc.2004.09.151

Chen, M. C., Cheng, Y. M., Sung, P. J., Kuo, C. E., & Fang, L. S. (2003). Molecular identification of Rab7 (ApRab7) in Aiptasia pulchella and its exclusion from phagosomes harboring zooxanthellae. *Biochemical and Biophysical Research Communications*, *308*(3), 586–595. https://doi.org/10.1016/S0006-291X(03)01428-1

Chrisman, C. J., Alvarez, M., & Casadevall, A. (2010). Phagocytosis of cryptococcus neoformans by, and nonlytic exocytosis from, Acanthamoeba castellanii. *Applied and Environmental Microbiology*, *76*(18), 6056–6062. https://doi.org/10.1128/AEM.00812-10

Cirl, C., Wieser, A., Yadav, M., Duerr, S., Schubert, S., Fischer, H., Stappert, D., Wantia, N., Rodriguez, N., Wagner, H., Svanborg, C., & Miethke, T. (2008). Subversion of Toll-like receptor signaling by a unique family of bacterial Toll/interleukin-1 receptor domain-containing proteins. *Nature Medicine*, *14*(4), 399–406. https://doi.org/10.1038/nm1734

Coats, D. W. (1999). Parasitic life styles of marine dinoflagellates. *Journal of Eukaryotic Microbiology*, *46*(4), 402–409. https://doi.org/10.1111/j.1550-7408.1999.tb04620.x

Coffroth, M. A., Lewis, C. F., Santos, S. R., & Weaver, J. L. (2006). Environmental populations of symbiotic dinoflagellates in the genus Symbiodinium can initiate symbioses with reef cnidarians. *Current Biology*, *16*(23), R985–R987. https://doi.org/10.1016/j.cub.2006.10.049

Collins, A. G. (2009). Recent Insights into Cnidarian Phylogeny. *Smithsonian*, *000*(August 2008), 139–149. http://www.si.edu/marinescience/pdf/SCMS_Collins.pdf

References

Costanza, R., de Groot, R., Sutton, P., van der Ploeg, S., Anderson, S. J., Kubiszewski, I., Farber, S., & Turner, R. K. (2014). Changes in the global value of ecosystem services. *Global Environmental Change*, *26*(1), 152–158. https://doi.org/10.1016/j.gloenvcha.2014.04.002

Coutinho, M. F., Prata, M. J., & Alves, S. (2012). Mannose-6-phosphate pathway: A review on its role in lysosomal function and dysfunction. *Molecular Genetics and Metabolism*, *105*(4), 542–550. https://doi.org/10.1016/j.ymgme.2011.12.012

Cumbo, V. R., Baird, A. H., Moore, R. B., Negri, A. P., Neilan, B. A., Salih, A., van Oppen, M. J. H., Wang, Y., & Marquis, C. P. (2013). Chromera velia is endosymbiotic in larvae of the reef corals acropora digitifera and A. tenuis. *Protist*, *164*(2), 237–244. https://doi.org/10.1016/j.protis.2012.08.003

Cumbo, V. R., Baird, A. H., & van Oppen, M. J. H. (2013). The promiscuous larvae: Flexibility in the establishment of symbiosis in corals. *Coral Reefs*, *32*(1), 111–120. https://doi.org/10.1007/s00338-012-0951-7

Daly, M., Brugler, M. R., Cartwright, P., Collins, A. G., Dawson, M. N., Fautin, D. G., France, S. C., McFadden, C. S., Opresko, D. M., Rodriguez, E., Romano, S. L., & Stake, J. L. (2007). The phylum Cnidaria: A review of phylogenetic patterns and diversity 300 years after Linnaeus. *Zootaxa*, *1668*, 127–182. https://doi.org/10.11646/zootaxa.1668.1.11

Davies, S. W., Strader, M. E., Kool, J. T., Kenkel, C. D., & Matz, M. v. (2017). Modeled differences of coral life-history traits influence the refugium potential of a remote Caribbean reef. *Coral Reefs*, *36*(3), 913–925. https://doi.org/10.1007/s00338-017-1583-8

Davy, S. K., Allemand, D., & Weis, V. M. (2012). Cell Biology of Cnidarian-Dinoflagellate Symbiosis. *Microbiology and Molecular Biology Reviews*, *76*(2), 229–261. https://doi.org/10.1128/MMBR.05014-11

de Vargas, C., Audic, S., Henry, N., Decelle, J., Mahe, F., Logares, R., Lara, E., Berney, C., le Bescot, N., Probert, I., Carmichael, M., Poulain, J., Romac, S., Colin, S., Aury, J.-M., Bittner, L., Chaffron, S., Dunthorn, M., Engelen, S., … Velayoudon, D. (2015). Eukaryotic plankton diversity in the sunlit ocean. *Science*, *348*(6237), 1261605–1261605. https://doi.org/10.1126/science.1261605

Deguine, J., & Barton, G. M. (2014). MyD88: A central player in innate immune signaling. *F1000Prime Reports*, *6*(November), 1–7. https://doi.org/10.12703/P6-97

Desalvo, M. K., Sunagawa, S., Voolstra, C. R., & Medina, M. (2010). Transcriptomic responses to heat stress and bleaching in the elkhorn coral Acropora palmata. *Marine Ecology Progress Series*, *402*(2006), 97–113. https://doi.org/10.3354/meps08372

Dishon, S., Schumacher, A., Fanous, J., Talhami, A., Kassis, I., Karussis, D., Gilon, C., Hoffman, A., & Nussbaum, G. (2018). Development of a novel backbone cyclic peptide

inhibitor of the innate immune TLR/IL1R signaling protein MyD88. *Scientific Reports*, *8*(1), 1–12. https://doi.org/10.1038/s41598-018-27773-8

Douglas, A. E. (1995). The Ecology of Symbiotic Micro-organisms. In *Advances in Ecological Research* (Vol. 26, Issue C). https://doi.org/10.1016/S0065-2504(08)60064-1

Douglas, A. E. (2003). Coral bleaching - How and why? *Marine Pollution Bulletin*, *46*(4), 385–392. https://doi.org/10.1016/S0025-326X(03)00037-7

Downs, C. A., Kramarsky-winter, E., Martinez, J., Kushmaro, A., Woodley, C. M., & Loya, Y. (2009). *Symbiophagy as a cellular mechanism for coral bleaching*. *February*, 211–216.

Dunkelberger, J. R., & Song, W. C. (2010). Complement and its role in innate and adaptive immune responses. In *Cell Research* (Vol. 20, Issue 1, pp. 34–50). https://doi.org/10.1038/cr.2009.139

Dunn, C. W. (2005). Complex colony-level organization of the deep-sea siphonophore Bargmannia elongata (Cnidaria, Hydrozoa) is directionally asymmetric and arises by the subdivision of pro-buds. *Developmental Dynamics*, *234*(4), 835–845. https://doi.org/10.1002/dvdy.20483

Dunn, S. R., Bythell, J. C., le Tissier, M. D. A., Burnett, W. J., & Thomason, J. C. (2002). Programmed cell death and cell necrosis activity during hyperthermic stress-induced bleaching of the symbiotic sea anemone Aiptasia sp. *Journal of Experimental Marine Biology and Ecology*, *272*(1), 29–53. https://doi.org/10.1016/S0022-0981(02)00036-9

Dunn, S. R., Thomason, J. C., le Tissier, M. D. A., & Bythell, J. C. (2004). Heat stress induces different forms of cell death in sea anemones and their endosymbiotic algae depending on temperature and duration. *Cell Death and Differentiation*, *11*(11), 1213–1222. https://doi.org/10.1038/sj.cdd.4401484

Dunn, S. R., & Weis, V. M. (2009). Apoptosis as a post-phagocytic winnowing mechanism in a coral-dinoflagellate mutualism. *Environmental Microbiology*, *11*(1), 268–276. https://doi.org/10.1111/j.1462-2920.2008.01774.x

Epstein, H. E., Torda, G., Munday, P. L., & van Oppen, M. J. H. (2019). Parental and early life stage environments drive establishment of bacterial and dinoflagellate communities in a common coral. *ISME Journal*, *13*(6), 1635–1638. https://doi.org/10.1038/s41396-019-0358-3

Fadok, V. A., Bratton, D. L., Konowal, A., Freed, P. W., Westcott, J. Y., & Henson, P. M. (1998). Macrophages that have ingested apoptotic cells in vitro inhibit proinflammatory cytokine production through autocrine/paracrine mechanisms involving TGF-β, PGE2, and PAF. *Journal of Clinical Investigation*, *101*(4), 890–898. https://doi.org/10.1172/JCI1112

References

Fautin, D. G. (2002). Reproduction of Cnidaria. *Canadian Journal of Zoology*, *80*(10), 1735–1754. https://doi.org/10.1139/z02-133

Fay, S. A., Weber, M. X., & Lipps, J. H. (2009). The distribution of Symbiodinium diversity within individual host foraminifera. *Coral Reefs*, *28*(3), 717–726. https://doi.org/10.1007/s00338-009-0511-y

Fitt, W. K., & Trench, R. K. (1983). Endocytosis of the symbiotic dinoflagellate symbiodinium microadriaticum Freudenthal by endodermal cells of the scyphistomae of Cassiopeia xamachana and resistance of the algae to host digestion. *Journal of Cell Science*, *64*, 195–212. https://doi.org/10.1111/j.1469-8137.1983.tb03456.x

Flannagan, R. S., Cosío, G., & Grinstein, S. (2009). Antimicrobial mechanisms of phagocytes and bacterial evasion strategies. In *Nature Reviews Microbiology* (Vol. 7, Issue 5, pp. 355–366). https://doi.org/10.1038/nrmicro2128

Franzenburg, S., Fraune, S., Künzel, S., Baines, J. F., Domazet-Lošo, T., & Bosch, T. C. G. (2012). MyD88-deficient Hydra reveal an ancient function of TLR signaling in sensing bacterial colonizers. *Proceedings of the National Academy of Sciences of the United States of America*, *109*(47), 19374–19379. https://doi.org/10.1073/pnas.1213110109

Geller, J. B., Fitzgerald, L. J., & King, C. E. (2005). Fission in sea anemones: Integrative studies of life cycle evolution. *Integrative and Comparative Biology*, *45*(4), 615–622. https://doi.org/10.1093/icb/45.4.615

Ghosh, D., & Stumhofer, J. (2014). Do You See What I See: Recognition of Protozoan Parasites by Toll-Like Receptors. *Current Immunology Reviews*, *9*(3), 129–140. https://doi.org/10.2174/1573395509666131203225929

Gilbert, A. S., Seoane, P. I., Sephton-Clark, P., Bojarczuk, A., Hotham, R., Giurisato, E., Sarhan, A. R., Hillen, A., Velde, G. vande, Gray, N. S., Alessi, D. R., Cunningham, D. L., Tournier, C., Johnston, S. A., & May, R. C. (2017). Vomocytosis of live pathogens from macrophages is regulated by the atypical MAP kinase ERK5. *Science Advances*, *3*(8), 1–8. https://doi.org/10.1126/sciadv.1700898

Gleason, D. F., & Hofmann, D. K. (2011). Coral larvae: From gametes to recruits. *Journal of Experimental Marine Biology and Ecology*, *408*(1–2), 42–57. https://doi.org/10.1016/j.jembe.2011.07.025

Gomez, F. (2012). A quantitative review of the lifestyle, habitat and trophic diversity of dinoflagellates (Dinoflagellata, Alveolata). *Systematics and Biodiversity*, *10*(3), 267–275. https://doi.org/10.1080/14772000.2012.721021

Grawunder, D., Hambleton, E. A., Bucher, M., Wolfowicz, I., Bechtoldt, N., & Guse, A. (2015). Induction of Gametogenesis in the Cnidarian Endosymbiosis Model Aiptasia sp. *Scientific Reports*, *5*, 1–11. https://doi.org/10.1038/srep15677

Gu, Z., Eils, R., & Schlesner, M. (2016). Complex heatmaps reveal patterns and correlations in multidimensional genomic data. *Bioinformatics*, *32*(18), 2847–2849. https://doi.org/10.1093/bioinformatics/btw313

Guiry, M. D. (2012). How many species of algae are there? *Journal of Phycology*, *48*(5), 1057–1063. https://doi.org/10.1111/j.1529-8817.2012.01222.x

Haeckel, E. (1873). Die Gastraea-Theorie, die phylogenetische Classification des Thierreiches und die Homologie der Keimblätter. *Jenaische Zeitschrift Für Naturwissenschaft*, *8*, 1–55.

Hambleton, E. A., Guse, A., & Pringle, J. R. (2014). Similar specificities of symbiont uptake by adults and larvae in an anemone model system for coral biology. *Journal of Experimental Biology*, *217*(9), 1613–1619. https://doi.org/10.1242/jeb.095679

Hambleton, E. A., Jones, V. A. S., Maegele, I., Kvaskoff, D., Sachsenheimer, T., & Guse, A. (2019). Sterol transfer by atypical cholesterol-binding NPC2 proteins in coral-algal symbiosis. *ELife*, *8*, 1–26. https://doi.org/10.7554/eLife.43923

Hardiman, G., Rock, F. L., Balasubramanian, S., Kastelein, R. A., & Bazan, J. F. (1996). Molecular characterization and modular analysis of human MyD88. *Oncogene*, *13*(11), 2467–2475.

Harrison, P. (2011). Sexual Reproduction of Scleractinian Corals. In *Coral Reefs: An Ecosystem in Transition* (pp. 59–85). https://doi.org/10.1007/978-94-007-0114-4

Hemmrich, G., Miller, D. J., & Bosch, T. C. G. (2007). The evolution of immunity: a low-life perspective. *Trends in Immunology*, *28*(10), 449–454. https://doi.org/10.1016/j.it.2007.08.003

Hoegh-Guldberg, O., McCloskey, L. R., & Muscatine, L. (1987). Expulsion of zooxanthellae by symbiotic cnidarians from the Red Sea. *Coral Reefs*, *5*(4), 201–204. https://doi.org/10.1007/BF00300964

Hoegh-Guldberg, O., & Smith, J. (1989). The effect of sudden changes in temperature, light and salinity on the population density and export of zooxanthellae from the reef corals Stylophora pistillata Esper and Seriatopora hystrix Dana. *Genetics and Ceff Biology*, *129*, 279–303.

Hollingsworth, L. L., Kinzie, R. A., Lewis, T. D., Krupp, D. A., & Leong, J. A. C. (2005). Phototaxis of motile zooxanthellae to green light may facilitate symbiont capture by coral larvae. *Coral Reefs*, *24*(4), 523. https://doi.org/10.1007/s00338-005-0063-8

Huynh, K. K., Eskelinen, E. L., Scott, C. C., Malevanets, A., Saftig, P., & Grinstein, S. (2007). LAMP proteins are required for fusion of lysosomes with phagosomes. *EMBO Journal*, *26*(2), 313–324. https://doi.org/10.1038/sj.emboj.7601511

References

Jacobovitz, M. R., Rupp, S., Voss, P. A., Maegele, I., Gornik, S. G., & Guse, A. (2021). Dinoflagellate symbionts escape vomocytosis by host cell immune suppression. *Nature Microbiology*, *6*(6), 769–782. https://doi.org/10.1038/s41564-021-00897-w

Jaumouillé, V., & Grinstein, S. (2016). Molecular Mechanisms of Phagosome Formation. *Microbiology Spectrum*, *4*(3), 1–18. https://doi.org/10.1128/microbiolspec.MCHD-0013-2015

Johnston, S. A., & May, R. C. (2010). The human fungal pathogen Cryptococcus neoformans escapes macrophages by a phagosome emptying mechanism that is inhibited by arp2/3 complex- mediated actin polymerisation. *PLoS Pathogens*, *6*(8), 27–28. https://doi.org/10.1371/journal.ppat.1001041

Kanehisa, M., & Goto, S. (2000). KEGG: Kyoto Encyclopedia of Genes and Genomes. *Nucleic Acids Research*, *28*(1), 27–30. https://doi.org/10.1093/nar/28.1.27

Kawai, T., & Akira, S. (2007). Signaling to NF-κB by Toll-like receptors. *Trends in Molecular Medicine*, *13*(11), 460–469. https://doi.org/10.1016/j.molmed.2007.09.002

Kayal, E., Bentlage, B., Sabrina Pankey, M., Ohdera, A. H., Medina, M., Plachetzki, D. C., Collins, A. G., & Ryan, J. F. (2018). Phylogenomics provides a robust topology of the major cnidarian lineages and insights on the origins of key organismal traits. *BMC Evolutionary Biology*, *18*(1), 1–18. https://doi.org/10.1186/s12862-018-1142-0

Keeling, P. J., & Burki, F. (2019). Progress towards the Tree of Eukaryotes. *Current Biology*, *29*(16), R808–R817. https://doi.org/10.1016/j.cub.2019.07.031

Keith, S. A., Maynard, J. A., Edwards, A. J., Guest, J. R., Bauman, A. G., van Hooidonk, R., Heron, S. F., Berumen, M. L., Bouwmeester, J., Piromvaragorn, S., Rahbek, C., & Baird, A. H. (2016). Coral mass spawning predicted by rapid seasonal rise in ocean temperature. *Proceedings of the Royal Society B: Biological Sciences*, *283*(1830). https://doi.org/10.1098/rspb.2016.0011

Knowlton, N., Grottoli, A., Kleypas, J., Obura, D., Corcoran, E., de Goeij, J., Felis, T., Harding, S., Mayfield, A., Miller, M., Osuka, K., Peixoto, R., Randall, C., Voolstra, C., Wells, S., Wild, C., & Ferse, S. (2021). Rebuilding Coral Reefs: A Decadal Grand Challenge. *International Coral Reef Society and Future Earth Coasts*, 56. http://coralreefs.org/wp-content/uploads/2021/07/ICRS_2021_Policy_Brief_high_resol.pdf

Kraus, Y., & Technau, U. (2006). Gastrulation in the sea anemone Nematostella vectensis occurs by invagination and immigration: An ultrastructural study. *Development Genes and Evolution*, *216*(3), 119–132. https://doi.org/10.1007/s00427-005-0038-3

Kvennefors, E. C. E., Leggat, W., Kerr, C. C., Ainsworth, T. D., Hoegh-Guldberg, O., & Barnes, A. C. (2010). Analysis of evolutionarily conserved innate immune components in

coral links immunity and symbiosis. *Developmental and Comparative Immunology*, *34*(11), 1219–1229. https://doi.org/10.1016/j.dci.2010.06.016

Lajeunesse, T. C., Bhagooli, R., Hidaka, M., deVantier, L., Done, T., Schmidt, G., Fitt, W., & Hoegh-Guldberg, O. (2004). Closely related Symbiodinium spp. differ in relative dominance in coral reef host communities across …. *Marine Ecology-Progress Series-*, *284*, 147–161. http://www.int-res.com/articles/meps2004/284/m284p147.pdf%5Cnpapers2://publication/uuid/41AD47B4-CEF4-47E8-8C7C-40DF51B4969E

LaJeunesse, T. C., Parkinson, J. E., Gabrielson, P. W., Jeong, H. J., Reimer, J. D., Voolstra, C. R., & Santos, S. R. (2018). Systematic Revision of Symbiodiniaceae Highlights the Antiquity and Diversity of Coral Endosymbionts. *Current Biology*, *28*(16), 2570-2580.e6. https://doi.org/10.1016/j.cub.2018.07.008

Lehnert, E. M., Mouchka, M. E., Burriesci, M. S., Gallo, N. D., Schwarz, J. A., & Pringle, J. R. (2014). Extensive Differences in Gene Expression Between Symbiotic and Aposymbiotic Cnidarians. *G3: Genes|Genomes|Genetics*, *4*(2), 277–295. https://doi.org/10.1534/g3.113.009084

Lema, K. A., Bourne, D. G., & Willis, B. L. (2014). Onset and establishment of diazotrophs and other bacterial associates in the early life history stages of the coral Acropora millepora. *Molecular Ecology*, *23*(19), 4682–4695. https://doi.org/10.1111/mec.12899

Lesser, M. P., Stat, M., & Gates, R. D. (2013). The endosymbiotic dinoflagellates (Symbiodinium sp.) of corals are parasites and mutualists. *Coral Reefs*, *32*(3), 603–611. https://doi.org/10.1007/s00338-013-1051-z

Levitz, S. M., Nong, S. H., Seetoo, K. F., Harrison, T. S., Speizer, R. A., & Simons, E. R. (1999). Cryptococcus neoformans resides in an acidic phagolysosome of human macrophages. *Infection and Immunity*, *67*(2), 885–890.

Lewis, C. L., & Coffroth, M. A. (2004). The acquisition of exogenous, algal symbionts by an octocoral after bleaching. *Science*, *304*(5676), 1490–1492. https://doi.org/10.1126/science.1097323

Lin, K. L., Wang, J. T., & Fang, L. S. (2000). Participation of glycoproteins on zooxanthellal cell walls in the establishment of a symbiotic relationship with the sea anemone, Aiptasia pulchella. *Zoological Studies*, *39*(3), 172–178.

Liss, V., Swart, A. L., Kehl, A., Hermanns, N., Zhang, Y., Chikkaballi, D., Böhles, N., Deiwick, J., & Hensel, M. (2017). Salmonella enterica Remodels the Host Cell Endosomal System for Efficient Intravacuolar Nutrition. *Cell Host and Microbe*, *21*(3), 390–402. https://doi.org/10.1016/j.chom.2017.02.005

References

Littman, R. A., Willis, B. L., & Bourne, D. G. (2009). Bacterial communities of juvenile corals infected with different Symbiodinium (dinoflagellate) clades. *Marine Ecology Progress Series*, *389*(Ritchie 2006), 45–59. https://doi.org/10.3354/meps08180

Loiarro, M., Sette, C., Gallo, G., Ciacci, A., Fantó, N., Mastroianni, D., Carminati, P., & Ruggiero, V. (2005). Peptide-mediated interference of TIR domain dimerization in MyD88 inhibits interleukin-1-dependent activation of NF-κB. *Journal of Biological Chemistry*, *280*(16), 15809–15814. https://doi.org/10.1074/jbc.C400613200

Love, M. I., Huber, W., & Anders, S. (2014). Moderated estimation of fold change and dispersion for RNA-seq data with DESeq2. *Genome Biology*, *15*(12), 1–21. https://doi.org/10.1186/s13059-014-0550-8

Luo, W., & Brouwer, C. (2013). Pathview: An R/Bioconductor package for pathway-based data integration and visualization. *Bioinformatics*, *29*(14), 1830–1831. https://doi.org/10.1093/bioinformatics/btt285

Ma, H., Croudace, J. E., Lammas, D. A., & May, R. C. (2006). Expulsion of Live Pathogenic Yeast by Macrophages. *Current Biology*, *16*(21), 2156–2160. https://doi.org/10.1016/j.cub.2006.09.032

Ma, X. N., Chen, T. P., Yang, B., Liu, J., & Chen, F. (2016). Lipid production from Nannochloropsis. *Marine Drugs*, *14*(4). https://doi.org/10.3390/md14040061

Madan, R., Rastogi, R., Parashuraman, S., & Mukhopadhyay, A. (2012). Salmonella acquires lysosome-associated membrane protein 1 (LAMP1) on phagosomes from golgi via SipC protein-mediated recruitment of host syntaxin6. *Journal of Biological Chemistry*, *287*(8), 5574–5587. https://doi.org/10.1074/jbc.M111.286120

Magie, C. R., Daly, M., & Martindale, M. Q. (2007). Gastrulation in the cnidarian Nematostella vectensis occurs via invagination not ingression. *Developmental Biology*, *305*(2), 483–497. https://doi.org/10.1016/j.ydbio.2007.02.044

Mandel, M. J. (2010). Models and approaches to dissect host-symbiont specificity. *Trends in Microbiology*, *18*(11), 504–511. https://doi.org/10.1016/j.tim.2010.07.005

Mansfield, K., & Gilmore, T. (2018). Innate immunity and cnidarian-Symbiodiniaceae mutualism. *Developmental and Comparative Immunology*.

Mansfield, K., Nguyen, L., Carter, N., Alshanbayeva, A., Williams, L., Crowder, C., Penvose, A., Finnerty, J., Weis, V., Siggers, T., & Gilmore, T. (2017). Conserved transcription factor NF-κB is modulated by symbiotic status in a sea anemone model for cnidarian bleaching. *Proceedings of the National Academy of Sciences*, *June*, 1–14. https://doi.org/10.1038/s41598-017-16168-w

Martindale, M. Q., Pang, K., & Finnerty, J. R. (2004). Investigating the origins of triplosblasty: "Mesodermal" gene expression in a diploblastic animal, the sea anemone Nematostella vectensis (phylum, Cnidaria; class, Anthozoa). *Development*, *131*(10), 2463–2474. https://doi.org/10.1242/dev.01119

Massagué, J. (2012). TGFβ signalling in context. *Nature Reviews Molecular Cell Biology*, *13*(10), 616–630. https://doi.org/10.1038/nrm3434

Matthews, J. L., Crowder, C. M., Oakley, C. A., Lutz, A., Roessner, U., Meyer, E., Grossman, A. R., Weis, V. M., & Davy, S. K. (2017). Optimal nutrient exchange and immune responses operate in partner specificity in the cnidarian-dinoflagellate symbiosis. *Proceedings of the National Academy of Sciences*, 201710733. https://doi.org/10.1073/pnas.1710733114

Matthews, J. L., Sproles, A. E., Oakley, C. A., Grossman, A. R., Weis, V. M., & Davy, S. K. (2016). Menthol-induced bleaching rapidly and effectively provides experimental aposymbiotic sea anemones (Aiptasia sp.) for symbiosis investigations. *Journal of Experimental Biology*, *219*(3), 306–310. https://doi.org/10.1242/jeb.128934

McCloskey, L. R., Cove, T. G., & Verde, E. A. (1996). Symbiont expulsion from the anemone Anthopleura elegantissima (Brandt) (Cnidaria; Anthozoa). *Journal of Experimental Marine Biology and Ecology*, *195*(2), 173–186. https://doi.org/10.1016/0022-0981(95)00079-8

McDevitt-Irwin, J. M., Baum, J. K., Garren, M., & Vega Thurber, R. L. (2017). Responses of coral-associated bacterial communities to local and global stressors. *Frontiers in Marine Science*, *4*(AUG), 1–16. https://doi.org/10.3389/fmars.2017.00262

Mcgourty, K., Thurston, T. L., Matthews, S. A., Pinaud, L., Mota, L. J., & Holden, D. W. (2012). Salmonella Inhibits Retrograde Trafficking of Mannose-6-Phosphate. *Science*, *November*, 963–967. https://doi.org/10.1126/science.1227037

Medrano, E., Merselis, D. G., Bellantuono, A. J., & Rodriguez-Lanetty, M. (2019). Proteomic basis of symbiosis: A heterologous partner fails to duplicate homologous colonization in a novel cnidarian-symbiodiniaceae mutualism. *Frontiers in Microbiology*, *10*(MAY), 1–15. https://doi.org/10.3389/fmicb.2019.01153

Mellman, I. (1986). Acidification of the Endocytic and Exocytic Pathways. *Annual Review of Biochemistry*, *55*(1), 663–700. https://doi.org/10.1146/annurev.biochem.55.1.663

Mercier, A., & Hamel, J. F. (2010). Synchronized breeding events in sympatric marine invertebrates: Role of behavior and fine temporal windows in maintaining reproductive isolation. *Behavioral Ecology and Sociobiology*, *64*(11), 1749–1765. https://doi.org/10.1007/s00265-010-0987-z

References

Méresse, S., Steele-Mortimer, O., Moreno, E., Desjardins, M., Finlay, B., & Gorvel, J.-P. (1999). Controlling the maturation of pathogen-containing vacuoles: a matter of life and death. *Nature Cell Biology*, *1*(7), E183–E188. https://doi.org/10.1038/15620

Miller, D. J., Hemmrich, G., Ball, E. E., Hayward, D. C., Khalturin, K., Funayama, N., Agata, K., & Bosch, T. C. G. (2007). The innate immune repertoire in Cnidaria - Ancestral complexity and stochastic gene loss. *Genome Biology*, *8*(4). https://doi.org/10.1186/gb-2007-8-4-r59

Mohamed, A. R., Cumbo, V., Harii, S., Shinzato, C., Chan, C. X., Ragan, M. A., Bourne, D. G., Willis, B. L., Ball, E. E., Satoh, N., & Miller, D. J. (2016). The transcriptomic response of the coral Acropora digitifera to a competent Symbiodinium strain: The symbiosome as an arrested early phagosome. *Molecular Ecology*, *25*(13), 3127–3141. https://doi.org/10.1111/mec.13659

Mohamed, A. R., Cumbo, V. R., Harii, S., Shinzato, C., Chan, C. X., Ragan, M. A., Satoh, N., Ball, E. E., & Miller, D. J. (2018). Deciphering the nature of the coral-Chromera association. *ISME Journal*, *12*(3), 776–790. https://doi.org/10.1038/s41396-017-0005-9

Molestina, R. E., & Sinai, A. P. (2005a). Detection of a novel parasite kinase activity at the Toxoplasma gondii parasitophorous vacuole membrane capable of phosphorylating host lκBα. *Cellular Microbiology*, *7*(3), 351–362. https://doi.org/10.1111/j.1462-5822.2004.00463.x

Molestina, R. E., & Sinai, A. P. (2005b). Host and parasite-derived IKK activities direct distinct temporal phases of NF-κB activation and target gene expression following Toxoplasma gondii infection. *Journal of Cell Science*, *118*(24), 5785–5796. https://doi.org/10.1242/jcs.02709

Moran, N. A. (n.d.). *Symbiosis*. *16*(20), 866–871.

Muscatine, L. (1990). The role of symbiotic algae in carbon and energy flux in coral reefs. In *Ecosystems of the world* (Vol. 25, pp. 75–87).

Muscatine, L., Goiran, C., Land, L., Jaubert, J., Cuif, J. P., & Allemand, D. (2005). Stable isotopes (δ13C and δ15N) of organic matrix from coral skeleton. *Proceedings of the National Academy of Sciences of the United States of America*, *102*(5), 1525–1530. https://doi.org/10.1073/pnas.0408921102

Muscatine, L., & Porter, J. W. (1977a). Reef Corals: Mutualistic Symbioses Adapted to Nutrient-Poor Environments. *BioScience*, *27*(7), 454–460. https://doi.org/10.2307/1297526

Muscatine, L., & Porter, J. W. (1977b). Reef Corals: Mutualistic Symbioses Adapted to Nutrient-Poor Environments. *BioScience*, *27*(7), 454–460. https://doi.org/10.2307/1297526

Ndungu, F. M., Urban, B. C., Marsh, K., & Langhorne, J. (2005). Regulation of immune response by Plasmodium-infected red blood cells. *Parasite Immunology*, *27*(10–11), 373–384. https://doi.org/10.1111/j.1365-3024.2005.00771.x

Neubauer, E.-F., Poole, A. Z., Neubauer, P., Detournay, O., Tan, K., Davy, S. K., & Weis, V. M. (2017). A diverse host thrombospondin-type-1 repeat protein repertoire promotes symbiont colonization during establishment of cnidarian-dinoflagellate symbiosis. *ELife*, *6*, 1–26. https://doi.org/10.7554/elife.24494

Nüchter, T., Benoit, M., Engel, U., Özbek, S., & Holstein, T. W. (2006). Nanosecond-scale kinetics of nematocyst discharge. *Current Biology*, *16*(9), 316–318. https://doi.org/10.1016/j.cub.2006.03.089

Nyholm, S. v., & McFall-Ngai, M. J. (2004). The winnowing: Establishing the squid - Vibrios symbiosis. *Nature Reviews Microbiology*, *2*(8), 632–642. https://doi.org/10.1038/nrmicro957

Oakley, C. A., Ameismeier, M. F., Peng, L., Weis, V. M., Grossman, A. R., & Davy, S. K. (2016). Symbiosis induces widespread changes in the proteome of the model cnidarian Aiptasia. *Cellular Microbiology*, *18*(7), 1009–1023. https://doi.org/10.1111/cmi.12564

Parkinson, J. E., Tivey, T. R., Mandelare, P. E., Adpressa, D. A., Loesgen, S., & Weis, V. M. (2018). Subtle differences in symbiont cell surface glycan profiles do not explain species-specific colonization rates in a model cnidarian-algal symbiosis. *Frontiers in Microbiology*, *9*(MAY), 1–12. https://doi.org/10.3389/fmicb.2018.00842

Peralta, A. L., Malinarich, F., & Hermoso, M. A. (2007). *TLRs are key participants in innate immune responses.pdf*. *2*, 97–112.

Picelli, S., Faridani, O. R., Björklund, Å. K., Winberg, G., Sagasser, S., & Sandberg, R. (2014). Full-length RNA-seq from single cells using Smart-seq2. *Nature Protocols*, *9*(1), 171–181. https://doi.org/10.1038/nprot.2014.006

Poole, A. Z., Kitchen, S. A., & Weis, V. M. (2016). The role of complement in cnidarian-dinoflagellate symbiosis and immune challenge in the sea anemone Aiptasia pallida. *Frontiers in Microbiology*, *7*(APR). https://doi.org/10.3389/fmicb.2016.00519

R Core Team. (2018). *R: A language and environment for statistical computing* (3.5.2).

Rahman, M. M., & McFadden, G. (2011). Modulation of NF-κB signalling by microbial pathogens. *Nature Reviews Microbiology*, *9*(4), 291–306. https://doi.org/10.1038/nrmicro2539

Rana, R. R., Simpson, P., Zhang, M., Jennions, M., Ukegbu, C., Spear, A. M., Alguel, Y., Matthews, S. J., Atkins, H. S., & Byrne, B. (2011). Yersinia pestis TIR-domain protein

forms dimers that interact with the human adaptor protein MyD88. *Microbial Pathogenesis*, *51*(3), 89–95. https://doi.org/10.1016/j.micpath.2011.05.004

Reaka-Kudla, M. L. (1997). The Global Biodiversity of Coral Reefs: A Comparison with Rain Forests. In *Biodiversity II:Understanding and Protecting Our Biological Resources* (pp. 83–108).

Rodriguez-Lanetty, M., Wood-Charlson, E. M., Hollingsworth, L. L., Krupp, D. A., & Weis, V. M. (2006). Temporal and spatial infection dynamics indicate recognition events in the early hours of a dinoflagellate/coral symbiosis. *Marine Biology*, *149*(4), 713–719. https://doi.org/10.1007/s00227-006-0272-x

Ros, M., Suggett, D. J., Edmondson, J., Haydon, T., Hughes, D. J., Kim, M., Guagliardo, P., Bougoure, J., Pernice, M., Raina, J. B., & Camp, E. F. (2021). Symbiont shuffling across environmental gradients aligns with changes in carbon uptake and translocation in the reef-building coral Pocillopora acuta. *Coral Reefs*, *40*(2), 595–607. https://doi.org/10.1007/s00338-021-02066-1

Rosales, C., & Uribe-Querol, E. (2017). Phagocytosis: A Fundamental Process in Immunity. *BioMed Research International*, *2017*. https://doi.org/10.1155/2017/9042851

Rosenstiel, P., Philipp, E. E. R., Schreiber, S., & Bosch, T. C. G. (2009). Evolution and function of innate immune receptors - Insights from marine invertebrates. *Journal of Innate Immunity*, *1*(4), 291–300. https://doi.org/10.1159/000211193

Ruggiero, V., Loiarro, M., & Sette, C. (2010). Targeting TLR/IL-1R signalling in human diseases. *Mediators of Inflammation*, *2010*. https://doi.org/10.1155/2010/674363

Rumpho, M. E., Pelletreau, K. N., Moustafa, A., & Bhattacharya, D. (2011). The making of a photosynthetic animal. *Journal of Experimental Biology*, *214*(2), 303–311. https://doi.org/10.1242/jeb.046540

Sacks, D., & Sher, A. (2002). Evasion of innate immunity by parasitic protozoa. In *Nature Immunology* (Vol. 3, Issue 11, pp. 1041–1047). https://doi.org/10.1038/ni1102-1041

Salcedo, S. P., Marchesini, M. I., Degos, C., Terwagne, M., Bargen, K. von, Lepidi, H., Herrmann, C. K., Santos Lacerda, T. L., Imbert, P. R. C., Pierre, P., Alexopoulou, L., Letesson, J. J., Comerci, D. J., & Gorvel, J. P. (2013). BtpB, a novel Brucella TIR-containing effector protein with immune modulatory functions. *Frontiers in Cellular and Infection Microbiology*, *4*(JUL), 1–13. https://doi.org/10.3389/fcimb.2013.00028

Salinas-Saavedra, M., Rock, A. Q., & Martindale, M. Q. (2018). Germ layer-specific regulation of cell polarity and adhesion gives insight into the evolution of mesoderm. *ELife*, *7*, 1–28. https://doi.org/10.7554/eLife.36740

Schindelin, J., Arganda-Carreras, I., Frise, E., Kaynig, V., Longair, M., Pietzsch, T., Preibisch, S., Rueden, C., Saalfeld, S., Schmid, B., Tinevez, J. Y., White, D. J., Hartenstein, V., Eliceiri, K., Tomancak, P., & Cardona, A. (2012). Fiji: An open-source platform for biological-image analysis. *Nature Methods*, *9*(7), 676–682. https://doi.org/10.1038/nmeth.2019

Schwarz, J. A. (2008). Understanding the intracellular niche in Cnidarian-Symbiodinium symbioses: Parasites lead the way. *Vie et Milieu*, *58*(2), 141–151.

Schwarz, J. A., Krupp, D. A., & Weis, V. M. (1999). Late Larval Development and Onset of Symbiosis in the Scleractinian Coral Fungia scutaria. *The Biological Bulletin*, *196*(1), 70–79. https://doi.org/10.2307/1543169

Seoane, P. I., & May, R. C. (2020). Vomocytosis: What we know so far. *Cellular Microbiology*, *22*(2), 1–6. https://doi.org/10.1111/cmi.13145

Shinzato, C., Shoguchi, E., Kawashima, T., Hamada, M., Hisata, K., Tanaka, M., Fujie, M., Fujiwara, M., Koyanagi, R., Ikuta, T., Fujiyama, A., Miller, D. J., & Satoh, N. (2011). Using the Acropora digitifera genome to understand coral responses to environmental change. *Nature*, *476*(7360), 320–323. https://doi.org/10.1038/nature10249

Smith, L. M., Dixon, E. F., & May, R. C. (2015). The fungal pathogen Cryptococcus neoformans manipulates macrophage phagosome maturation. *Cellular Microbiology*, *17*(5), 702–713. https://doi.org/10.1111/cmi.12394

Souter, D., Planes, S., Wicquart, J., Logan, M., Obura, D., & Staub, F. (2020). Status of Coral Reefs of the World : 2020. *Global Coral Reef Monitoring Network*.

Spalding, M. D., & Grenfell, A. M. (1997). New estimates of global and regional coral reef areas. *Coral Reefs*, *16*(4), 225–230. https://doi.org/10.1007/s003380050078

Steele, R. D. (1977). *THE SIGNIFICANCE OF ZOOXAN- THELLA-CONTAINING PELLETS EX- TRUDED BY SEA ANEMONES*. *27*(3), 591–594.

Steinmetz, P. R. H. (2019). A non-bilaterian perspective on the development and evolution of animal digestive systems. *Cell and Tissue Research*, *377*(3), 321–339. https://doi.org/10.1007/s00441-019-03075-x

Stoecker, D. K. (1999). Mixotrophy among dinoflagellates. *Journal of Eukaryotic Microbiology*, *46*(4), 397–401. https://doi.org/10.1111/j.1550-7408.1999.tb04619.x

Subramanian, K., & Balch, W. E. (2008). NPC1/NPC2 function as a tag team duo to mobilize cholesterol. *Proceedings of the National Academy of Sciences of the United States of America*, *105*(40), 15223–15224. https://doi.org/10.1073/pnas.0808256105

References

Takeuchi, O., & Akira, S. (2010). Pattern Recognition Receptors and Inflammation. *Cell*, *140*(6), 805–820. https://doi.org/10.1016/j.cell.2010.01.022

Takeuchi, R., Jimbo, M., Tanimoto, F., Iijima, M., Yamashita, H., & Suzuki, G. (2021). *N -Acetyl- D -Glucosamine-Binding Lectin in Acropora tenuis*. 1–11.

Taylor, F. J. R., Hoppenrath, M., & Saldarriaga, J. F. (2008). Dinoflagellate diversity and distribution. *Biodiversity and Conservation*, *17*(2), 407–418. https://doi.org/10.1007/s10531-007-9258-3

Technau, U. (2020). Gastrulation and germ layer formation in the sea anemone Nematostella vectensis and other cnidarians. *Mechanisms of Development*, *163*(June), 103628. https://doi.org/10.1016/j.mod.2020.103628

Technau, U., Steele, R. E., Technau, U., & Steele, R. E. (2012). Evolutionary crossroads in developmental biology: Cnidaria. *Development (Cambridge)*, *139*(23), 4491. https://doi.org/10.1242/dev.090472

Uribe-Querol, E., & Rosales, C. (2020). Phagocytosis: Our Current Understanding of a Universal Biological Process. *Frontiers in Immunology*, *11*, 1066. https://doi.org/10.3389/fimmu.2020.01066

van Oppen, M. J. H., & Blackall, L. L. (2019). Coral microbiome dynamics, functions and design in a changing world. *Nature Reviews Microbiology*. https://doi.org/10.1038/s41579-019-0223-4

Vanier, M. T., & Millat, G. (2004). Structure and function of the NPC2 protein. *Biochimica et Biophysica Acta - Molecular and Cell Biology of Lipids*, *1685*(1–3), 14–21. https://doi.org/10.1016/j.bbalip.2004.08.007

von Euw, S., Zhang, Q., Manichev, V., Murali, N., Gross, J., Feldman, L. C., Gustafsson, T., Flach, C., Mendelsohn, R., & Falkowski, P. G. (2017). Biological control of aragonite formation in stony corals. *Science*, *356*(6341), 933–938. https://doi.org/10.1126/science.aam6371

Voolstra, C. R., Schwarz, J. A., Schnetzer, J., Sunagawa, S., Desalvo, M. K., Szmant, A. M., Coffroth, M. A., & Medina, M. (2009). The host transcriptome remains unaltered during the establishment of coral-algal symbioses. *Molecular Ecology*, *18*(9), 1823–1833. https://doi.org/10.1111/j.1365-294X.2009.04167.x

Voss, P. A., Gornik, S. G., Jacobovitz, M. R., Rupp, S., Dörr, M. S., Maegele, I., & Guse, A. (2019). *Nutrient-dependent mTORC1 signaling in coral-algal symbiosis*. 1–24.

Waghabi, M. C., Keramidas, M., Feige, J. J., Araujo-Jorge, T. C., & Bailly, S. (2005). Activation of transforming growth factor β by Trypanosoma cruzi. *Cellular Microbiology*, *7*(4), 511–517. https://doi.org/10.1111/j.1462-5822.2004.00481.x

Wahl, S. M. (1994). Transforming Growth Factorβ: The Good, the Bad, and the Ugly. *Journal of Experimental Medicine*, *180*(5), 1589–1590. https://doi.org/10.1084/jem.180.5.1587

Wartosch, L., Bright, N. A., & Luzio, J. P. (2015). Lysosomes. *Current Biology*, *25*(28), R315–R316. https://doi.org/10.1055/s-0028-1111504

Watkins, R. A., Andrews, A., King, J. S., Barisch, C., Wynn, C., & Johnston, S. A. (2018). Cryptococcus neoformans Escape From Dictyostelium Amoeba by Both WASH-Mediated Constitutive Exocytosis and Vomocytosis. *Frontiers in Cellular and Infection Microbiology*, *8*(April), 1–11. https://doi.org/10.3389/fcimb.2018.00108

Weis, V. M., Davy, S. K., Hoegh-Guldberg, O., Rodriguez-Lanetty, M., & Pringle, J. R. (2008). Cell biology in model systems as the key to understanding corals. *Trends in Ecology and Evolution*, *23*(7), 369–376. https://doi.org/10.1016/j.tree.2008.03.004

Winchester, B. G. (2001). Lysosomal membrane proteins. *European Journal of Paediatric Neurology*, *5*(SUPPL. A), 11–19. https://doi.org/10.1053/ejpn.2000.0428

Wolfowicz, I., Baumgarten, S., Voss, P. A., Hambleton, E. A., Voolstra, C. R., Hatta, M., & Guse, A. (2016). Aiptasia sp. larvae as a model to reveal mechanisms of symbiont selection in cnidarians. *Scientific Reports*, *6*, 1–12. https://doi.org/10.1038/srep32366

Wood-Charlson, E. M., Hollingsworth, L. L., Krupp, D. A., & Weis, V. M. (2006). Lectin/glycan interactions play a role in recognition in a coral/dinoflagellate symbiosis. *Cellular Microbiology*, *8*(12), 1985–1993. https://doi.org/10.1111/j.1462-5822.2006.00765.x

Xiang, T., Hambleton, E. A., Denofrio, J. C., Pringle, J. R., & Grossman, A. R. (2013). Isolation of clonal axenic strains of the symbiotic dinoflagellate Symbiodinium and their growth and host specificity1. *Journal of Phycology*, *49*(3), 447–458. https://doi.org/10.1111/jpy.12055

Yellowlees, D., Rees, T. A. v., & Leggat, W. (2008). Metabolic interactions between algal symbionts and invertebrate hosts. *Plant, Cell and Environment*, *31*(5), 679–694. https://doi.org/10.1111/j.1365-3040.2008.01802.x